UNIVERSITÀ DEGLI STUDI DI PADOVA

Università degli studi di Padova

Dipartimento di Biologia

SCUOLA DI DOTTORATO IN BIOSCIENZE E BIOTECNOLOGIE
INDIRIZZO DI NEUROBIOLOGIA
CICLO XXVI

Mechanism of activation and function of the odorant receptor expressed at the axon terminus – growth cone of olfactory sensory neurons

Direttore della scuola: Ch. mo Prof. Giuseppe Zanotti
Coordinatore: Ch. ma Prof.ssa Daniela Pietrobon
Supervisore: Dott.ssa Claudia Lodovichi

Dottorando: Sira Angela Franchi

Index

Summary

A unique feature in the topographic organization of the olfactory bulb is the “dual role” of the odorant receptor. It detects odorants and it has been suggested to play a critical role in the axonal convergence of olfactory sensory neurons to form glomeruli in specific loci of the olfactory bulb. This spatial segregation of sensory afferents results in the sensory map. A role of the odorant receptors in axon guidance was suggested by genetic experiments demonstrating that manipulations of odorant receptor sequences perturb the sensory map (Wang et al., 1998). This hypothesis was confirmed by subsequent works (Barnea et al., 2004, Strotmann et al., 2004) that revealed the presence of the olfactory receptor in the most distal portion of the axon and at the growth cone. The open question to be addressed was whether the odorant receptor expressed at the axon terminal was functional and if yes, what was the signalling pathway coupled to its activation. In a previous study, Maritan et al., 2009, demonstrated, for the first time, that the odorant receptor expressed at the axon terminus - growth cone is functional and coupled to local increases of Ca^{2+} and cAMP. Although cAMP and Ca^{2+} are the primary second messengers produced upon activation of the odorant receptor, cGMP is also synthesized and takes part in several key processes such as adaptation, neuronal development and long term cellular responses to odorant stimulation. Many aspects of the regulation of cGMP in olfactory sensory neurons (OSNs) were still unknown, as the mechanism of coupling to odorant receptors (ORs) and downstream targets. To address these points, we investigated the dynamics and the intracellular distribution of cGMP in living rat OSNs in culture transfected with a genetically encoded sensor for cGMP. We demonstrated that OSNs treated with pharmacological stimuli able to activate particulate or soluble guanylyl cyclases (pGC and sGC) presented an increase in cGMP in the whole neuron, from cilia - dendrite to the axon terminus - growth cone. Upon odorant stimulation, a rise in cGMP was again found in the entire neuron, including the axon terminal, where it is locally synthesized. The odorant - dependent rise in cGMP is due to sGC activation by NO and requires an increase of cAMP. The link between cAMP and NO synthase appears to be the rise in $[Ca^{2+}]_c$ elicited by either plasma membrane Ca^{2+} channel activation and Ca^{2+} mobilization from

stores via the guanine nucleotide exchange factor Epac. Finally we show that a cGMP rise can elicit the phosphorylation of nuclear CREB both *in vitro* and *in vivo*. The local synthesis of cGMP, coupled to the OR expressed at the axon terminal, suggested that not only cAMP, but also cGMP can contribute to OSN axonal convergence.

The question then arose on the mechanism of activation, i.e. the possible natural ligands, of the olfactory receptor at the axon terminal. We hypothesized that a few molecules expressed in gradient in the olfactory bulb could bind and activate the odorant receptor expressed at the axon terminal, regulating in this way the axon pathfinding to its final target. To test our hypothesis we studied the spatio - temporal dynamics of Ca^{2+} and cAMP in response to molecules from the bulb. We found that a pool of these molecules is capable of eliciting a rise in Ca^{2+} and cAMP in the axon terminus - growth cone of OSNs loaded with fura-2 or transfected with the sensor for cAMP. To assess whether the Ca^{2+} and cAMP rises were due to the activation of the olfactory receptor at the axon terminal, we expressed specific odorant receptors in HEK cells. The Ca^{2+} rise was observed only in HEK cells transfected with specific receptors, but not in HEK cells transfected with the empty vector (controls). All together, our data demonstrate the presence of a pool of active molecules in the bulb able to activate the OR expressed at the axon terminus - growth cone. To assess the physiological meaning of the variation in Ca^{2+} and cAMP levels on the turning behaviour of the olfactory sensory neuron axons, real - time imaging experiments on isolated olfactory sensory neurons were performed. We analyzed the behaviour of olfactory sensory neuron growth cone in response to gradients of molecules capable of modulating Ca^{2+} and cAMP levels at the axon terminus - growth cone, such as forskolin, a generic activator of adenylyl cyclase, odors and the active pool of molecules from the olfactory bulb. We found that all these molecules, including the ones from the bulb, were able to regulate the turning behaviour of the olfactory sensory neuron axons.

All together our data suggest that molecules from the olfactory bulb, via activation of the odorant receptor expressed at the axon terminus – growth cone, contribute in providing the olfactory sensory neuron axons with instruction to reach the proper target in the olfactory bulb.

Sommario

Una caratteristica peculiare dell'organizzazione topografica del bulbo olfattivo è il "duplice ruolo" del recettore olfattivo. Esso non solo è in grado di riconoscere gli odori, ma sembra anche svolgere un ruolo chiave nella convergenza assonale dei neuroni sensoriali olfattivi a formare i glomeruli in specifiche posizioni nel bulbo olfattivo. Questa segregazione spaziale delle afferenze assonali porta alla formazione della mappa sensoriale. Un ruolo del recettore olfattivo nei processi di "axon guidance" (orientamento assonale) è stato suggerito da esperimenti genetici (Wang et al., 1998) e successivamente confermato da studi che hanno rivelato la presenza del recettore olfattivo a livello della porzione distale dell'assone e nel cono di crescita (Barnea et al., 2004, Strotmann et al., 2004). La questione che rimane da affrontare è se il recettore olfattivo espresso al cono di crescita sia funzionale e se si, quale sia la cascata di segnalazione intracellulare accoppiata alla sua attivazione. In uno studio precedente, Maritan et al. (2009), hanno dimostrato, per la prima volta, che il recettore olfattivo espresso al cono di crescita è funzionale ed associato a locali incrementi di cAMP e Ca^{2+}. Sebbene l' cAMP e il Ca^{2+} siano i principali secondi messaggeri prodotti in seguito all'attivazione del recettore olfattivo, anche il cGMP viene sintetizzato e prende parte a processi quali l'adattamento, lo sviluppo neuronale e le risposte a lungo termine alla stimolazione odorosa. Molti aspetti della regolazione del cGMP nei neuroni sensoriali olfattivi, come il meccanismo di accoppiamento al recettore olfattivo e i "target" a valle, rimangono poco conosciuti. Per far luce su questi punti, abbiamo studiato le dinamiche e la distribuzione intracellulare del cGMP in neuroni sensoriali olfattivi di ratto in coltura transfettati con un sensore per il cGMP geneticamente codificato. Abbiamo dimostrato che neuroni sensoriali olfattivi trattati con stimoli farmacologici capaci di attivare le guanilato ciclasi solubili o di membrana presentavano un incremento del cGMP nell'intero neurone, dalle cilia al cono di crescita. In seguito alla stimolazione con gli odori, un incremento nei livelli di cGMP è stato nuovamente osservato in tutta la cellula, incluso il cono di crescita, dove il cGMP viene localmente prodotto. L'aumento odore - dipendente del cGMP è dovuto all'attivazione della guanilato ciclasi solubile ad opera dell'ossido nitrico (ON) e richiede un aumento di cAMP. Il collegamento

tra l' cAMP e l' ON sembra essere costituito dall'aumento dei livelli di Ca^{2+} citosolico indotto sia dall'attivazione dei canali Ca^{2+} sulla membrana plasmatica, sia dalla mobilitazione del Ca^{2+} dai depositi intracellulari attraverso lo scambiatore di nucleotidi ciclici Epac. Infine abbiamo dimostrato che l'incremento di cGMP può indurre la fosforilazione di CREB a livello nucleare sia *in vitro* che *in vivo*. La sintesi locale di cGMP, accoppiata al recettore olfattivo espresso al cono di crescita, suggerisce che anche questo secondo messaggero, assieme all' cAMP, può contribuire alla convergenza assonale dei neuroni sensoriali olfattivi.

A questo punto ci siamo chiesti quale possa essere il meccanismi di attivazione, in particolare quali possano essere i ligandi del recettore olfattivo espresso al cono di crescita. Abbiamo ipotizzato che alcune molecole, espresse in gradiente nel bulbo olfattivo, possano legare e attivare il recettore olfattivo all'assone terminale.

Per testare la nostra ipotesi, abbiamo studiato le dinamiche spazio – temporali di Ca^{2+} e cAMP in risposta alle molecole estratte dal bulbo olfattivo. I nostri dati dimostrano che un set di molecole è in grado di indurre un aumento di Ca^{2+} e cAMP nel cono di crescita di neuroni sensoriali olfattivi caricati col fura-2 o transfettati con un sensore per l' cAMP. Al fine di dimostrare che tali incrementi di Ca^{2+} e cAMP erano effettivamente dovuti all'attivazione del recettore al cono di crescita, abbiamo espresso specifici recettori olfattivi in cellule HEK. L'aumento di Ca^{2+} è stato osservato esclusivamente nelle cellule HEK transfettate con diversi recettori olfattivi, ma non in quelle transfettate con il vettore vuoto (mancanti del recettore olfattivo), usate come controllo. Questi dati dimostrano la presenza di un set di molecole attive nel bulbo olfattivo in grado di attivare il recettore espresso al cono di crescita. Per capire il significato fisiologico delle variazioni di Ca^{2+} e cAMP sul comportamento di "turning" degli assoni dei neuroni sensoriali olfattivi, abbiamo svolto esperimenti di "real – time imaging" su neuroni sensoriali olfattivi isolati. Abbiamo quindi analizzato il comportamento del cono di crescita in risposta a un gradiente di molecole capaci di modulare Ca^{2+} e cAMP a livello del cono di crescita, come la forscolina, un attivatore generico delle adenilato ciclasi, gli odori e anche le molecole provenienti dal bulbo olfattivo. Da questi esperimenti emerge che la

forskolina, gli odori e anche le molecole del bulbo, sono capaci di regolare il comportamento di “turning” del cono di crescita dei neuroni sensoriali olfattivi.

Nel complesso, i nostri dati suggeriscono che alcune molecole del bulbo olfattivo, attraverso l’attivazione del recettore espresso al cono di crescita, contribuiscono a fornire ai neuroni sensoriali olfattivi le informazioni necessarie per raggiungere il corretto bersaglio nel del bulbo olfattivo.

1. Introduction

1.1 The olfactory system

Most organisms are able to recognize and discriminate a huge number of chemical signals, i.e. odors, in the environment. Odors deeply influence the behavior of most animals and provide them with essential information for their survival. The olfactory system regulates a wide range of multiple and integrative tasks such as reproductive functions, social behaviours, physiological regulation and emotional responses. To accomplish this large variety of functions, most animals take advantage of two anatomically separate sensory organs. The accessory olfactory system consists of the vomeronasal organ and the accessory olfactory bulb, whose cells project to the amygdala and the hypothalamus. It is specialized to sense specific chemical compounds, i.e. the pheromones. The main olfactory system includes the olfactory epithelium, the main olfactory bulb and the associated cortical areas. It recognizes more than a thousand airborne volatile molecules called odorants (Lledo et al., 2005). In this thesis I focused my attention on the main olfactory system, in particular on the main olfactory epithelium.

1.1.1 The olfactory epithelium

The olfactory system sits at the interface of the environment and the central nervous system. It is responsible for coding sensory information from thousands of odorous stimuli. To understand the logic of olfactory information processing, it is necessary to appreciate the coding rules generated at each level, from the odorant receptors up to the olfactory cortex. In mammals, the initial event of odor detection takes place in the olfactory epithelium (OE), located in the posterior end of the nasal cavity (Lledo et al., 2005). The olfactory epithelium is a specialized pseudostratified neuroepithelium which covers the turbinates, a set of cartilaginous flaps located in the posterior part of the nasal cavity (Firestein 2001). It contains three major cell types: the olfactory sensory neurons (OSNs; the only neuronal cell type), the supporting or sustentacular cells (a kind of glial cells, which possess microvilli on their apical surface) and several types of basal cells, including the olfactory stem cells (Figure 1).

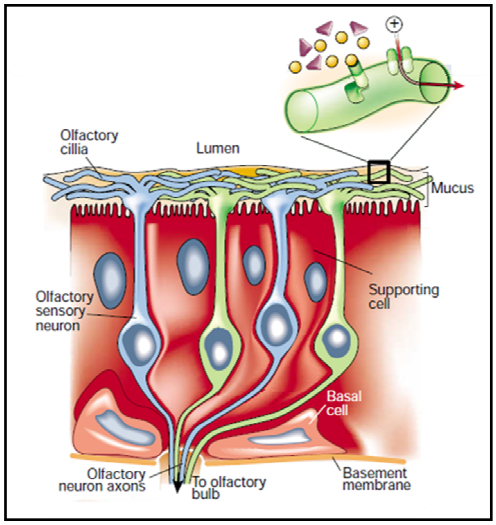

Figure 1: schematic representation of the olfactory epithelium. Three different cell types can be distinguished: the olfactory sensory neurons, whose cilia are immersed in the mucus and protrude in the nasal cavity, sustentacular cells and basal cells. The cilia are the sites of the odorant receptors, which bind odorants and initiate the olfactory signaling cascade. (Firestein 2001)

The olfactory sensory neurons represent the 70 - 80% of the whole population of cells within the olfactory epithelium and they constantly regenerate during the entire life of the organism with an emilife of 60 – 90 days. Olfactory sensory neurons are bipolar neurons with a thin axon that directly projects from the proximal pole of the soma to the olfactory bulb. From the apical pole of the cell body, a single and unbranched dendrite extends to the surface of the olfactory epithelium and ends in a knob – like swelling from which several cilia protrude (Figure 2).

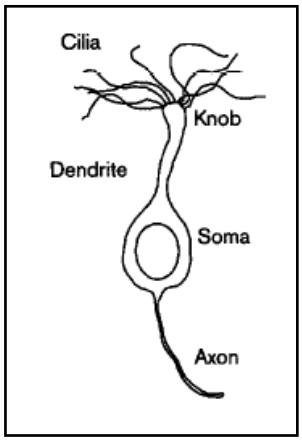

Figure 2: schematic representation of an olfactory sensory neuron. It is notable the typical bipolar morphology: a unique unbranched dendrite ending in a knob – like swelling, from which several cilia originate and a single thin axon. (Menini 1999)

These cilia are the site of the sensory transduction apparatus and invade the mucus lining the nasal cavity. The mucus is secreted by the sustentacular cells and Bowman glands and it is thought to create an optimal environment for the odor detection. It includes mucopolysaccharides, enzymes, salts and olfactory binding proteins. Olfactory binding proteins are a family of proteins secreted in the nasal mucosa that may help transport odorant molecules through the mucus. The odorant molecules are dissolved in the mucus and they bind the odorant receptors on the cilia. Once the receptor has bound the odorant molecule, a cascade of intracellular events is initiated and it culminates with the propagation of an action potential to the olfactory bulb.

The sustentacular cells function as metabolic and physical support for the olfactory cells. Indeed, they electrically isolate the olfactory sensory neurons and release the components of the mucus lining the nasal cavity and growth factors essential for the development of the olfactory sensory neurons. Finally, they contain enzymes which have an inactivating action on the odorants.

The olfactory stem cells (named also basal cells) are located in the basal lamina of the olfactory epithelium and they are capable of division and differentiation into new olfactory sensory neurons.

1.1.2 The olfactory receptors

Odorants are typically small organic molecules of less than 400 Da and they can vary in a number of parameters, including size, shape, functional groups, and charge. The perception of odors depends on the structure of the odorant molecule. For example when the hydroxyl group of octanol is replaced by a carboxyl group to give octanoic acid, its perceived odor changes from orange and rose – like to rancid and sweaty (Arctander 1969).

The perceived odor can be influenced also by other parameters, such as the concentration of the odorant and the individual variability. Indole, for example, has a putrid odor when concentrated but it is perceived as floral when diluted. In addition, there can be individual differences in olfactory perception. Androstenone, a pig pheromone, is a good example. At a low concentration, it is perceived as a mild, pleasant odor to some, while other people perceive it as a

disgusting urinous odor. Still others cannot smell it at all (Malnic et al., 1999). The odorant detection is mediated by the odorant receptors (ORs), which belong to the G protein - coupled receptors (GPCRs) family. They are expressed on the cilia of the olfactory sensory neurons, within the olfactory epithelium. The odorant receptors share many features with others GPCRs, such as a structure that predicts seven α – helical membrane – spanning domains connected by intracellular and extracellular loops of variable lengths, and numerous conserved short sequences. However, there are certain characteristics specific to the odorant receptors, such as an unusually long second extracellular loop, an extra pair of conserved cysteines in that loop, and other short sequences. Within the odorant receptor family, there is a range of similarity from less than 40% to over 90% identity. Most interesting, there is a region of hypervariability, where the sequences show a particularly strong divergence, in the third, fourth and fifth transmembrane regions. In three – dimensional models of the GPCRs, these three regions are thought to face each other and form a pocket where the binding with the ligand is thought to occur (Figure 3). Moreover, the variability observed among the odorant receptors in these regions provides the first molecular basis for understanding the range, diversity and large number of olfactory molecules that can be detected and discriminated (Firestein 2001).

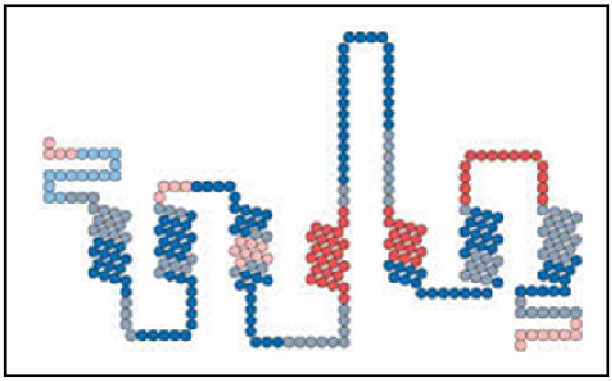

Figure 3: structure of an odorant receptor. More conserved amino acid residues are represented in blue shades, while residues characterized by a higher variability are stained in the red shades. (Firestein 2001)

The genes encoding the odorant receptors constitute a large gene family and in mammals they represent the largest gene superfamily in the genome. It has been estimated that there are ~1000 odorant receptors in the mouse and rat (it may account for as much as 2% of the genome), and ~500 - 800 in human. The genes encoding the odorant receptors are intronless. Mammalian odorant

receptor genes are typically organized in clusters of ten or more members and located on many chromosomes. The chromosomal distribution of odorant receptors is extremely biased, with six chromosomes (1, 6, 9, 11, 14 and 19) accounting for 73% of the repertoire and the remaining 27% scattered on most other chromosomes (Zozulya et al., 2001, Glusman et al., 2001). In the human genome more than 60% of the odorant receptor genes seem to be pseudogenes. In contrast, only about 20% of mouse odorant receptors are pseudogenes, giving mice over three times as many intact genes than humans. Furthermore, some apparently intact human odorant receptor genes lack motifs that are very highly conserved in intact mouse odorant receptor genes, suggesting that not all human genes encode functional odorant receptor proteins. The expression of odorant receptor genes occurs only in mature olfactory sensory neurons, namely cells expressing a functional odorant receptor, and it starts already during embryonic life, before the axon reaches the olfactory bulb. A known marker of mature olfactory sensory neurons is the olfactory marker protein (OMP). OMP is a 19 kDa cytoplasmic protein exclusively expressed by mature olfactory sensory neurons (Monti - Graziadei et al., 1977). In rodent olfactory sensory neurons, OMP can be detected 3 – 4 days after their morphological development. Indeed, its expression starts at embryonic day 13 – 14 (E13 - E14) in mice and at embryonic day 18 (E18) in rats (Monti - Graziadei et al., 1980).

Each olfactory sensory neuron expresses only one type of odorant receptor gene in a repertoire of more than 1000 odorant receptor genes. Moreover, each olfactory sensory neuron is functionally distinct and can be identified by the type of receptor expressed. In each neuron, each cluster of receptor genes is inactive on one of the two chromosomes. This mechanism is thought to assure that individual neurons express only one receptor gene (Chess et al., 1994). Thus, the odorant receptor defines the molecular receptive range of that neuron, namely it determines the range of odors which can be recognized and bound by the olfactory sensory neuron (Malnic et al., 1999).

Each odorant receptor recognizes a specific structure within the odorant molecule (odotope). The two main classes of odotopes characterizing odorants are: the stereochimichal structure of hydro carbonic chain and the position of the lateral functional groups. Each odorant can contain several odotopes thus

each odor can be recognized by different odorant receptors. Moreover, each odorant receptor can recognize different odors but carrying the same odotope. Thus, each odorant can be coded by a specific combination of activated odorant receptors and each receptor can be considered as a component of the combinatorial receptor code for several odors (Malnic et al., 1999). The olfactory system uses this combinatorial receptor coding scheme to encode odor identities (Figure 4).

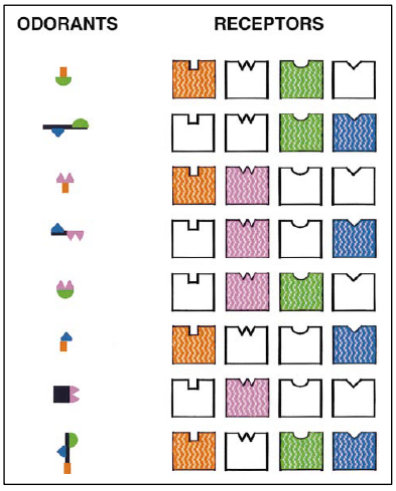

Figure 4: combinatorial receptor codes for odorants. Receptors shown in colour are those that recognize the odorant on the left. The identities of different odorants are encoded by different combinations of receptors. However, each odorant receptor can serve as one component of the combinatorial receptor codes for many odorants. Given the immense number of possible combinations of odorant receptors, this scheme could allow for the discrimination of an almost unlimited number and variety of different odorants. (Malnic et al., 1999)

1.1.3 Mechanism of transduction of the olfactory signal in the olfactory sensory neurons

The olfactory transduction is activated by the binding of the odorants to specific odorant receptors and involves two main second messengers: the cyclic AMP and Ca^{2+}. Once the odorants enter the nasal cavity, they dissolve in the mucus and bind the odorant receptors expressed at the cilia. The odorant receptor, upon binding odorant ligands, activates a specific stimulatory G protein, G_{olf}, that stimulates the type III adenylyl cyclase (ACIII) to synthesize cAMP. Cyclic AMP directly activates cyclic nucleotide gated (CNG) channels, driving an influx of Ca^{2+} and Na^{+} within the cell. The Ca^{2+} rise induces a Cl^{-} outward current (through Ca^{2+} - activated Cl^{-} channels) and therefore a further depolarization, leading to action potential generation. These action potentials are conducted along the axon to the olfactory bulb (Figure 5).

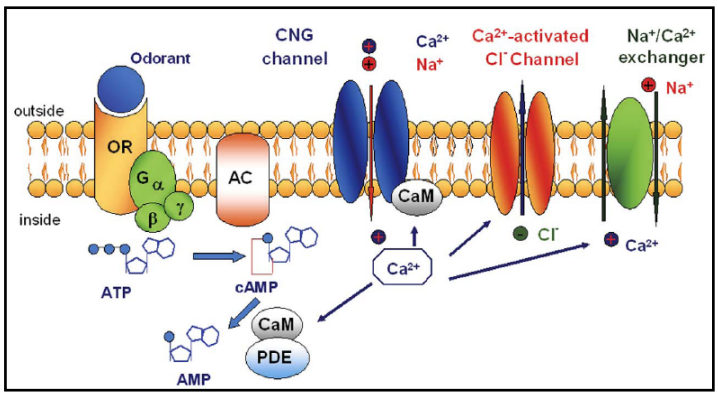

Figure 5: signaling transduction cascade at the cilia of olfactory sensory neurons. Upon binding odorant ligand, the odorant receptor (OR) activates G_{olf}, that in turn stimulates ACIII to produce cAMP. The increase in cAMP level opens CNG channels driving an influx of Ca^{2+} and Na^{+} within the cell. The Ca^{2+} rise, in turn, induces the opening of Cl^{-} channels, allowing an efflux of Cl^{-} and a further depolarization. (Pifferi et al., 2006)

Following excitation, the intracellular level of Ca^{2+} is thought to be restored to pre – stimulus levels by a Na^{+} - Ca^{2+} exchanger, whose presence in the olfactory dendrite and cilia was suggested by Ca^{2+} imaging studies (Noe et al., 1997). The functional role of this exchanger has been also established by replacing Na^{+} with another cation that does not support exchange extrusion of Ca^{2+}. Under these conditions, the response to odor stimulation is prolonged, indicating a persistent elevation of intracellular Ca^{2+} and opening of Ca^{2+} - activated Cl^{-} channels, and recovery from olfactory adaptation is retarded. The increased concentration of Ca^{2+} at the cilia, upon odorant stimulation, regulates not only activation, but also desensitization of the olfactory sensory neurons. Elevated Ca^{2+} level reduces the sensitivity of the CNG channels to cAMP, through a direct interaction between the CNG channels and the Ca^{2+} - calmodulin complex (Matthews and Reisert, 2003). Moreover, Ca^{2+} shows an inhibitory action on the ACIII, blocking the synthesis of cAMP, and an activating action on type 1C2 phosphodiesterase (PDE1C2), increasing the cAMP degradation (Pifferi et al., 2006).

Olfactory sensory neurons express at least two $G\alpha_s$, homologs, G_s and G_{olf} (G olfactory protein), both able of activating adenylyl cyclases. During embryogenesis, the level of G_s in olfactory sensory neurons exceeds that of G_{olf}. However, in postnatal stages of development, G_{olf} level rises and greatly exceeds that of G_s. Thus, G_{olf} is mainly expressed in mature olfactory sensory neurons and associated with the odorant receptor on the cilia, where it takes

part in the olfactory signal transduction. Indeed, G_{olf} knock – out mice show a dramatic reduction in the electrophysiological response of the primary olfactory sensory neurons to a large range of odorants.

The odorants exposure leads not only to an increase of cAMP and Ca^{2+} levels, but also of cyclic GMP (cGMP), another second messenger. Cyclic GMP exhibits a slow and sustained rise. This dynamics suggested that cGMP may not be involved in initial stimulus detection events but rather may be involved in several long term cellular responses to odorant stimulation. A number of studies indicate that, in olfactory sensory neurons, cGMP is involved in a variety of signal processes such as adaptation, neuronal development, and long – term cellular responses. The mechanisms underpinning the synthesis and degradation of cGMP in the olfactory sensory neurons are still poorly understood (Moon et al., 2005).

1.1.4 Metabolism and effectors of cAMP

1.1.4.1 cAMP synthesis

Cyclic adenosine monophosphate (cAMP) is a key second messenger in many biological processes. Cyclic AMP is synthesized from ATP by adenylyl cyclases located on the inner side of the plasma membrane. Adenylyl cyclases (ACs) are ATP - pyrophosphate lyases which catalyze the conversion of ATP to 3' - 5' - cyclic AMP (cAMP) and pyrophosphate. Currently, nine mammalian transmembrane ACs are recognized, with a tenth "soluble" form that has distinct catalytic and regulatory properties. Mammalian transmembrane ACs share a similar topology of a variable N – terminus and two repeats of a membrane – spanning domain followed by a cytoplasmic domain. All the transmembrane ACs are activated by a stimulatory G protein (G_s), while the soluble isoform is activated by HCO^-_3 and Ca^{2+}. Table 1.1 resumes some characteristics of the membrane ACs.

AC isoform	G protein regulators		Protein kinases		Calcium	RGS2	Other
	stimulatory	inhibitory	stimulatory	inhibitory			
Group I							
AC1	Gsα	Gα i, z, o, Gβγ	PKCα (weak)	CaMK IV	↑ CaM		PAM
AC8	Gsα	Gβγ			↑ CaM		PP2A
AC3	Gsα	Gβγ	PKCα (weak)	CaMK II	↑ CaM*	↓	
Group II							
AC2	Gsα, Gβγ		PKCα				
AC4	Gsα, Gβγ			PKCα			
AC7	Gsα, Gβγ		PKCα				PAM
Group III							
AC5	Gsα, Gβγ	Gα i, z	PKC (α, ζ)	PKA	↓ free Ca^{2+}	↓	PAM, Ric8a
AC6	Gsα, Gβγ	Gα i, z		PKA, PKC (δ, ε)	↓ free Ca^{2+}	↓	PAM, Snapin
Group IV							
AC9	Gsα			PKC	↓ via calcineurin		

Table 1.1: regulatory properties of transmembrane ACs isoforms. Transmembrane ACs are regulated by several factors, such as G proteins (Gsα, Gβγ, Gαi, z, o), protein kinases A and C (PKA and PKC, respectively), calmodulin (CaM) and CaM – dependent kinases (CaMKs). There also are other secondary regulators, including RGS2 (regulator of G protein signaling), PAM (protein associated with Myc), Ric8a (guanine nucleotide exchange protein for heterotrimeric G proteins), Sinapsin (member of SNAP – 25/Snare complex in hippocampal neurons) and PP2a (protein phosphatase 2a). (Sadana and Dessauer, 2009)

Membrane - bound ACs are often classified into four different groups based on regulatory properties. Group I consists of Ca^{2+} - stimulated AC1, 3 and 8; group II consists of Gβγ stimulated AC2, 4 and 7; group III is comprised of Giα/Ca^{2+} - inhibited AC5 and 6; while group IV contains forskolin (a generic activator of ACs) insensitive AC9 (Sadana and Dessauer, 2009). It is well established that AC2, AC3 and AC4 are all expressed in the cilia of the olfactory sensory neurons (Wong et al., 2000). In particular, AC3 is involved in the odorant transduction cascade. Recently it has been demonstrated that AC3 is expressed not only at the cilia but also at the axonal terminal of olfactory sensory neurons.

1.1.4.2 cAMP degradation

Cyclic nucleotide phosphodiesterases (PDEs), which are ubiquitously distributed in mammalian tissues, play a major role in cell signalling by hydrolyzing cAMP and cGMP. At present, eleven different PDE families have been identified, each consisting of several isoforms.

As you can see from the Table 1. 2, PDE families are characterized by different substrate specificity (cAMP and cGMP). On this basis, three main groups can be distinguished: PDEs that specifically hydrolyze cAMP, cGMP specific PDEs, and PDEs which hydrolyze both cyclic nucleotides. cAMP and cGMP dependent PDEs can be classified also basing on their regulatory properties. The main

PDE modulators are cGMP itself, which can act both as activator and inhibitor, Ca^{2+} - CaM complex, protein kinases PKA and PKG.

PDE family	Substrate	Property
PDE1	cAMP, cGMP	Ca-calmodulin-activated
PDE2	cAMP, cGMP	cGMP-activated,
PDE3	cAMP, cGMP	cGMP-inhibited
PDE4	cAMP	cGMP-insensitive
PDE5	cGMP	PKA/PKG-phosphorylated
PDE6	cGMP	Transducin-activated
PDE7	cAMP	Rolipram-insensitive
PDE8	cAMP	Rolipram-insensitive IBMX-insensitive
PDE9	cGMP	IBMX-insensitive
PDE10	cAMP, cGMP	Unknown
PDE11	cAMP, cGMP	Unknown

Table 1. 2: classification of the PDEs family. PDE4, 7 and 8 are cAMP – specific, while PDE5, 6 and 9 are cGMP – specific. PDE1, 2, 3, 10 and 11 are specific for both cyclic nucleotides. PDEs can be regulated by cGMP, Ca^{2+} - CaM complex, PKA and PKG. IBMX is a generic pharmacological inhibitor of PDEs and Rolipram is a specific inhibitor of PDE4. Transducins are G proteins specific for the retina. (Lugnier 2006)

In the olfactory sensory neurons, PDE1, 2 and 4 have been identified (Moon et al., 2005). Type 1 phosphodiesterase (PDE1) is highly localized in olfactory cilia and is a Ca^{2+}/calmodulin - dependent PDE, which is activated by an increase in Ca^{2+} level via calmodulin. All PDE1 isoforms can hydrolyze both cAMP and cGMP, although the affinity for each nucleotide varies according to the isoform. Among these isoforms, PDE1C2, is highly expressed in olfactory sensory neurons. PDE1C2 is activated by calcium via calmodulin and inhibited by PKA. Moreover, PDE1C2 displays a higher affinity for cAMP than cGMP and, interestingly, is colocalized with AC type III.

Type 2 phosphodiesterase (PDE2) is expressed in olfactory cilia, olfactory sensory neuron cell bodies and axons. It is specific for both cAMP and cGMP and allosterically activated by the bound with cGMP.

Type 4 phosphodiesterase (PDE4) is localized in the dendritic knob, olfactory sensory neuron soma and axons. It is specific for cAMP and it has been demonstrated that its phosphorylation by PKA increases the catalytic activity (Lugnier 2006).

1.1.4.3 cAMP effectors

cAMP regulates multiple intracellular targets, such as cyclic nucleotide – gated (CNG) channels, protein kinase A (PKA), and exchange protein directly activated by cAMP (Epac).

Cyclic nucleotide – gated channels (CNG channels) were first identified in rod and cone photoreceptors (Kaupp and Seifert 2002). They were found also in olfactory sensory neurons (Nakamura and Gold 1987). In mammals, a family of six genes codes for four "A" subunits (CNGA1 - 4) and two "B" subunits (CNGB1 and CNGB3). In olfactory sensory neurons, the CNG channels consist of three different subunits with a $CNG(A2)_2$ – A4 – B1b stechiometry. The two modulatory subunits A4 and B1b play the essential role of increasing the sensitivity to cAMP and making the feedback inhibition by Ca^{2+} - CaM rapid and state independent (Bradley et al., 2005). CNG channels are nonselective cation channels with a considerable Ca^{2+} permeability under physiological conditions. Moreover, they do not desensitize or inactivate when exposed to cyclic nucleotides. However, they can undergo a feedback regulation, especially via Ca^{2+} - mediated mechanisms. Olfactory CNG channels show similarity with the family of voltage – gated ion channels. They are indeed constituted by six transmembrane domains (TMDs), the pore loop is located between TMD5 and 6, and both their N - and C - termini are intracellular and include functional regions for channel regulation (Figure 6)(Bradley et al., 2005, Gordon and Zagotta, 1995). Finally, CNG channels of olfactory cells show a higher affinity for cGMP than for cAMP and this affinity can be modulated by phosphorylation, bivalent cations and by the interaction with the Ca^{2+} - calmodulin complex (Nakamura 2000).

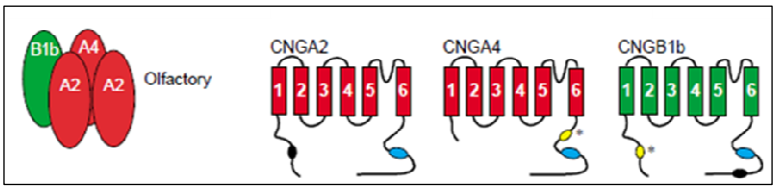

Figure 6: subunits and stechiometry of CNG channels in olfactory sensory neurons. cAMP binding sites are represented in blue, while CaM binding sites in yellow and black. (Bradley et al., 2005)

Protein kinase A (PKA) is the main effector of cAMP and its activity depends on the cellular levels of cAMP. PKA is an holotetramer composed by two

regulatory and two catalytic subunits. Its activation leads to the dissociation of the catalytic subunits from the regulatory ones. The dissociated catalytic subunits can phosphorylate cytoplasmic substrates and/or diffuse into the nucleus, where they trigger some of the long – term effects of cAMP (Zaccolo et al., 2000). For example, the catalytic subunits can phosphorylate cAMP response element binding protein (CREB) and thus regulate gene expression. Down regulation of PKA occurs by a feedback mechanism: PKA can phosphorylate PDEs inducing them to quickly hydrolyze cAMP. Therefore they reduces cAMP levels that can in turn activate PKA.

Exchange protein directly activated by cAMP (Epac) is a guanine nucleotide exchange factor directly activated by cAMP. In the rat nervous system Epac exists in two isoforms, Epac1 and Epac2, whose structure differs only in that Epac2 contains two instead of one cAMP binding sites. The expression of Epac is developmentally regulated: Epac1 is highly expressed at embryonic and neonatal stages of development, while Epac2 is dramatically up regulated in adult cells (Murray and Shewan, 2008).

1.1.4.4 Methods for measuring cAMP dynamics

Alterations in intracellular cAMP levels govern fundamental metabolic, electrical, cytoscheletal and transcriptional responses within cells. In the past, cellular cAMP levels have been measured in cell lysates by radioimmuno assays (RIAs). Such an approach estimated total cAMP rather than free cAMP and offered very poor temporal resolution and no spatial resolution. Therefore it was inadequate to study the fine details of cAMP signalling.

Subsequently, the development of new technologies based on the green fluorescent protein (GFP) and FRET (Fluorescence Resonance Energy Transfer) has introduced a new perspective in the study of cAMP signalling. Indeed, real - time imaging of fluorescent biosensors made it possible to visualize cAMP dynamics directly as they happen in intact, living cells. In these genetically encoded sensors, the FRET between the two fluorescent moieties is dependent on the levels of cAMP. FRET is a physiochemical phenomenon describing energy transfer between two chromophores, called donor and acceptor. The two chromophores are chosen so that the donor emission

spectrum overlaps with the acceptor absorption spectrum (Figure 7). Thus, the excited – state energy of a donor fluorophore is directly transferred to an acceptor molecule, which can then emit its own characteristic fluorescence. However, FRET efficiency is strictly dependent on the distance between the donor and the acceptor, and the optimal distance is typically in the range of 1 – 10 nm.

FRET efficiency (E) is described by Förster equation:

$$E = \frac{1}{1 + (r/R_0)^6}$$

where *r* is the donor – acceptor distance and R_0 is the Förster distance, where the energy transfer efficiency is 50%. Therefore, when *r* is doubled to *2r*, the efficiency moves from E = 50% to E = 1,5%. Thus, FRET is highly sensitive to intramolecular distances and conformational changes. Generally, the two essential components of a FRET – based indicator include: (i) a sensor, which may consist of two interacting protein domains or a protein domain undergoing a conformational change upon ligand binding and (ii) a donor and an acceptor chromophores fused to the sensor.

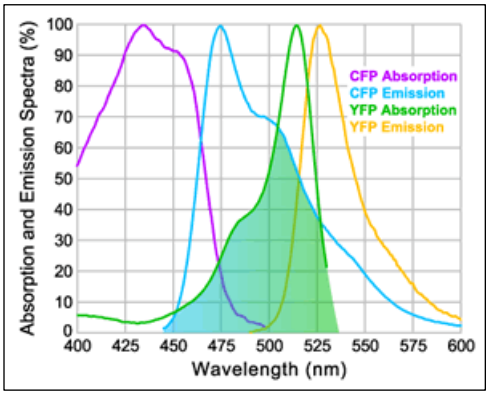

Figure 7: adsorption and emission spectra of CFP and YFP fluorophores. In green is represented the overlapping area between CFP emission and YFP adsorption spectrum.

Zaccolo and coll. (2000) created one of the first genetically encoded sensor for cAMP. This sensor, characterized by high spatial and temporal resolution, represented a breakthrough in the field of second messenger intracellular signalling, since it allowed to begin to monitor cAMP levels *in vivo*, with high

spatial and temporal resolution. This genetically encoded sensor relies on FRET and is based on PKA.

In this project we used two different probes: the first based on PKA, and the second one on Epac. As well known, both proteins represent cAMP targets.

As mentioned before, PKA is a tetrameric enzyme constituted by two catalytic subunits (C) and two regulatory ones (R). The sensor has been genetically modified so that two appropriate mutants of green fluorescent protein (GFP) have been fused to PKA subunits and they can be used as donor and acceptor chromophores. In particular, cyan fluorescent protein (CFP) is fused to the regulatory subunit, while yellow fluorescent protein (YFP) is fused to the catalytic one. In conditions of low cAMP, the PKA sensor is in its inactive holotetrameric conformation and FRET is maximal. Upon excitation of the donor CFP at its proper excitation wavelength (430 nm), part of its excited – state energy is transferred to the acceptor YFP that then emits at its own wavelength (545 nm). When cAMP rises, it binds to R, inducing a conformational change that releases active C. Thus, CFP and YFP diffuse apart and FRET is abolished (Figure 8).

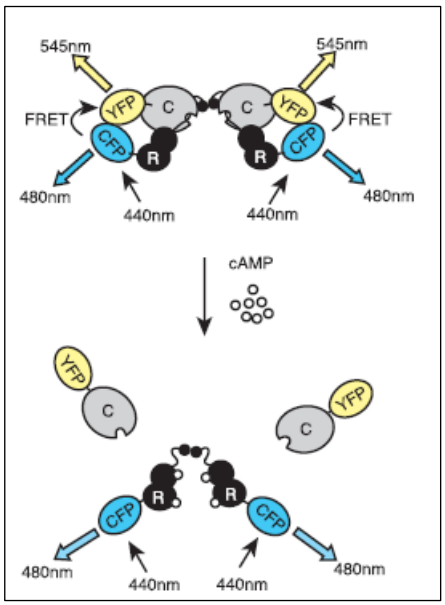

Figure 8: schematic illustration of the genetically encoded cAMP sensor, based on PKA. R and C subunits of PKA have been fused to CFP and YFP, respectively. At low cAMP levels, subunits are associated and FRET occurs. At higher cAMP levels, R and C diffuse apart and FRET is abolished. Thus, 545 nm emission decreases and CFP/YFP ratio increases. (Zaccolo and Pozzan 2002)

FRET can be easily monitored as the ratio of donor (480 nm) over acceptor emission (545 nm) intensities. Changes in the fluorescence ratio (480 nm / 545 nm) are directly correlated to changes in C and R subunits association and thus correspond to changes in cAMP levels (Zaccolo and Pozzan 2002).

A second type of sensor is based on Epac. As mentioned before, Epac is a guanine nucleotide exchange factor (GEF) and it acts on Rap1 and Rap2. Rap GTPases cycle between an inactive GDP – bound and an active GTP – bound state, through the action of GEF proteins which exchange GDP with GTP. Epac probe consists of a C – terminal catalytic domain and an N – terminal regulatory domain, which contains a cAMP – binding site similar to those of PKA. Moreover, it includes a DEP domain that mediates membrane attachment. At low cAMP levels, Epac is folded in an inactive conformation, thus preventing Rap binding due to the steric restraint. When cAMP level increases, it binds Epac and unfolds it, allowing Rap to bind. Epac1 probe we used, is sandwiched between CFP and YFP and displays a significant energy transfer (Figure 9). Compared with PKA sensor, Epac – based cAMP indicator outperforms the first one in several aspects (Ponsioen et al., 2004).

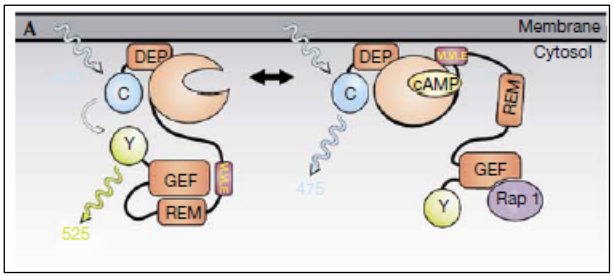

Figure 9: schematic representation of Epac1 – based cAMP sensor. N – and C – termini are fused to CFP and YFP, respectively. At low cAMP levels, the sensor is in its inactive conformation and the two fluorophores are sufficiently close to have FRET. Upon binding cAMP, the probe assumes an extended conformation, CFP and YFP diffuse apart and FRET is abolished. (Ponsioen et al., 2004)

1.1.5 Methods for measuring Ca^{2+} dynamics in the olfactory sensory neurons

Changes in calcium levels inside the cells are measured with Ca^{2+} indicators, which are high selective fluorescent molecules capable of responding to the local calcium concentration by changing their fluorescent properties.

Two main classes of calcium indicators exist: chemical indicators and genetically encoded calcium sensors. In order for a fluorescent probe to provide

useful information about its environment, it is necessary that its fluorescent properties change in a suitable manner in response to changes in the parameter to be measured. Thus, any one of the following three property changes are appropriate: a change in fluorescent yield, a shift in the excitation or emission spectrum and finally a combination of the two. Chemical indicators are small molecules able to chelate Ca^{2+} ions. They are based on BAPTA, a pH – sensitive evolution of the widely used Ca^{2+} - selective EGTA. EGTA is related to EDTA but it exhibits a higher affinity for Ca^{2+} than for Mg^{2+}. All such chemical indicators share a modular design consisting of a metal – binding site (sensor) coupled to a fluorescent dye. This group of indicators includes Fura – 2, Indo – 1, Fluo – 3, Fluo – 4 and Calcium Green. They are generally used with the chelator carboxyl groups masked as acetoxymethyl esters, which render the molecule lipophilic and allow their easy entrance into the cell. Once the indicator is inside the cell, the cellular esterases free the carboxyl and the indicator is able to bind Ca^{2+}. Binding of Ca^{2+} to a fluorescent indicator leads to either an increase in quantum yield of fluorescence or emission/excitation wavelength shift. In our project we used Fura – 2 AM calcium indicator (Figure 10), a ratiometric fluorescent dye which binds to free intracellular calcium. Fura – 2 is excited at 340 nm (calcium bound) and 380 nm (calcium free) and it emits at 510 nm. Upon binding Ca^{2+}, Fura – 2 exhibits an adsorption shift that can be observed by scanning the excitation spectrum between 300 and 400 nm, while monitoring the emission at 510 nm. The ratio of the emissions at those wavelengths is directly correlated to the amount of intracellular calcium. Moreover, the use of the ratio automatically cancels out confounding variables, such as variable dye concentration, cell thickness and photobleaching problems. Fura – 2 has become the dye of choice for ratio – imaging microscopy, in which it is more practical to change excitation wavelength than emission wavelength.

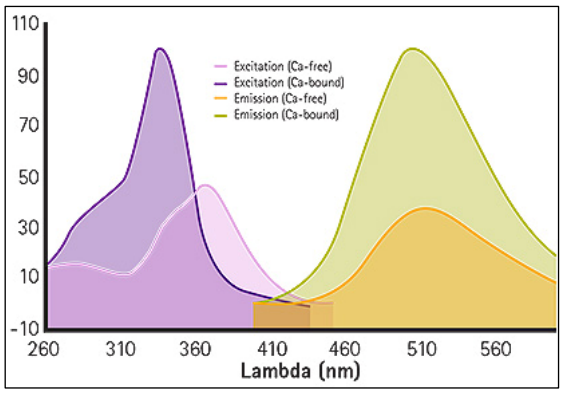

Figure 10: emission and absorption spectra of Fura – 2 AM calcium indicator. Fura – 2 is excited at 340 nm (calcium bound) and 380 nm (calcium free), and it emits at 510 nm.

However, small – molecule indicators have many drawbacks that prevent their applicability in neuroscience for a wide variety of questions. For instance, they cannot be easily targeted to specific cell types, populations, or subcellular locations. For these purposes, genetically encoded calcium sensors (i. e. GCaMP, Pericams and Cameleons) have been generated. They allow to address many of chemical indicators limitations and provide an alternative to small – molecule calcium dyes. Indeed, they can be targeted to specific cell types, populations or subcellular compartments allowing the imaging of structures such as synapses, axons and dendrites. These indicators are fluorescent proteins derived from green fluorescent protein (GFP) or its variants (e. g. YFP, CFP) fused with calmodulin (CaM) and the M13 domain of the myosin light chain kinase, which is able to bind CaM. These sensors are genetically encoded without cofactors and are targetable to specific intracellular locations.

1.1.6 Metabolism and effectors of cGMP

1.1.6.1 cGMP in olfactory sensory neurons

Cyclic GMP levels are generally regulated by two distinct classes of guanylyl cyclases (GCs): soluble (sGCs) and particulate GCs (pGCs). Soluble GCs are activated by gaseous messengers, such as NO and CO. Particulate GCs are activated by either extracellular ligands or Ca^{2+} and Ca^{2+} - binding proteins, on

the intracellular side. Both GCs are expressed in the olfactory sensory neurons (Moon et al., 1998).

NO and CO are synthesized by nitric oxide synthase (NOS) and heme oxygenase (HO), respectively. **Nitric oxide synthase** is transiently expressed in developing and regenerating olfactory sensory neurons and its expression rapidly declines after birth becoming entirely absent by postnatal day 7. Thus, NO – mediated cGMP signals could be involved in the proliferation or maturation of developing and regenerating olfactory sensory neurons (Ingi and Ronnett, 1995, Moon et al., 2005). Experimental evidences demonstrated that NO not only promotes basal cell proliferation, but is also involved in the formation of synaptic connections both during embryonic development and continuous neurogenesis occurring in this type of neurons. NOS null mice indeed exhibit an alteration in the turnover of the olfactory sensory neuron population (proliferation and cell death) and in the glomerular formation (Roskams et al., 1994, Chen et al., 2004). Van Wagenen and coll. (1999) investigated the effects of NO on the axon guidance processes in *Helisoma Trivolvis.* They demonstrated that NO donors elicited rapid filopodial elongation and a reduction in the number of filopodia on growth cones. To better elucidate NO effects on growth cones, inhibitors of GCs have been used and in these conditions NO effects were completely abolished. Moreover, a direct cGMP injection in the olfactory sensory neurons mimicked the effects of NO donors on filopodia. These cGMP injections promoted a rapid and transient Ca^{2+} rise in the growth cones, suggesting that NO action is mediated by cGMP through its action on CNG channels. This hypothesis has been also corroborated by a cGMP analogue administration, which induced a Ca^{2+} increase in the axon terminal. Thus, NO could function, via cGMP, as a messenger to influence the growth cone's navigational tasks by modifying its action radius (Kafitz et al., 2000). **Heme oxygenase** is highly expressed in adult, suggesting a possible role of CO – induced cGMP signals in the odor – mediated events (Moon et al., 2005). Two isoforms of HO have been identified: HO – 1 and HO – 2. The first one is an heat – shock protein mostly abundant in spleen and liver, while HO – 2 is expressed at high levels in the brain, in the olfactory sensory neurons and in the granule cell layer of the olfactory bulb (Ingi and Ronnett, 1995). Biochemical studies have shown a decrease in cGMP levels when the HO

activity was abolished by ZnPP - 9 and ZnBG, while no alterations were detectable when NOS was inhibited. Therefore, CO may be a physiological mediator of the changes in endogenous cGMP levels (Ingi and Ronnett, 1995). To support the physiological role for CO in the olfactory sensory neurons, *in situ* hybridization assays for HO – 2 and soluble GCs demonstrated that these two enzymes colocalize in large degree (Verma et al., 1993, Ingi and Ronnett, 1995). However, when HO – 2 inhibition is achieved, cGMP synthesis in olfactory sensory neurons is not completely abolished. This result suggests that also particulate GCs could be involved in the basal production of this second messenger, although the mechanisms underlying this process are still unknown. A unique subset of olfactory sensory neurons expresses the orphan GC – D, suggested to respond to hormones and pheromones. This small population of neurons is located within a single topographic zone in the olfactory epithelium (Kuhn et al., 2003). GC – D expressing olfactory sensory neurons lack of the canonical components of the odor signal transduction, including G_{olf}, ACIII, Ca^{2+} - calmodulin – dependent PDE1C, cAMP – specific PDE4A, CNG channel subunits CNGA2 and CNGB1b. Instead, these neurons express a cGMP – specific CNG channel subunit (CNGA3) and a cGMP – stimulated PDE (PDE2). Finally, GC – D expressing olfactory sensory neurons project their axons to a distinct group of glomeruli, known as necklace glomeruli. These results suggest that GC – D expressing olfactory sensory neurons may use a different signalling pathway respect to the canonical one (Golf → ACIII → cAMP) and participate in the transduction of different environmental stimuli (Leinders – Zufall et al., 2007, Juilfs et al., 1997).

Cyclic GMP is also implicated in the odorant response. This second messenger and its effectors are indeed implicated in several aspects of olfaction. It has been demonstrated that odorants increase cGMP levels in isolated olfactory cilia (Moon et al., 1998) and inhibition of GCs completely abolishes these responses in cultured olfactory sensory neurons (Moon et al., 2005). Due to its slow kinetics, cGMP is thought to participate to adaptation (Leinders – Zufall et al., 1996, Zufall and Leinders – Zufall, 1998) and long term response to odor stimulation. But what is the mechanism underpinning cGMP synthesis upon odorant stimulation? Odor – induced cGMP increase is abolished when NOS is selectively inhibited. According to the first proposed model explaining this

mechanism, odor – induced Ca^{2+} signal may mediate the activation of NOS; NO, in turn, may activate soluble GCs. However, NOS is expressed in developing and regenerating neurons, but not in mature ones, so NO is not likely to activate soluble GCs in odor – responsive olfactory sensory neurons. Therefore, the other gaseous messenger, CO, was investigated (Moon et al., 2005). Several studies suggest that the major regulator of intracellular cGMP levels in olfactory sensory neurons is soluble GC activated by CO (Verma et al., 1993, Ingi and Ronnett 1995, Leinders – Zufall et al., 1995) .

Although the majority of the cGMP pool is contributed by soluble GCs, a consistent amount is generated by particulate GCs. A likely site for this activity are the olfactory cilia. Indeed, isolated olfactory cilia are responsive to odors and express high levels of particulate GCs. Although most particulate GCs are activated by extracellular ligands, the olfactory form may be more similar to retinal GCs, which are regulated by a guanylyl cyclase – activating protein (GCAP).

Odor – induced cGMP signal is characterized by two important properties:

- its formation depends on the stimulus strength and only occurs with stronger odor stimuli;
- cGMP build-up is slow, reaches only low levels and is sustained over time (Breer et al., 1993).

These characteristics suggest that the odor – induced cGMP increase is not involved in initial signaling events but rather in adaptation and in other long - term responses (Moon et al., 1998, Moon et al., 1999). Odorant adaptation begins at the level of olfactory sensory neurons and it refers to the ability of the olfactory system of regulating its responsiveness depending on the stimulus strength. This mechanism prevents the saturation of the signal transduction system and allows the olfactory sensory neurons to preserve their high sensitivity, in spite of continuous and repeated stimuli. In olfactory sensory neurons, adaptation processes occur through modulation of their transduction machinery. It has been reported that the Ca^{2+} signal mediates both signaling transduction and adaptation. Indeed, Ca^{2+} - calmodulin complex changes the affinity of CNG channels for their ligands and this phenomenon is known as short term adaptation. Farther, cGMP is able to modulate CNG channels itself. Low concentrations of 8 – Br – cGMP (a membrane permeable cGMP

analogue) are sufficient to down – regulate the sensitivity of olfactory sensory neurons to their natural stimuli causing a sustained Ca^{2+} influx through CNG channels (Leinders – Zufall et al., 1996). This kind of adaptation is known as long – lasting adaptation (LLA) and is induced by tonic activation of CNG channels. LLA is associated with a persistent background Ca^{2+} current through CNG channels (Zufall et al., 1997). Ca^{2+}, in turn, modulates cAMP – dependent signal transduction cascade, reducing olfactory sensory neurons responsiveness to odorant stimuli (Leinders – Zufall et al., 1997). LLA is abolished when CO production is inhibited by ZnPP – 9 (HO inhibitor) and this result supports the additional role for CO in odorant adaptation. However, is not known the mechanism linking the physiological odorant stimulation to the CO endogenous synthesis and how a gaseous messenger can modulate the adaptation of the same cell within which it is produced.

1.1.6.2 cGMP in the axon guidance processes

It is known that cGMP levels at the axon terminal influence the response of the growth cone to several axon guidance cues. It has been demonstrated that in cultured *Xenopus* spinal neurons, a microscopic gradient of Semaphorin III induced a repulsive effect on the growth cone of these neurons. However, when a cGMP agonist (8 – Br – cGMP) was applied, nearly all growth cones displayed an attractive behavior toward the Sema III gradient and the same effect has been observed after a treatment with a GC activator. Thus, the levels of cGMP can regulate the direction of growth cone turning in response to the same gradient of an axon guidance molecule, i.e. Sema III (Song et al., 1998).
Subsequently, Nishiyama and coll. (2003) investigated the response of *Xenopus* spinal neurons toward a Netrin1 gradient. They demonstrated that the turning responses correlated with the ratio of cAMP and cGMP signaling: a high ratio favoured attraction, whereas a low ratio favoured repulsion. How do cAMP and cGMP signaling pathways modulate Netrin1 signals? It has been previously demonstrated (Hong et al., 2000) that in *Xenopus* neurons, Netrin1 – induced attraction requires Ca^{2+} entry through voltage – dependent channels, including LCCs. These channels are known to be activated by cAMP but inactivated by cGMP signaling pathways. Ca^{2+} levels also regulate growth cone's responses to the guidance cues. For example, in *Xenopus*, low Ca^{2+} levels abolish Netrin1 –

mediated responses of the growth cone (Ming et al., 1997). Ca^{2+} can achieve its function at both the growth cone through local mechanisms, and at a nuclear level regulating the genetic expression. The levels of these second messengers can be modulated by neuromodulators, neurotransmitters, as well as by spontaneous and evoked activity. Thus, a complex network of modulations is exerted on these second messengers, which in turn act on multiple targets.

1.1.6.3 Methods for measuring cGMP dynamics

In the past, cGMP levels have been measured through radioimmunoassay technique, which allows their measurement in small amounts of tissue despite their presence in very low concentrations. However, this technique shows an important limitation: the measurement of cGMP can be done only on fixed and lysate cells. Therefore, it doesn't give any information on spatial and temporal dynamics of cGMP in living cells.

In order to measure cGMP levels with a high spatial and temporal resolution, genetically encoded sensors for cGMP have been generated. These sensors allow to investigate spatio – temporal dynamics of cGMP and they are based on the fluorescence resonance energy transfer (FRET) principle (see 1.1.4.4 chapter). At present, several genetically encoded sensors for cGMP are available and they are based on cGMP – binding domain B from cGMP – dependent protein kinase I (GKI) or on the regulatory domain from PDEs.

These new sensors respond to cGMP changes with a decrease (GKI construct) or increase (PDE construct) in FRET.

In our project we used Cygnet 2.1 sensor, which is characterized by a high cGMP selectivity (Figure 11)(Nikolaev et al., 2006, Honda et al., 2001).

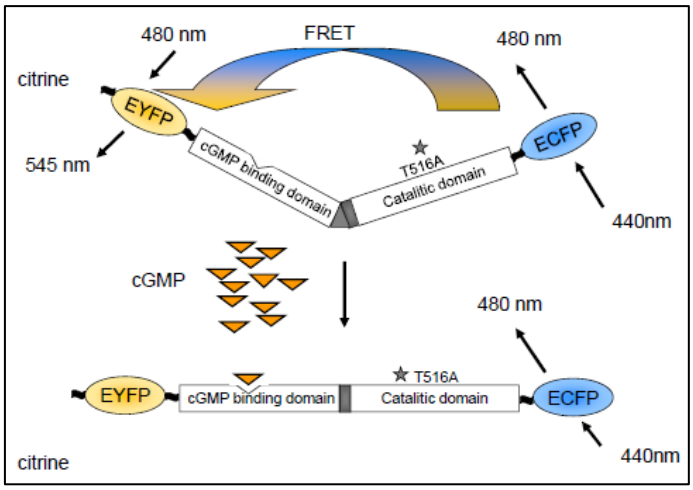

Figure 11: schematic representation of PKG - based cGMP sensor, Cygnet 2.1.

Cygnet 2.1 probe is constituted by PKG lacking of 1 – 77 residues and sandwiched between CFP and YFP. This sensor shows a cytosolic localization and is enzimatically inactive due to a Thr^{516} - Ala mutation within the catalytic site. Cygnet 2.1 is a monomolecular probe, is highly selective for cGMP (cGMP/cAMP selectivity > 600) and sensitive to cGMP changes (K ½ 1.7 μM). At low cGMP levels, Cygnet 2.1 appears in a conformation in which CFP and YFP are close to each other. Indeed, when the donor CFP is excited at its proper wavelength (430 nm), a part of its excited – state energy is transferred to the acceptor YFP, that in turn emits at its proper wavelength (545 nm). In these conditions FRET is maximal. When cGMP increases, it binds to the regulatory site of the probe inducing its conformational change: CFP and YFP diffuse apart and FRET is abolished. FRET can be easily monitored as the ratio of donor (480 nm) over acceptor emission (545 nm) intensities, when the cells are excited at donor wavelength (430 nm). Finally, changes in fluorescence ratio (480 nm / 545 nm) are directly correlated to changes in intracellular cGMP level.

1.1.7 The olfactory bulb

The olfactory bulb is a part of the vertebrate forebrain and it consists of two symmetrical ovoid structures immediately localized above the nasal cavities in rodents. As other cerebral areas, it consists of three different types of neurons: afferent neurons, efferent neurons and interneurons. The afferent neurons are the olfactory sensory neurons, which constitute the sensory afferences to the olfactory bulb. Their amyelinic and unbranched axons (0.2 μm of diameter) pass

through the cribriform plate and reach the olfactory bulb (Figure 12). The mitral and tufted cells represent the projection neurons (the efferent neurons) of the olfactory bulb while periglomerular and granule cells represent the interneurons of the olfactory bulb .

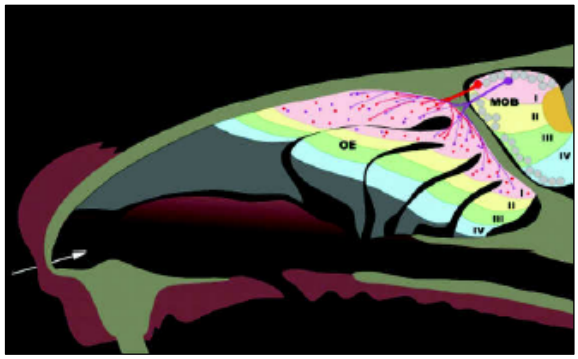

Figure 12 : sagital view of a mouse head. The arrow indicates the entering point of the air containing the odorant molecules. The olfactory epithelium (OE) covers the turbinates and is subdivided into four zones, represented with different colours. The axons of olfactory sensory neurons project to the olfactory bulb (OB), where they converge to form glomeruli. (Firestein 2001)

These different cells types are distributed in specific layers. The olfactory bulb indeed exhibits a typical laminar structure, in which different layers can be easily identified, from the surface to the centre: the olfactory nerve layer (ONL), the glomerular layer (GL), the external plexiform layer (EPL), the mitral cell layer (MCL),internal plexiform layer (IPL) and the granule cell layer (GCL)(Figure 13). In turn, each layer consists of different cell types.

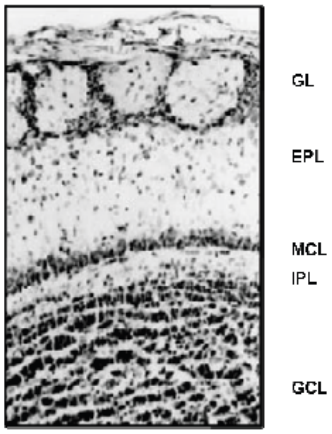

Figure 13 : olfactory bulb (OB) section after Nissl staining. It is possible to distinguish the different layers composing the OB: glomerular layer (GL), external plexiform layer (EPL), mitral cell layer (MCL), internal plexiform layer (IPL) and granule cell layer (GCL).

The **olfactory nerve layer** is composed by the axons of the olfactory sensory neurons. They pass through the basal lamina, within the olfactory epithelium, and then they cross the cribriform plate to finally reach the olfactory bulb.

Within the **glomerular layer**, the axons of the olfactory sensory neurons form excitatory synapses on the dendrites of the post synaptic neurons of the olfactory bulb, namely the mitral, the tufted and the periglomerular cells. These synaptic contacts form the glomeruli. Glomeruli are spherical structures of neuropil (with a diameter in the range of 50 – 100 μm in mice) localized on the surface of each olfactory bulb. Each glomerulus results from the synapses between the axons of the olfactory sensory neurons expressing the same odorant receptor and the related postsynaptic cells, namely periglomerular, mitral and tufted cells. Each glomerulus is also surrounded by glial cells (Mori et al., 1999).

Periglomerular cells and **granule cells**, represent the interneurons of the olfactory bulb. They both regenerate constantly and originate from the subventricular zone, around the lateral ventricles. They migrate through the rostral migratory stream to reach the olfactory bulb. Once they arrive into the olfactory bulb, they migrate radially and differentiate into mature interneurons. Periglomerular cells include different cellular types, such as periglomerular cells, short axon cells and external tufted cells. These cells not only form synapses with dendrites of mitral and tufted cells, but also with the terminal axons of the olfactory sensory neurons. Periglomerular cells constitute a morphologically and biochemically heterogeneous population. They use different types of neurotransmitters, such as GABA, nitric oxide, NADPH, dopamine and neuropeptide Y. Their synapses with both pre – and post – synaptic cells in the olfactory bulb exert a modulatory effect, although their exact role remains to be understood (Shipley and Ennis 1996).

The **external plexiform layer** lies immediately below the glomeruli. It primarily consists of a dense neuropil formed by the mitral (M)/tufted (T) cell dendrites and GABAergic granule cell dendrites, which ascend into the external plexiform layer from the deeper, mitral cell and granule cell layers, respectively. Within the external plexiform layer, the lateral dendrites of the mitral and tufted cells synapse with the granule cell dendrites (Hamilton et al., 2005).

Mitral and tufted cells represent the output neurons of the olfactory bulb and they constitute the efferent pathway forming the lateral olfactory tract. Tufted cells are a more heterogeneous population divided in external, medial and internal, according to the location of the cell body. Both mitral and tufted cells possess a single primary dendrite, which enters one single glomerulus, where it forms an extended harborization. Both mitral and tufted cells present secondary dendrites which horizontally extend into the external plexiform layer and form dendro – dendritic synapses with granule cells. The axons of mitral and tufted cells exit the olfactory bulb and constitute the lateral olfactory tract, sending the information to the olfactory cortex. External tufted cells (ETCs) belong to the interneurons family. Even biochemically, external tufted cells represent an heterogeneous population of cells, using several types of neurotransmitters, such as cholecystokinin (CCK), GABA, corticotrophin – releasing factor (CRF), and vasoactive intestinal peptide (VIP).

The **mitral cell layer** is a single layer composed by the cellular bodies of glutamatergic mitral cells.

The **internal plexiform layer** is a thin layer, below the mitral cell layer, composed by few cellular bodies, which mainly belong to granule cells and short axon cells and axons of external tufted cells, mitral and tufted cells.

Finally, the **granule cell layer** is located immediately under the internal plexiform layer, in the central part of the olfactory bulb. It contains the cellular bodies of the granule cells. Granule cells are GABAergic interneurons lacking the axon. They form inhibitory synapses on the lateral dendrites of mitral and tufted cells (Figure 14)(Shipley et al., 1996).

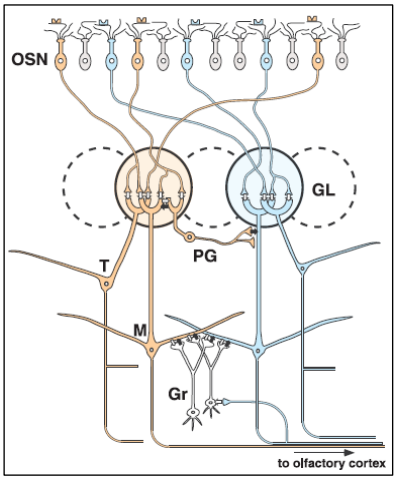

Figure 14 : basic circuit diagram summarizing the synaptic organization of the mammalian olfactory bulb. Two glomerular modules (blue and brown) represent two different types of odorant receptors. Mitral cells (M) and tufted cells (T) are output neurons, granule cells (Gr) and periglomerular cells (PG) are local interneurons. (Mori et al., 1999)

1.1.8 The sensory map

Sensory systems represent the interface between the external and the internal world. In the vertebrate sensory systems, peripheral neurons project to specific loci of the brain to give rise to topographic maps, i.e., sensory maps. A sensory map refers to an orderly representation of some physical features of the outside world.

The olfactory system differs somehow from this general scheme of organization due to the lack an orderly representation of receptor cells in the periphery. Olfactory sensory neurons expressing the same olfactory receptor are confined within a broad but circumscribed area of the epithelium (Ressler et al., 1993, Vassar et al., 1993, Serizawa et al., 2004, Serizawa et al., 2005). However, within a given zone, neurons expressing different olfactory receptors intermingle, showing a widely dispersed distribution (Ressler et al., 1993, Vassar et al., 1993, Serizawa et al., 2004, Serizawa et al., 2005). Odorant receptors with highly homologous amino acid sequences tend to be localized within the same zone of the olfactory epithelium (Mori et al., 1999). Although the olfactory epithelium presents only a coarse organization, a highly specific spatial order is achieved in the olfactory bulb, where a proper topographic map can be observed. The axons of sensory neurons expressing the same odorant receptor converge with extreme precision to form glomeruli in specific loci, both

on the medial and the lateral side of each olfactory bulb. Each glomerulus defines a functional unit, so called “odor column”, by analogy with the ocular dominance and orientation columns of the primary visual cortex. Each odor column consists of the mitral, tufted and periglomerular cells receiving input from a specific group of olfactory sensory neurons, along with the granule cells connected to those cells. The odor columns associated with the same olfactory receptor are known as isofunctional odor columns (Shepherd 1998).

In 1996, Moamberts and coll., developed an elegant genetic approach to “visualize the olfactory map”. In this classic study, the P2 receptor was genetically modified to co – express a tau – LacZ reporter. Thus, after X – gal staining, olfactory sensory neurons expressing P2 receptor could be easily visualized in their entire morphology, from the cilia to the axon terminal (Figure 15). In these “P2 – LacZ” mice, the P2 – expressing axons converge in a specific location to form P2 – glomeruli on the medial and the lateral sides of each olfactory bulb. In this way, olfactory sensory neurons expressing a given receptor can be identified within the olfactory epithelium and olfactory bulb. This approach allowed to visualize the olfactory map within the olfactory bulb .

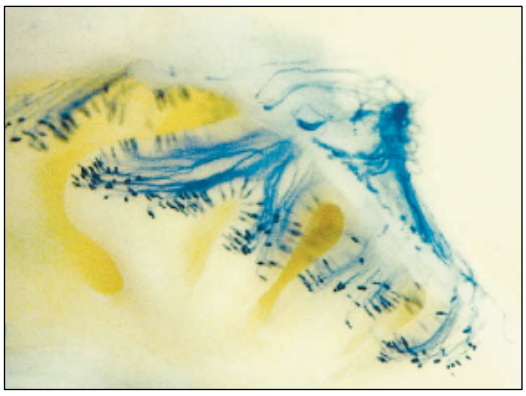

Figure 15 : whole mount view of turbinates and medial side of bulb in a P2 – IRES – tau – LacZ transgenic mouse, after X – gal staining. All olfactory sensory neurons expressing P2 receptor also express tau – LacZ and are thus easily visible in blue. Blue axons can be seen at the level of the olfactory epithelium projecting toward a single glomerulus in the medial side of the olfactory bulb. (Mombaerts et al., 1996)

Subsequently, tau – LacZ marker has been replaced with the green florescent protein (GFP), whose visualization is possible in living animals (Treolar et al., 2002).

As a result of the initial sensory projections, each olfactory bulb presents two mirror symmetric maps of homologous glomeruli. It has been demonstrated that the isofunctional odor columns are specifically and reciprocally

interconnected through a mutually inhibitory circuit with excellent topographic specificity, related to the external tufted cells (Lodovichi et al., 2003). In the intrabulbar link, axons of external tufted cells form a projection just underneath the homologous glomerulus on the opposite side of the bulb, in the internal plexiform layer. At this level, the axons of the external tufted cells form excitatory synapses on the dendrites of the granule cells. These granule cells, in turn, form inhibitory synapses on the external tufted cells connected to the homologous glomerulus (Figure 16). This connection is reciprocal.

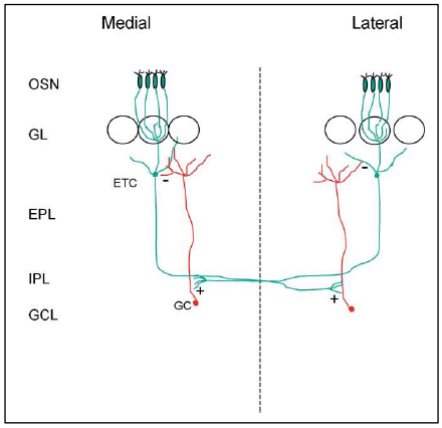

Figure 16: schematic representation of the inhibitory circuit connecting isofunctional odor columns in the two halves of each bulb. Axons of external tufted cells (ETC), connected to a given glomerulus, form excitatory synapses (+) onto the dendrites of the granule cells (GC) in a restricted region of the internal plexiform layer (IPL) on the opposite side of the bulb. These GC, in turn, form inhibitory synapses (-) on the ETC connected to the homologous glomerulus. This connection is reciprocal. GL, glomerular layer; EPL, external plexiform layer; GCL, granule cell layer. (Lodovichi et al., 2003)

The olfactory bulb presents therefore two levels of topographic organization: i) the sensory map, that results form the convergence of olfactory sensory neurons expressing the same odorant receptor to form glomeruli on the medial and on the lateral side of each olfactory bulb; ii) the intrabulbar link, that specifically and reciprocally connects homologous (i.e. isofunctional) glomeruli (Lodovichi et al., 2003).

It is worth noticing that a certain correlation between the location of the olfactory sensory neurons in the epithelium and the location of the corresponding glomeruli in the olfactory bulb is maintained (Figure 17). For instance, olfactory sensory neurons located in the dorsal part of the olfactory epithelium form glomeruli in the dorsal region of the olfactory bulb. Whereas, olfactory sensory

neurons ventrally located in the olfactory epithelium, project their axons to the ventral area of the olfactory bulb (Mori et al., 1999).

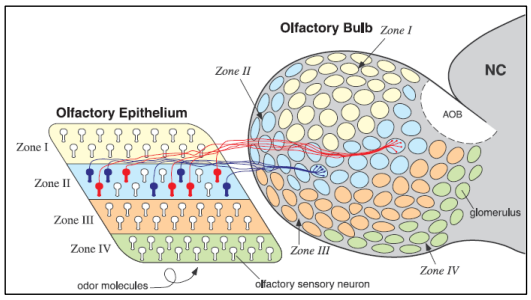

Figure 17: schematic diagram illustrating the axonal connectivity pattern between the olfactory epithelium (OE) and the olfactory bulb (OB). The OE in mice is divided into four zones, that are defined by the expression of odorant receptors. Olfactory sensory neurons (OSNs) in a given zone of the OE project to glomeruli located in a corresponding zone of the OB. Axons of ONSs expressing the same receptor (red or dark blue) converge to only a few defined glomeruli. NC, neocortex; AOB, accessory olfactory bulb. (Mori et al., 1999)

Not only the homologous glomeruli in the same olfactory bulb are interconnected but also the isofunctional glomeruli located in the two olfactory bulbs are linked to each other (Yan et al., 2008). It is known that a cortical area, called anterior olfactory nucleus, contains neurons that project to the controlateral olfactory bulb. Within the anterior olfactory nucleus, the anterior olfactory nucleus pars externa, receives inputs from the ipsilateral olfactory bulb and projects exclusively to the granule cell layer of the controlateral olfactory bulb. Thus, it forms an interbulbar association system.

1.1.8.1 Development of the sensory map in the olfactory bulb

The formation of glomeruli in specific loci of the olfactory bulb, i.e. the sensory map, is the result of a developmental process. Initially, axons expressing the same odorant receptor terminate in a rather broad but circumscribed area on the surface of the olfactory bulb. Only postnatally they segregate into completely distinct glomeruli (Strotmann et al., 2006). During early stages of development, in both medial and lateral side of each bulb, some glomeruli are innervated by axons of neurons that do not express the same receptor (heterogeneous glomeruli). Through the rearrangement and removal of “wrong” axonal projections, these heterogeneous glomeruli normally disappear with age.

To clarify the process that leads to the formation of glomeruli, here I report the development of two different types of glomeruli innervated by olfactory sensory neurons expressing different receptors.

P2 expressing axons project to the nerve fiber layer at E14.5. By E15.5 these axons penetrate the underlying glomerular layer in which they terminate diffusely. By E18.5, P2 axons form two to three tufts that are interconnected by bundles of axons. Between E18.5 and PD7.5, these tufts either condensed and form a single glomerulus or instead separate into two discrete glomeruli that are connected by a bundle of axons. By PD14.5 all interconnected glomeruli are separated and form discrete glomeruli. Thus, discrete P2 glomeruli emerge slowly and the navigational errors occur for up to 10 days of development (Royal and Key 1999).

The axons of olfactory sensory neurons expressing M71 and M72 receptors start forming proto – glomeruli only in the first postnatal days, PD2 – PD3. By PD10, M71 and M72 glomeruli can be clearly identified, but they are often multiple, at either the medial or lateral half – bulbs. However, between PD10 and PD40, a progressive removal of supernumerary glomeruli is achieved and by PD40 single glomeruli are generally observed in both the medial and lateral half – bulbs. It is important to note that M72 glomeruli can be initially innervated also by M71 - positive axons. Indeed, M71 and M72 receptors are highly homologous, with 96% identity in their amino acid sequences. However, during development, multiple glomeruli are removed.

1.1.9 Axon guidance process: the growth cone

In the central nervous system the formation of precise neural circuits depends on the correct pathfinding and target recognition by the growing tip of an axon, the so called growth cone. Growth cones are characterized by a high motility, which allows them to respond to the surrounding environment by rapidly changing direction and branching in response to various stimuli. Each growth cone presents two kinds of structures: filopodia and lamellipodia. **Filopodia** are fine extensions of the growth cone and they contain bundles of actin filaments (F – actin). They are bound by membrane which contains receptors and cell adhesion molecules that are important for axon growth and guidance. **Lamellipodia** are flat regions of dense actin network and they are located

between filopodia. In growth cones, new filopodia usually emerge from these inter – filopodia veils. The actin network is also associated with microtubules, which transiently enter the growth cone. The growth cones motility is due to their continuous build - up through the extension of the plasma membrane and construction of actin microfilaments. Indeed, the actin filaments continuously polymerize and depolymerize within filopodia and lamellipodia. These constant changes in the cytoskeleton structure depend on the activity of important regulators, called Rho proteins, belonging to the GTPases family (Figure 18). Developing axons are guided to their targets by extracellular cues, i.e., axon guidance molecules. These molecular cues can be in the form of diffusible or substrate – bound molecules. They can exert on the growth cone an attractive or a repulsive effect, depending on the intracellular pathways they trigger. These pathways regulate cytoskeletal components and therefore influence the direction of growth cone extension (Ming et al., 1997, Dontchev and Letourneau 2002).

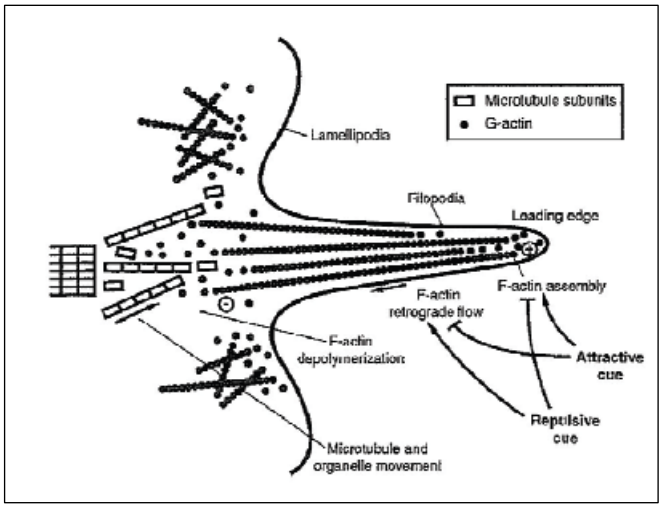

Figure 18: schematic representation of a growth cone. Lamellipodia contain a dense actin network, while filopodia motility depends on a continuous polymerization and depolymerization of F – actin filaments. (Huber et al., 2003)

1.1.9.1 Role of Ca^{2+} and cAMP in the axon guidance

Ca^{2+} plays an important role in the axon guidance processes. It has been reported to have many effects on the growth cones of the extending axons, that depend on several factors, including the spatio - temporal characteristics of the Ca^{2+} changes, the Ca^{2+} effectors present in the domain of elevated Ca^{2+} and

possibly the particular Ca^{2+} channel types involved in generating Ca^{2+} changes. After Ca^{2+} enters the cytosol, it acts on specific downstream Ca^{2+} - binding partners and subsequent cytoscheletal effectors (Gomez and Zheng, 2006). For instance, Ca^{2+} regulates proteins that are involved in the organization and movement of actin filaments. Dynamic changes in the actin filament network are required for rapid protrusion and retraction of filopodia and lamellipodia.

Although many proteins can interact with Ca^{2+} to regulate growth cone behavior, in this thesis I focused on a few candidates that have been investigated by recent studies.

A Ca^{2+} rise in the growth cone activates several target proteins and cellular machineries. The most largely characterized Ca^{2+} - binding protein is **calmodulin** (CaM), which acts as an intracellular Ca^{2+} sensor. It is abundant in growth cone filopodia and central domains and binds Ca^{2+} also at low concentrations. Interestingly, Ca^{2+} interaction with CaM persists for about one minute following brief electrical activity in the neuron (Henley and Poo, 2004). Calcium – calmodulin complex interacts with several targets, such as kinases and phosphodiesterases, inducing different signaling cascades. In particular, binding of Ca^{2+} to CaM leads to the activation of **Ca^{2+}/calmodulin – dependent kinases** (CaMKs). These kinases represent an important family of Ca^{2+} - activated proteins including five identified members. Among them, CaMKII is unique for its capacity to autophosphorylate and plays a central role in neural development and plasticity. Moreover, it seems to function in both growth cone turning and branching. Different CaMKII isoforms are expressed at different stages of development and they differ in their affinity for calcium – calmodulin complex. Among these isoforms, β – CaMKII is the most interesting as it is expressed at early developmental stages, is anchored to actin filaments and is able to modulate neurite extension. CaMKII seem to be involved in Ca^{2+} - dependent attraction. Studies in *Xenopus* growth cones demonstrated that β – CaMKII is crucial for Ca^{2+} - dependent attraction in response to extracellular cues (Zheng et al., 1994, Wen et al., 2004). In some cell types, these effects of CaMKII are mediated by the activation of Cdc42, a member of the Rho – family GTPases, which are known to regulate growth cone morphology and steering (Gomez and Zheng, 2006). Binding of Ca^{2+} to CaM also directly activates the Ca^{2+}/CaM – dependent phosphatase **calcineurin**, thought to be required for

Ca^{2+} - dependent repulsion in response to small local Ca^{2+} signals. Calcineurin is the only Ca^{2+}/CaM – dependent phosphatase that is highly enriched in the brain and has been previously implicated in Ca^{2+} regulation of axon extension. Its activation by Ca^{2+} in growth cones appears to dephosphorylate and activate other phosphatases, resulting in repulsive growth cone turning (Gomez and Zheng, 2006). Changes in intracellular Ca^{2+} levels also regulate guanine nucleotide exchange factors (GEFs) and GTPase – activating proteins (GAPs), which modulate **Rho – GTPases**. Rho family of small GTPases represents one of the main regulators of actin filaments assembly and organization during cell locomotion. Rho – GTPases family includes RhoA, Rac1 and Cdc42. RhoA takes part in growth cone collapse and repulsion, while Rac1 and Cdc42 participate in growth cone advance. Rho - GTPases are activated by GEFs, whereas inactivated by GAPs. GEFs and GAPs often contain other signaling motifs, such as CaMKII phosphorylation sites, which serve as additional regulatory mechanism. Ca^{2+}/CaM can also directly bind to certain **microtubule – associated proteins** (MAP1B, MAP2, tau) and compete for their association with tubulin, thus inhibiting the assembly of microtubules. Therefore, Ca^{2+}/CaM – dependent phosphorylation of many MAPs can lead to microtubule disassembly. Moreover, elevated Ca^{2+} levels inhibit casein kinase II activity, leading to decreased MAP1B phosphorylation and decreased binding to tubulin, favoring disassembly of microtubules. Concluding, Ca^{2+} serves as regulator of actin and microtubule dynamics to provide a mechanism by which the intracellular Ca^{2+} concentration can influence growth cone extension and steering.

Along with Ca^{2+}, also alterations in cAMP levels have been shown to influence neurite outgrowth and growth cone motility (Rydel and Greene, 1988, Tsuda et al., 1989, Sano et al., 1990, Greene et al., 1986, Lankford et al., 1988). In 1992, Poo and coll. developed a new method of repetitive pulse application in order to create reproducible chemical gradients. They demonstrated that an asymmetric distribution of cytosolic cAMP is sufficient to initiate a turning response of the growth cone. However, differences in cAMP – dependent activity in a neuron may result in opposite turning behaviors of the growth cone in response to the same guidance cue (Song et al., 1997, Song et al., 1998). For instance, a gradient of brain – derived neurotrophic factor (BDNF) normally triggers an

attractive turning response of the growth cone of *Xenopus* spinal neurons in culture. However, the same gradient induces repulsive turning in these growth cones in presence of a competitive analogue of cAMP or of a specific inhibitor of protein kinase A (PKA). Thus, in presence of other factors modulating neuronal cAMP – dependent activity, the same guidance cue can trigger opposite turning responses of the growth cone during its pathfinding. An important role for cAMP in the axonal targeting of olfactory sensory neurons was further supported by the observations that genetic ablation of ACIII perturbed the formation of glomeruli and the accurate convergence of odorant receptor – specific axons in the anterior – posterior axis of the olfactory bulb (Col et al., 2007, Zou et al., 2007).

1.1.10 Formation of the sensory maps: role of axon guidance molecules and electrical activity

1.1.10.1 Axon guidance molecules

How sensory neurons expressing the same odorant receptor coalesce in specific loci of the olfactory bulb to form glomeruli, that in turn give rise to the sensory map?

The development of the sensory maps is regulated by the complex interaction between spatially and temporally regulated axon guidance molecules and neuronal activity.

The glomerular location can be determined by modulating a few spatial coordinates: dorso – ventral, antero – posterior and latero – medial. Anatomical studies have shown that the zonal organization of the olfactory epithelium is coarsely reflected in the dorsal – ventral topography of the bulb (Myamichi et al., 2005, Sakano 2010). Namely, dorso – ventral position of olfactory sensory neurons in the olfactory epithelium determines the dorso – ventral region of axonal projections to the olfactory bulb. The dorso - ventral distribution of axonal projection to the olfactory bulb has been demonstrated to be guided by two sets of repulsive ligands/receptor molecules: Slit1/Robo2 (Cloutier et al., 2004) and neuropilin2/semaphorin3F (Nrp2/Sema3F)(Cloutier et al., 2002, Cloutier et al., 2004).

Robo2, a receptor for Slit chemorepellents, has been shown to be expressed in a high dorso – medial to low ventro – lateral gradient in the olfactory epithelium throughout development and in the adulthood (Cho et al., 2007). Interestingly, subsets of axons normally projecting to the dorsal region of the olfactory bulb are misrouted to the ventral part of the bulb in Robo2 mutant mice (Cho et al., 2007). Furthermore, the chemorepellent Slit1 is expressed in the ventral region of the olfactory bulb and ablation of its expression causes axonal targeting defects similar to those observed in Robo2 mutant mice. Therefore, Slit1 - Robo2 interactions prevent the entry of dorsally targeting axons into the ventral region of the olfactory bulb promoting the dorso – ventral segregation of olfactory sensory neuron axons in the olfactory bulb.

The axon guidance - receptor Nrp2 and its repulsive ligand Sema3F are both expressed by the axons of olfactory sensory neurons in a complementary manner (i.e. when one is high the other is low, and vice versa) to regulate dorso – ventral projections (Takeuchi et al., 2010). Loss – of – function and gain – of – function experiments demonstrated that Nrp2 regulates the axonal projection of olfactory sensory neurons along this axis. Sema3F is secreted by early – arriving axons of olfactory sensory neurons and is deposited in the anterodorsal portion of the olfactory bulb to repel Nrp2 – positive axons that arrive later. Therefore, sequential arrival of the axons of olfactory sensory neurons as well as the graded and complementary expression of Nrp2 and Sema3F by olfactory sensory neurons help to form the topographic order along the D – V axis (Takeuchi et al., 2010).

The antero - posterior distribution of axonal projection to the olfactory bulb is regulated by other axon guidance molecules. In particular, the secreted chemorepellent Sema3A has been shown to direct the antero – posterior targeting of olfactory sensory neuron axons. Sema3A is expressed in the nerve layer in the ventral region of the olfactory bulb as well as in mitral cells of the bulb (Schwarting et al., 2000). The Sema3A receptor, Nrp1, is expressed in subsets of olfactory sensory neurons and Nrp1 – positive axons segregate to either the medial or lateral side of the olfactory bulb according to their targeting position along the antero – posterior axis. In Sema3A mutant mice, the medio – lateral segregation of Nrp1 – positive axons is lost causing alterations in the olfactory map formation (Taniguchi et al., 2003). Indeed, $Nrp1^{+}$ glomeruli in

Sema3A - deficient olfactory bulb spread ectopically into the anteromedial and ventral regions, in which Sema3A is expressed in the wild – type olfactory bulb.
The position of glomeruli along the antero – posterior axis of the olfactory bulb is also regulated by other molecules, such as EphrinA3 and EphrinA5 and their Eph receptors. In particular, EphA5 and EphrinA5 are expressed in non – overlapping populations of olfactory sensory neurons in the olfactory epithelium. It has been demonstrated that the expression of EphrinA5 in the axons of olfactory sensory neurons correlates with the identity of the odorant receptor expressed in those neurons. EphrinA5 is present in a mosaic pattern in the bulb, with neurons expressing different receptors also containing different EphrinA5 levels. On the other hand, EphA5 expression is not graded in any dimension in the olfactory bulb. Rather, it has been observed a uniform level of EphA5 in both projection neurons and interneurons in the bulb (Cutforth et al., 2003). It has been demonstrated that mice lacking EphrinA5 exhibit a significant posteriorization of the glomeruli examined (P2 and SR1). Whereas, the over expression of EphrinA5 results in an anterior shift of the same glomeruli (Cutforth et al., 2003). Therefore, ephrins – As participate in the formation of a topographic map in the olfactory bulb. A complementary expression of EphA5/EphrinA5 has been demonstrated (Serizawa et al., 2006). Indeed, in each subset of olfactory sensory neurons, when one is high, the other is low, and vice versa. This complementary expression has been found not only in the olfactory epithelium, but also at a glomerular level, within the olfactory bulb.
In contrast to dorso – ventral targeting of olfactory sensory neuron axons, the position of glomeruli along the antero – posterior axis of the olfactory bulb appears to be independent of the zone of the olfactory epithelium and more dependent on the expressed odorant receptor species (Mombaerts et al., 1996, Wang et al., 1998, Feinstein and Mombaerts, 2004). Imai and coll. (2006) and Chesler and coll. (2007) demonstrated that the odorant receptor – derived signaling, cAMP, has a critical role in determining the antero - posterior location of the glomeruli. They performed experiments in which G – protein signalling and cAMP levels were altered in olfactory sensory neurons. The expression in olfactory sensory neurons of a mutated odorant receptor that does not interact with G – proteins or of a non – functional tagged receptor caused a lack of

axonal convergence. However, the expression of a constitutively active G_s protein rescued these defects and could also promote axonal convergence.

The segregation of olfactory sensory neurons along the medio - lateral axis seems to be regulated by the Insulin Growth Factor 1 (IGF1)(Scolnick et al., 2008). Genetic ablation of IGF1 or IGF1R induces a reduction in innervation of the lateral region of the bulb. The exact mechanism through which IGF1 controls the targeting of olfactory sensory neuron axons is not fully understood. Early in development, IGF1 is expressed in a low medial to high lateral gradient at the anterior part of the olfactory bulb and it can attract growing olfactory sensory neuron axons *in vitro*. Therefore, IGF1 could act as an attractant to promote the growth of axons into the lateral region of the bulb.

1.1.10.2 Electrical activity

It has been shown that electrical activity plays a critical role in shaping neural circuits in many sensory modalities (Zhang and Poo, 2001). Whether and how electrical activity modulate the formation of the glomerular map remains largely unknown and it is still a matter of significant debate.

To assess the role of evoked activity in circuit formation in the olfactory system, several genetic lines of mice have been created.

Mice lacking functional CNG channels, an essential component of the odorant receptor signalling pathway, failed to exhibit odor – evoked responses to a wide range of odorant stimuli (Lin et al., 2000). The sensory map in these mice was unaltered. Indeed, the axons of olfactory sensory neurons expressing a given receptor converge normally into specific glomeruli in the olfactory bulb of these mutant mice (Lin et al., 2000, Zheng et al., 2000). Subtle alterations in axonal convergence in CNG ko mice have been observed only for M72 expressing olfactory sensory neurons (Zheng et al., 2000).

Mice carrying a null mutation in G_{olf}, the G – protein coupled to the odorant receptor, resulted almost completely anosmic when tested electrophysiologically with the electro - olfactogram in the olfactory epithelium (Belluscio et al., 1998). Although a strong reduction in the electrophysiological responses of olfactory sensory neurons to odorants was observed, the sensory map again formed normally in these mice.

A completely different situation was observed when ACIII, an element of the signalling pathway coupled to the odorant receptor, was mutated (Dal Col et al., 2007, Zou et al., 2007). The mutation of ACIII results in the consequent lack of the synthesis of cAMP. In mice ko for ACIII the sensory map was affected in several ways. Most noticeably, the formation and organization of the glomeruli were perturbed. Indeed, the axons of olfactory sensory neurons targeted the olfactory bulb but they failed to form distinct and discrete glomeruli.
Imai and coll. (2006) generated a mouse line carrying a mutation in the DRY motif of the I7 – OR. This mutation modified the region of the odorant receptor that binds the G – protein. Therefore it results in olfactory sensory neurons that cannot produce cAMP and thus phenocopy the ACIII ko mice. In these mice, $I7^{+}$ axons targeted the olfactory bulb, but they remained into the nerve layer. This phenotype was rescued by the expression of a constitutively active G_s (caG_s). The axons expressing I7(RDY) - caG_s indeed converge to a specific site in the olfactory bulb. The rescue was also possible by the expression of a constitutively active PKA and a constitutively active variant of cAMP response element – binding protein (CREB). However, in the latter case, the axon termini were found within glomerular structures, but the convergence was still incomplete. The critical feature that differentiates the ACIII mutant mice from mice in which other components of the signalling pathway coupled to the odorant receptor have been mutated, could be represented by the cAMP levels. In the ACIII ko mice (Dal Col et al., 2007, Zou et al., 2007) as in the OR - DRY mutated mice (Imai et al., 2006), the synthesis of cAMP is hampered and the sensory map resulted perturbed.

Olfactory sensory neurons exhibit also spontaneous firing that is independent of odorant stimuli. In other sensory modalities, such as vision, spontaneous activity has been shown to play a critical role in the formation of neural circuits and in the topographic organization (Galli and Maffei 1988, Meister et al., 1991). Whether spontaneous firing in olfactory sensory neurons plays a role in the olfactory system remained unknown.
To explore the role of spontaneous electrical activity in circuit formation in the olfactory system, Yu and coll. (2004) generated a genetically modified mouse line: Kir2.1 mice. These mice are characterized by little spontaneous activity in

the olfactory sensory neurons due to the over expression of the inward rectifying potassium channel (Kir2.1) in these cells. In these mice (the Kir2.1 mice) the olfactory sensory neuron innervation to the olfactory bulb is delayed. Furthermore, olfactory sensory neurons expressing the same odorant receptor targeted multiple glomeruli. The sensory map was disrupted by the presence of additional glomeruli in Kir2.1 mice.

The exact mechanism by which the spontaneous activity influences the refinement of neural circuits in the olfactory bulb is still poorly understood. One possibility is that olfactory sensory neuron activity regulates cAMP and Ca^{2+} levels that in turn can affect axon elongation and retraction through local signaling (Song et al., 1997) and regulate gene expression (West and Greenberg, 2011). Another possibility arises from the observation that cyclic nucleotides locally produced at the axon terminal of olfactory sensory neurons seem to modulate synaptic transmission and the stabilization of synaptic contacts (Murphy and Isaacson, 2003). Recently, it has been demonstrated that the odorant receptor type determines not only the evoked activity but also the spontaneous firing rate in olfactory sensory neurons (Hallem et al., 2004, Reisert 2010, Connelly et al., 2013).

1.1.11 Role of the of the odorant receptor in the sensory map formation

A unique feature of the topographic organization of the olfactory bulb is the “dual role” of the odorant receptor. It detects odors at the cilia and it has been suggested to play a critical role in the axonal convergence of olfactory sensory neuron axons to form glomeruli in the olfactory bulb (Mombaerts et al., 1996). Evidence for this “dual role” in the function of the odorant receptor was first shown by Axel laboratory through genetic manipulations (Wang et al., 1998). These studies demonstrated that alterations of the odorant receptor sequences perturb the sensory map. Receptor substitution experiments showed that replacing the P2 receptor coding region with the coding region of the P3 receptor, which is a closely related receptor expressed in the same epithelial zone, caused the projection of the resulting P3 $\rightarrow$ P2 axons to converge in a glomerulus that was adjacent to, but not the same as, the endogenous P3

glomerulus. Similar findings were observed when the M71 coding sequence was swapped into the P2 gene locus in that the resulting M71→P2 glomerulus never occupied the same position as the endogenous M71 or P2 glomeruli; instead, it was usually located between them, displaced along the antero – posterior axis of the olfactory bulb. The degree to which the swapped glomerulus is shifted with respect to the endogenous one was influenced by a few parameters: 1) the sequence homology between the swapped genes, 2) the chromosomal loci where the genes are located, and 3) the epithelial zone occupied by olfactory sensory neurons endogenously expressing the odorant receptors. In general, the more similar odorant receptor genes are with respect to these factors, the closer the glomeruli that result from swapping their coding regions would be to their endogenous glomerular location. These data demonstrated that the odorant receptor plays an instructive role in the axon guidance process, but it is not the sole determinant.

Subsequently, Feinstein and coll. (2004) highlighted the relevance of the structure of the odorant receptor as a seven transmembrane G – protein coupled receptor in the axonal convergence of olfactory sensory neurons (Feinstein et al., 2004, Feinstein and Mombaerts 2004). When the odorant receptor sequence was replaced with another seven transmembrane receptor, V1R (which does not couple to the same class of G - proteins), the axons of the olfactory sensory neurons failed to converge and form glomeruli. Also in this experiment, as in Imai et al. (2006), it is highlighted the critical role of the odorant receptor - derived cAMP in axon targeting.

To seek to explain the role of the odorant receptor in the axonal convergence of olfactory sensor neurons it was hypothesized that the odorant receptor could be expressed at the axon terminal where it could act as an axon guidance molecule. This hypothesis was confirmed later by Barnea and Strotmann independently (Barnea et al., 2004, Strotmann et al., 2004), that found that the odorant receptor is expressed not only at the cilia but also in the most distal part of the axon. The odorant receptor is not present in the proximal part of the olfactory sensory neuron axon.

Later, Dubacq et al. (2009) found that mRNA of the odorant receptor is present at the axon terminal, suggesting that the odorant receptor is locally translated in this location.

The growth cone indeed functions as a semi – autonomous apparatus that contains all the machinery required to sense and respond to the extracellular environment (Campbell and Holt, 2001). This autonomous nature of the growth cone involves local mRNA translation and has been corroborated by the finding that the cue – induced responses of severed axons are hampered by protein synthesis inhibitors. Scientific evidence, in the last decade, indicates that the local mRNA translation plays a potentially important role in axon guidance. The local protein synthesis is indeed involved in regulatory mechanisms that orchestrate the chemotropic responses of growth cones to navigate precisely in the developing nervous system (Shigeoka et al., 2013).

The critical question that remained to be addressed was whether the odorant receptor at the axon terminal was functional and, if yes, what was the signalling pathway coupled to its activation. To address this question Maritan et al. (2009), in my laboratory, studied the spatio - temporal dynamics of cAMP and Ca^{2+} in olfactory sensory neurons transfected with a genetically encoded sensor for cAMP or loaded with the calcium indicator fura-2. They demonstrated, for the first time, that the odorant receptor at the axon terminal is functional and able to elicit local increases of cAMP and Ca^{2+}. Indeed, when they focally stimulated the axon terminus – growth cone with an odor puff, cAMP and Ca^{2+} rises could be observed exclusively in this compartment. Moreover, they demonstrated that the Ca^{2+} rise was due to the cAMP – dependent activation of the CNG channels since it was absent when an adenylyl cyclase blocker was applied. To assess whether the axonal signalling pathway observed in isolated olfactory sensory neurons was also present in a more intact olfactory system, the same experiments were performed in “hemi – head” preparations, where the connectivity of the olfactory bulb with both the olfactory epithelium and the brain was retained (Maritan et al., 2009). These data confirmed that the odorant receptor at the axon terminal is functional and coupled to local increases of cAMP and Ca^{2+}.

In this project I continued to study the signalling pathway coupled to the odorant receptor expressed at the axon terminal. In particular, we investigated the spatio – temporal dynamics of cGMP in olfactory sensory neurons transfected with a genetically encoded sensor for cGMP. This technique allows to highlight,

with a high spatio – temporal resolution, the cGMP regulation and thus its several functions in the olfactory sensory neurons. Subsequently I participated to the study aimed to understand the mechanisms of activation, i.e. the possible natural ligands, of the odorant receptor expressed at the axon terminus – growth cone. We hypothesized that a few molecules expressed in gradient in the olfactory bulb could bind and activate the odorant receptor expressed at the axon terminal of the olfactory sensory neurons. To test our hypothesis we studied the spatio - temporal dynamics of Ca^{2+} and cAMP in response to molecules from the olfactory bulb.

2. Materials and methods

2.1 Primary culture of olfactory sensory neurons

The olfactory epithelium was harvested from embryonic rats (E18 - E19) in ice cold HBSS. Tissue was enzimatically dissociated in 5 ml of 0.125 % trypsin at 37° C in a water bath for 15 min. The enzymatic dig estion was stopped by adding 1 ml of fetal bovine serum (FBS). The dissociated cells were then washed for 3 min three times with 5 ml of prewarmed HBSS. The cells were pelletted for two times by centrifugation (800 x g for 4 min), and the cell pellet was resuspended in 5 ml of prewarmed culture medium by gentle pipetting and plated onto 24 mm glass cover slips coated with poly – L - lysine (1 mg/mL). The cells were maintained in culture medium (D - Val Mem, 10% FBS, 5% Nu Serum, 1% Penstrep L - glutamine, 10 μM AraC and 25 ng/ml NGF) under standard conditions (Ronnet et al., 1991, Liu et al., 1998). After 6 - 24 h in culture, cells were transiently transfected with the protein - kinase G (PKG) - based sensor for cGMP (Cygnet 2.1)(Honda et al., 2001) or with the genetically encoded Ca^{2+} sensor, targeted to the endoplasmic reticulum, D1ER (Rudolf et al., 2006), or with the Epac – based sensor for cAMP (Ponsioen et al., 2004), using Transfectin transfection reagent (Biorad), or loaded with 5 μM Fura 2 - AM at 37° C for 30 min. After transfection, cells were maintained in culture for an additional 12 - 15 h before FRET imaging experiments to allow the genetically encoded sensor to be expressed. In transfected cells, the fluorescence is evenly distributed throughout the cytoplasm and is excluded from the nucleus. The morphology of OSNs transfected with Cygnet 2.1, D1ER or Epac appear normal and indistinguishable from non transfected cells.

2.2 cGMP and cAMP measurements in cultured neurons

FRET imaging experiments were performed on an inverted microscope Olympus IX 70 with 60X NA 1.4 oil - immersion objective. The microscope was equipped with an illumination system and CCD camera TILL - visION v3.3 equipped with the polychrome IV. Excitation was 430 nm. Emission wavelengths were separated with a dual - emission beam splitter (Multispec

Microimager; Optical Insights) with a 505 nm dichroic filter and 480 ± 15 and 545 ± 20 nm emission filters for CFP and YFP, respectively. All filters and dichroics were from Chroma Technology. Live images were acquired for 200 - 300 ms at 5 s intervals for cGMP dynamics and at 3 s intervals for cAMP dynamics.

The day of the experiment, cover slips were mounted in an imaging chamber at 37° C and maintained in Ringer's Solution as follow (in mM): 140 NaCl, 5 KCl, 1 $CaCl_2$, $2H_2O$, 1 $MgCl_2$, 10 HEPES, 10 glucose, 1 sodium pyruvate, pH 7.2. Images were acquired using TILLvisION v3.3 software and then processed off line using a custom - made software (Vimmaging, made in Mat Lab environment). FRET changes were measured as changes in the background - subtracted 480/545 nm fluorescence emission intensities on excitation at 430 nm and expressed as R/R_0, where R is the ratio at time t and R_0 is the ratio at time = 0 s. The time for half - maximal response (t ½), was evaluated as the time, after stimulus application, at which half - maximal response was reached, considering half - maximal response = $(R - R_0)/2 + R_0$, and $t = t - t_0$ where t_0 is stimulus application time and t is time at the peak of the response.

The changes in CFP/YFP ratios reported in all the experiments were always dependent on an antiparallel behaviour of CFP and YFP fluorescences. At longer times, during the experiments, the two wavelengths might decrease in parallel, probably due to an out of focus artefact and/or bleaching. The CFP/YFP ratio, however, compensates for this artefact, and the ratio trace remains practically constant. The ability of the ratio measurements to compensate for parallel changes in the two wavelengths is a well known advantage of this approach.

2.3 Ca^{2+} measurements in cultured neurons

Ca^{2+} imaging experiments were performed on an inverted Olympus IX 70 microscope with a 40X NA 1.3 oil - immersion objective (see above for details). The day of the experiment, cover slips were mounted in an imaging chamber maintained at 37° C in Ringer's solution (for details see above). Changes in intracellular calcium were visualized using 380/15 nm and 340/15 nm excitation filters and 510/40 nm emission filter. Live images were acquired for 100 - 200 ms every 5 s, and every 1 s in Ca^{2+} imaging experiments on OSN growth cone.

Images were then processed off - line using ImageJ software (National Institutes of Health). Changes in fluorescence (340/380 nm) were expressed as R/R_0 where R is the ratio at time t and R_0 is the ratio at time = 0 s.

2.4 cGMP and Ca^{2+} measurements in the same cultured neurons

After 6 - 24 h in culture, cells were transfected with PKG - based sensor for cGMP, as above. The day of the imaging experiments, neurons transfected with the PKG - based sensor were loaded with Fura 2 - AM. FRET experiments were conducted according to the standard protocol (see above). Changes in intracellular Ca^{2+} were visualized using a 380/15 nm excitation filter and 480 ± 15 and 454 ± 20 nm emission filters. Live images were acquired for 200 - 300 ms every 6 s. Images were then processed off - line using ImageJ (National Institutes of Health). To measure FRET ratios, bleed through of CFP and Fura - 2 was corrected. To analyze Fura - 2 fluorescence intensity, Fura - 2 emission from both channel was summed, and bleed through from CFP was corrected (Dunn et al., 2009).

2.5 Ca^{2+} measurements with a genetically encoded Ca^{2+} sensor, targeted to the endoplasmic reticulum (D1ER) in primary culture of OSNs

FRET imaging experiments were performed on an inverted Olympus IX 70 microscope with a 60X NA 1.4 oil - immersion objective (see above for details). In this case, FRET changes were measured as changes in the background - subtracted 545/480 nm fluorescence emission intensities on excitation at 430 nm. Live images were acquired for 200 - 300 ms at 5 s intervals.

2.6 Immunostaining

OMP. Cells in culture were fixed in ice - cold methanol 100% for 20 min at RT. Cells were then reacted with goat polyclonal antibodies specific for OMP (Wako Chemicals) at 1:1000 dilution. The bound primary antibody was visualized using Cy3 - conjugated anti - goat IgG (Jackson Laboratories).

Epac, sarcoendoplasmic reticulum Ca^{2+} ATPase, calreticulin. After 48 h in culture, cells were fixed with 4% paraformaldehyde in 0.1% phosphate buffer (PBS). Cells were then reacted with rabbit polyclonal antibody specific for Epac (1:100, Abcam), or mouse polyclonal antibody specific for sarcoendoplasmic reticulum Ca^{2+} ATPase (SERCA)(1:100, Sigma) or rabbit polyclonal antibody specific for calreticulin (1:100, Abcam). The bound primary antibody was visualized using FITC - conjugated anti - goat IgG (1:500, Sigma), Cy3 - conjugated anti - mouse IgG, and DyLight 488 - conjugated anti rabbit IgG (1:500, Jackson Laboratories), respectively.

Phosphorylated CREB (P – CREB) in vitro. Primary cultures of OSNs were treated with 8Br - cGMP (50 μM) and left in standard culture conditions for 20 - 30 min. Cells were then fixed with 4% paraformaldehyde in 0.1% phosphate buffer (PBS) for 20 min at RT and reacted with rabbit polyclonal antibody specific for phosphorylated (P) - CREB (1:2000, Millipore). The bound primary antibody was then visualized using the ABC kit (Vectastain, Vector Laboratories).

Phosphorylated CREB (P – CREB) in vivo. 18 mice (P15 - P30) were anesthetized with Zoletil 100 (a combination of zolazepam and tiletamine, 1:1, 10 mg/Kg; Laboratoire Virbac) and xilor (xilazine 2%, 0.06 ml/Kg; Bio98) and placed in stereotaxic apparatus. The scalp was resected, and a small portion of the bone over the two bulbs removed. 8Br - cGMP (250 μM, n = 4), odor mixture (1 mM, n = 4), or odor mixture (1 mM) in the presence of the sGC inhibitor LY83583 (250 μM, n = 5) or Ringer's Solution for controls (n = 5) were locally applied on the bulb with a pipette. To avoid possible effects due to diffusion of odors applied on the olfactory bulb, the experiments were performed under a chemical hood, and the nose of the animal was placed in a funnel connected to the vacuum for the entire duration of the experiment. After 30 - 40 min, animals were killed and transcardially perfused with 0.9% saline followed by 4% paraformaldehyde in 0.1% phosphate buffer (PBS). The epithelium was removed, postfixed overnight in a 4% paraformaldehyde, 0.1% phosphate buffer and then cryoprotected in 30% sucrose in PBS for 3 d. The epithelium was sectioned on the cryostat (20 – μm - tick section). Epithelium sections were

reacted with rabbit antibody specific for P - CREB (1:2000, Millipore). The bound primary antibody was visualized with the ABC kit (Vectastain; Vector laboratories).

P - CREB analysis. The signal intensity, background subtracted, of CREB phosphorylation in the nuclei of OSNs in culture and in olfactory epithelium coronal sections, was evaluated using ImageJ software. P - CREB levels were normalized to the P - CREB level present in controls. Student's t test, two tailed, not paired, was used to evaluate statistical significance. All data are presented as mean ± SE. Student's t test (two tailed, not paired) was performed to evaluate statistical significance (*p = 0.01< p <0.05; **p = 0.001< p <0.01; ***p < 0.001). The number of cells or animals analyzed is denoted by n.

2.7 Real – time imaging experiments on cultured neurons

Olfactory sensory neurons are maintained in culture for 24 hours. The day of the experiment, cover slips were mounted in an imaging chamber at 37° C and maintained in Ringer's solution as follow (in mM): 140 NaCl, 5 KCl, 1 $CaCl_2$, $2H_2O$, 1 $MgCl_2$, 10 HEPES, 10 glucose, 1 sodium pyruvate, pH 7.2.
Microscopic chemical gradients near the growth cone were created using a repetitive pulse application method (Lohof et al., 1992). The micropipette (tip opening of 1 µm) was filled with the stimulus solution (Ringer's solution, Frsk 5 mM, odors 1 mM, IEC fract2 5 µg/µL) and connected to an electrically gated pressure application system (Picospritzer, General valve Co.). The tip of the micropipette was placed 100 µm from the centre of the growth cone and with an angle between 45° and 70° with respect to the direc tion of neurite extension. A positive pressure of 3 psi was applied to the pipette with a frequency of 2 Hz and a duration of 4 ms. The images were obtained with a 50 x objective, collected using TILL visION v3.3 software and processed off line. The microscope was equipped with a CCD camera TILL visION v3.3. The direction of neurite extension was measured after 1 h's growth in presence of the gradient. The turning angle was defined by the angle between the original direction of neurite extension and a straight line connecting the positions of the growth cone at the onset and the end of the 1 - h period. Only growth cones with a turning response over a 7° angle were scored for the turning assay.

2.8 Ca^{2+} imaging on HEK 293T cells

HEK 293T cells were maintained in minimal essential medium (DMEM) containing 10% fetal bovine serum (FBS) and 1% Penstrep (Invitrogen) in a 37° C incubator with 5 % CO_2. When the desiderated confluence was reached, cells were passed and plated onto 24 mm glass cover slips coated with poly – L - lysine (1 mg/mL). After 12 hours, Lipofectamine 2000 (Invitrogen) was used to transfect cells with different odorant receptors (OREG, ORS6, Olfr62, OR23 and ORM71). In details, cells were co – transfected with cDNA for different receptors, RTP1s and RTP2 proteins to ensure the insertion of the OR into the plasma membrane, Gα15 protein, and pcDNA$_3$kate to visualize transfected cells. After transfection, HEK cells were maintained in culture for an additional 12 - 15 h before Ca^{2+} imaging experiments to allow the OR proteins to be expressed.

The day of the experiment, HEK cells were loaded with 5 μM Fura - 2 AM at 37° C for 30 min. The cover slips were mounted on an imaging chamber maintained at 37° C in Ringer's solution. Ca^{2+} imaging experiments were performed on an inverted Olympus IX 70 microscope with a 40X NA 1.3 oil - immersion objective (see above for details). Changes in intracellular calcium were visualized using 380/15 nm and 340/15 nm excitation filters and 510/40 nm emission filter, and were acquired for 100 - 200 ms every 3 s. Images were then processed off - line using ImageJ software (National Institutes of Health). Changes in fluorescence (340/380 nm) was expressed as R/R_0 where R is the ratio at time t and R_0 is the ratio at time = 0 s. HEK cells were continuously perfused with normal Ringer's Solution (1.5 ml/min) except during stimulus presentation.

2.9 Olfactory bulb lysate

Olfactory bulbs were collected from embryonic rats (E18 – E19). After dissection in ice cold HBSS, each tissue was frozen in liquid nitrogen in a cryotube and conserved at -80° C for at least one d ay, to favour the subsequent lysis. Good quantities of lysate proteins can be obtained from at least 60 rat embryos. The day of the experiment, the bulbs were powdered by pestle and mortar with liquid nitrogen (the pestle must be put in liquid nitrogen to chill it). The powder was then diluted in ice cold Lysis buffer added with protease and

dephosphatase inhibitors as follow: 140 mM NaCl, 5 mM KCl, 5 mM $NaHCO_3$, 1.2 mM Na_2HPO_4, 1 mM $MgCl_2$, 20 mM HEPES pH 7.4, 10 mM dextrose, 1.8 mM $CaCl_2$, 1 mM PMSF, 1 mM NaV, 5 mM NaF, 3 mM β – glycerol – P, Roche Complete Protease Inhibitor Cocktail with a 1:50 dilution. The lysate was incubated in ice for 30 – 40 min and centrifuged at 4° C for 30 min at 13.000 rpm to separate the surnatant (cytosolic fraction) from the pellet (membrane fraction). To remove salts and small contaminants, the surnatant was then dialysated with a slide – A – Lyzer Dialysis Cassette (3500 MWCO) in 20 mM HEPES and 100 mM NaCl, pH 7.3. Proteins were then quantified with a Bradford assay.

.

2.10 Chromatography procedures

The dialysate from the olfactory bulb was applied onto a HiTrap Desalting column (GE Healthcare) equilibrated with 20 mM Tris pH 7.4 and 100 mM NaCl. The proteins were eluted in a single peak, concentrated and further purified by a Superdex 200 prep - grade 300/10 column (GE Healthcare) equilibrated with 20 mM Tris – HCl, 100 mM NaCl (Gel Filtration Chromatography, GF). The peaks were separately collected. The third peak from the gel filtration chromatography was concentrated and diluted with 20 mM Tris (pH 8) several times until it contained 1 mM NaCl. The sample was then loaded onto a HiTrap Capto Q column (GE Healthcare) equilibrated with the buffer A (20 mM Tris, pH 8)(Ion Exchange Chromatography, IEC). During sample loading, the first peak (IEC fract1) was collected and concentrated. The column was washed with 10 ml of buffer A, and a linear gradient (0 - 30%, in 30 minutes at the flux of 1 ml/min) of buffer B (20 mM Tris, 1 M NaCl) was then applied. During the application of the gradient two subsequent peaks were collected (IEC fract2 and 3), whereas another one (IEC fract4) was collected when the column was washed with 100% of buffer B. All the collected fractions were concentrated and tested as describe above. All these chromatographies (desalting, gel filtration and ion exchange) were performed with an AKTA Fast Protein Liquid Chromatography (FPLC) system (GE Healthcare).

Proteins of IEC fract2 from the ion exchange chromatography were further purified through a C18 Reverse – Phase column (GE Healthcare) equilibrated

with the buffer A (0.1% trifluoroacetic acid (TFA) in 2% acetonitrile)(Reverse – Phase Chromatography, RPC). Several fractions were separately collected, concentrated and tested as described above.

2.11 Stimuli on OSNs *in vitro* and HEK cells

Pharmacological stimuli: atrial natriuretic peptide (ANP, 1 μM), activator of pGCs; S – nitroso - acetylpenicillamine (SNAP, 300 μM), an NO donor that activates sGCs; forskolin (Frsk, 25 μM), generic activator of adenylyl cyclase (AC); 8 Br - cGMP (50 μM), a membrane - permeable cGMP analogue; 1 – methyl – 3 - isobutylxanthine (IBMX, 250 μM), nonselective inhibitor of phosphodiesterases (PDEs); Zaprinast (250 μM, Alexis), inhibitor of the cGMP - specific PDE5; SQ22536 (30 μM, Biomol International), inhibitor of AC; LY83583 (10 μM, Calbiochem), inhibitor of sGC; zinc protoporfhyrin IX (ZnPP9, 10 μM, Calbiochem), inhibitor of HO that produces CO; 7 nitroindazole (7 – NI, 30 μM, Calbiochem), inhibitor of NOS that produces NO; H89 (10 μM, Biomol International), inhibitor of PKA; KT5720 (1 μM, Calbiochem), inhibitor of PKA; Ringer's Solution with high concentration of KCl (50 mM); 8 – CPT – 2' – O - Me cAMP (30 μM) activator of Epac; U73122 (30 μM), inhibitor of phospholipase Cε (PLCε); protease K (Invitrogen); ATP (100 μM); carbachol (CCH, 100 μM), all from Sigma, unless stated otherwise, were prepared in stocks and diluted to the final concentration (indicated in brackets) in the bath.

The odorant stimuli were represented by mixtures of several compounds, including the following: citralva, citronellal, menthone, carvone, eugenol, geraniol, acetophenone, hexanal, benzyl alcohol, heptanoic acid, propionic acid, benzaldeyde, and IBMP (all from Sigma) prepared as 1mM stock in Ringer's Solution and diluted to the final concentration of 1, 50, or 200 μM for each odorant in the bath. These odor concentrations are well within the range (1 nM - 1 mM) of those used in previous studies (Bozza and Kauer, 1998; Bhandawat et al., 2005, 2010) on dissociated OSNs. The stimuli bath applied were carefully and slowly delivered via an application pipette positioned far away (~ 3 mm) from the cell to obtain an homogeneous distribution of the stimulus in the bath, capable of stimulating the entire cell and not a specific compartment. Odor stimuli and chromatographic products focally applied to the growth cone of

OSNs in culture were delivered (with no perfusion) by a single - puff pressure ejection (Pneumatic pico - pump, WPI) with a glass micropipette (3 - 5 μm tip diameter, 3 s puff duration, 5 psi). The micropipette was positioned at 5 - 10 μm from the growth cone. Within the micropipette, the concentration of odors was 1 mM for each component of the mixture, while the concentration of the chromatographic products was 1 μg/μL. The volume ejected from the pipette was very small (5 - 10 nl) and got diluted in the Ringer's Solution of the chamber (1 ml). Thus, the concentration of the stimulus focally applied at the axon terminus - growth cone was much lower than the concentration of the stimulus present in the pipette, but sufficient to induce OR activation. The stimulus get even more diluted as it spreads away from the site of application. To focally applied stimuli at the axon termini, we modified the protocol used by Lohof et al., 1992.

The neurons were continuously perfused with normal Ringer's Solution (1.5 ml/min) except during stimulus presentation. Stimuli were bath applied for 4 - 10 s in Ca^{2+} imaging experiments, and for 5 - 7 min in FRET imaging experiments, or for the entire duration of the experiment. Stimuli applied *in vivo*, on the olfactory bulb (OB), had the following concentration: 8Br - cGMP, 250 μM; odors, 1 mM; LY83583, 250 μM.

3. Results

3.1 Primary culture of OSNs

In our study neurons remained in culture for a longer period of time than in most studies on isolated olfactory sensory neurons. We performed a series of control experiments to evaluate the healthy state of OSNs in the time window in which experiments were performed. We checked the morphology of the transfected OSNs in culture for 2 days (d). They showed the typical OSN bipolar morphology, without signs of sufferance (Figure 1A – D). They expressed specific markers of OSNs, such as OMP (Fig. 1A, B), as freshly plated OSNs. Moreover, the cultured OSNs, both transfected and nontransfected, had similar functional responses and did not exhibit differences respect to freshly plated neurons. In Figure 1 are shown examples of the $[Ca^{2+}]_i$ changes elicited by KCl depolarization or odors in cells kept in culture for 2 days. The cells were loaded with the Ca^{2+} indicator fura-2 and challenged with KCl (50 mM) and odors, at different concentrations (1, 50, and 200 μM). OSNs exhibited an immediate and transient rise in Ca^{2+} in response to KCl depolarization (n = 13; responsive cells = 90%; Figure 1E), as observed in previous studies (Bozza and Kauer, 1998; Bozza et al., 2002). All concentrations tested (1, 50, and 200 μM) were well within the range (1 nM – 1 mM) of those used in previous experiments on isolated OSNs (Bozza and Kauer, 1998; Bhandawat et al., 2005, 2010). At all these concentrations, odors elicited Ca^{2+} responses (Figure 1) similar to those obtained in freshly plated neurons. As expected, due to the partial cross - reactivity of each OR for different odors (Malnic et al., 1999), the higher odor mix concentration used (200 μM) elicited reliable responses in a larger number of cells (odor mix 1 μM, n = 29, responsive cells = 6%; odor mix 50 μM, n = 30, responsive cells = 16%; odor mix 200 μM, n = 39, responsive cells = 33%). In our study we worked with OSNs with unknown OR specificity and in each experiment a single cell was analyzed. Thus we decided to use, in all the following experiments that required odor stimulation, the higher odor mix concentration (200 μM) in order to increase the probability of finding responsive cells. Odor concentrations in the range of hundreds of micromolar have also been used in Ca^{2+} imaging experiments performed on isolated OSNs

expressing specific OR of known ligands (Touhara et al., 1999; Imai et al., 2006). Notable, when the odor mix was continuously present in the bath (at least 8 min)(Figure 1F) the Ca^{2+} signal did not completely return to baseline. However, when the odor mix was applied for 4 – 10 s and then washed away, the Ca^{2+} signal returned to baseline (Figure 1G). OSNs nonresponsive to the odor mix were subsequently challenged with KCl (50 mM) to test their viability. A prompt rise in Ca^{2+} was observed after KCl stimulation (Figure 1H). Therefore, the absence of response upon odor stimulation is due to the specificity of the OR expressed by OSNs and unspecific effects due to the odor mix application can be excluded. Together, these results demonstrate that OSNs in culture for 2 d are functionally indistinguishable from freshly plated cells.

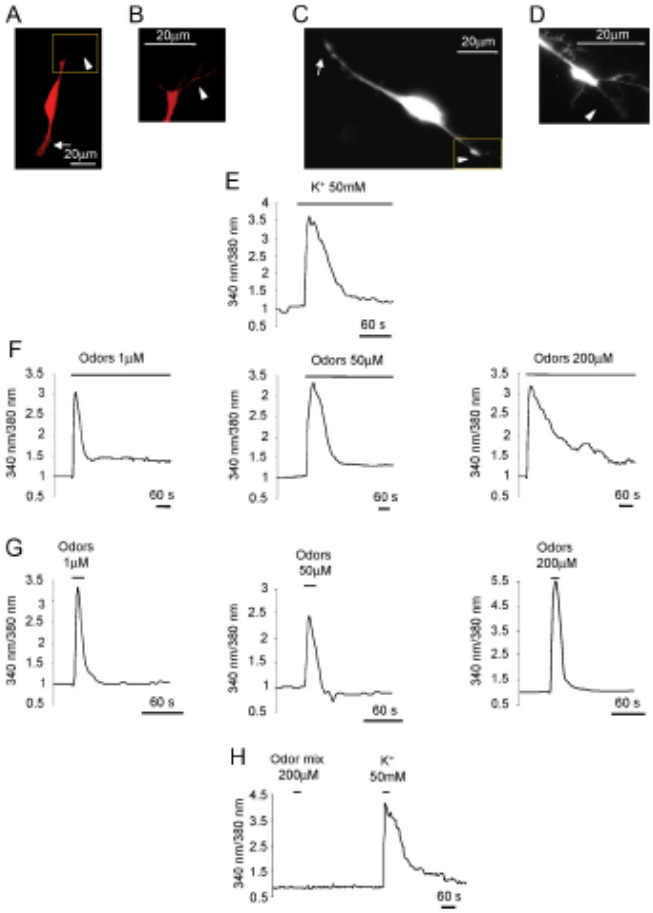

Figure 1: Ca^{2+} dynamics in OSNs in culture. **A**, example of an OSN immunopositive for OMP. **B**, higher magnification of the cilia indicated in the square in A. **C**, example of an OSN loaded with fura-2. **D**, higher magnification of the cilia emanating from the knob, indicated in the square in C. Arrows, axon terminus – growth cone; arrowheads, cilia – dendrite. Scale bar, 20 µm. **E – H**, normalized fluorescence ratio changes (340/380 nm) in OSNs loaded with fura-2 and challenged with KCl (50 mM), bath applied (**E**); odor mixture at 1, 50, 200 µM, bath applied (**F**); odor mixture at 1, 50, 200 µM, bath applied for 4 – 10s (**G**); example of a non responsive neuron to the odor mixture (200 µM, bath applied for 4 – 10s), but responsive to KCl (50 mM) bath applied for 4 – 10s (**H**).

3.2 cGMP dynamics in OSNs upon pharmacological stimulation

Primary cultures of OSNs were transiently transfected with the PKG - based sensor for cGMP, Cygnet 2.1 (Honda et al., 2001; Figure 2A). Changes in cGMP levels result in modifications of FRET between the CFP and YFP moieties, genetically fused to PKG, and a rise in CFP/YFP ratio reflects an increase in cGMP. Noticeable, Cygnet 2.1 is highly specific for cGMP and is practically insensitive to cAMP levels (selectivity for cGMP over cAMP is 100:1; Honda et al., 2001).

A first series of experiments was performed using drugs known to activate particulate and soluble GCs and/or to inhibit PDEs. As shown in Figure 2B, ANP (1 μM), an agent known to activate pGCs in several cell types, induced an increase in cGMP in the whole OSN, from cilia – dendrite to axon terminus - growth cone. Moreover, the cGMP rise began with no appreciable lag phase between stimulus application and its onset and remained sustained for the entire duration of the experiment (at least 8 min)(Figure 2B). The time to reach the half – maximal response ($t_{1/2}$) was faster at the cilia – dendrite and at the axon terminus – growth cone than at the soma level (n = 6, $t_{1/2}$: cilia - dendrite = 1.1 ± 0.2 min, soma = 1.5 ± 0.1 min, axon terminus - growth cone = 0.85 ± 0.2 min; *t* test $t_{1/2}$: cilia dendrite - soma, $*p = 0.02$; axon terminus - growth cone - soma, $**p = 0.005$; cilia dendrite - axon terminus growth cone, $p = 0.19$).

When the OSNs were treated with NO donors able to activate the sGCs, such as SNAP (300 μM), a prompt rise in cGMP was observed again in the entire neuron (Figure 2C) and also in this case no latency was observed between stimulus application and the onset of the response. The time to reach the half - maximal response was not statistically different in the three compartments analyzed (n = 6, $t_{1/2}$: cilia - dendrite = 1.6 ± 0.3 min; soma = 1.8 ± 0.4 min; axon terminus – growth cone = 1.6 ± 0.3 min).

In most cell types (including OSNs), cAMP is produced in resting cells also in the absence of external stimuli, due to the constitutively active ACs. To determine whether this occurs also for cGMP, OSNs were treated with Zaprinast (250 μM), an inhibitor of PDE5, that specifically hydrolyzes cGMP, or IBMX (250 μM), a nonspecific PDE blocker (Lugnier, 2006). As shown in Figure 2D, no cGMP increase could be detected in OSNs upon application of Zaprinast. However, all cells responded to ANP applied subsequently ($n = 4$)

with the same kinetics observed for ANP, used as first stimulus (Figure 2B). On the other hand, IBMX caused a substantial, slow rise in cGMP in the entire neuron (Figure 2E; n = 4, $t_{1/2}$: cilia – dendrite = 2.5 ± 0.4 min; soma = 3 ± 0.6 min; axon terminus - growth cone = 2.5 ± 0.5 min). It is significant that the cGMP increases elicited by the above - mentioned drugs have been observed in the majority (90%) of the neurons tested.

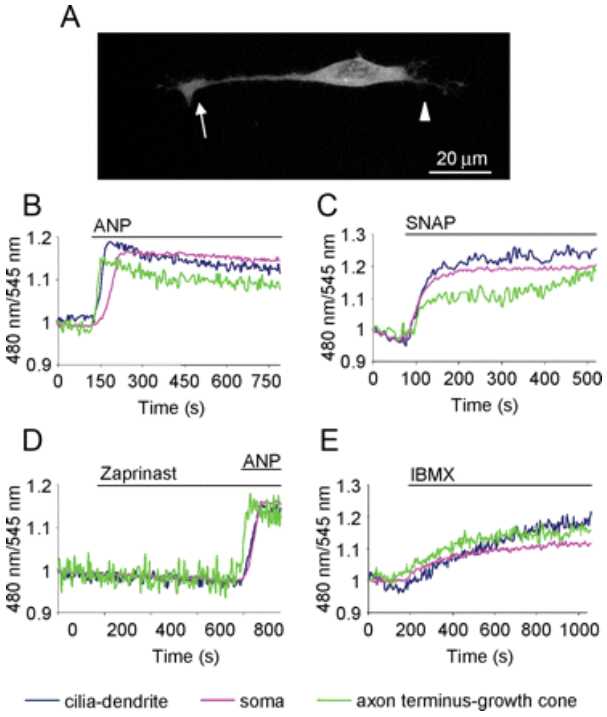

Figure 2: cGMP dynamics in OSNs upon pharmacological stimuli. **A**, example of an OSN transfected with the sensor for cGMP. The fluorescence is distributed throughout the cytoplasm with the exclusion of the nucleus. Arrow, axon terminus - growth cone; arrowhead, cilia - dendrite. Scale bar, 20 µm. **B – E**, normalized kinetics of fluorescence emission intensities (480/545 nm) recorded in cilia - dendrite, soma, and axon terminus - growth cone in OSNs transfected with the PKG - based sensor for cGMP and challenged with different stimuli, all bath applied. **B – E**, ANP (1 µM) activator of pGC (**B**); SNAP (300 µM) NO donor, which activates sGC (**C**); zaprinast (250 µM), inhibitor of the cGMP - specific PDE5 and subsequently with ANP (1 µM) (**D**); and IBMX (250 µM), nonselective inhibitor of PDEs (**E**). Blue line, CFP/YFP in cilia - dendrite; pink line, CFP/YFP in soma; green line, CFP/YFP in axon terminus - growth cone.

3.3 cGMP dynamics in OSNs upon physiological stimuli (odors)

We then investigated the spatio - temporal dynamics of cGMP in OSNs upon physiological stimulation (i.e., odors). Upon application of an odormix at different concentrations (1, 50, and 200 µM, bath applied; Figure 3A – C) a slow and sustained rise in cGMP was observed in the entire neuron (1 µM, n = 3, $t_{1/2}$ cilia - dendrite = 3 ± 0.3 min, soma = 4.2 ± 0.3 min, axon terminus - growth cone = 2.9 ± 0.2 min; *t* test $t_{1/2}$ cilia – dendrite - soma $*p = 0.04$, axon terminus -

growth cone - soma *p = 0.02, cilia dendrite - axon terminus - growth cone p = 0.8; 50 µM, n = 6, $t_{1/2}$, cilia - dendrite = 2.7 ± 0.5 min, soma = 3.1 ± 0.5 min, axon terminus - growth cone = 2.4 ± 0.5 min, *t* test $t_{1/2}$ cilia - dendrite - soma *p = 0.03, axon terminus - growth cone - soma *p = 0.02, cilia - dendrite - axon terminus growth cone p = 0.4; 200 µM, n = 20, $t_{1/2}$ cilia - dendrite = 2.2 ± 0.3 min; soma = 2.4 ± 0.4 min; axon terminus - growth cone = 2 ± 0.3 min; *t* test $t_{1/2}$ cilia - dendrite - soma *p = 0.03; axon terminus - growth cone - soma *p = 0.02, cilia - dendrite - axon terminus - growth cone p = 0.3). The higher odor concentration (200 µM) elicited cGMP responses very similar, in terms of kinetics, to those observed with the lower concentrations. At all the concentrations tested, the time for half - maximal response ($t_{1/2}$) was slightly, but significantly, faster at the cilia - dendrite and at the axon terminus - growth cone than at the soma (Figure 3A – C). As expected, given the specificity of the OR expressed by each OSN, only a fraction of the tested neurons responded at the odor concentrations used. The higher concentration (200 µM) evoked Ca^{2+} responses in a higher number of cells (1 µM, n = 62, responsive cells = 5%; 50 µM, n = 50, responsive cells = 12%; 200 µM, n = 67, responsive cells = 30%). Therefore, we decided to use, in all the experiments that required odor stimulation, the concentration of 200 µM, a condition that increases the probability of finding responsive cells. In a few cells, a variable lag phase (0.5 – 4 min) was observed between stimulus application and the onset of the response. The cGMP signal remained sustained for the entire duration of the experiment (at least 10 min, during which the stimulus, odor mixture, was present in the bath). However, the cGMP increase was reversible upon removal of the stimulus (bath applied for 5 – 7 min; n = 6; Figure 3D). Finally, the odor mixture was locally applied to the axon terminus - growth cone with a pipette in which the odor concentration was 1 mM. Under these conditions, a rise in cGMP was observed exclusively at the axon terminus - growth cone (n = 4, $t_{1/2}$ = 1.5 ± 0.2 min; Figure 3E), without appreciable changes in cGMP level in the other compartments.

In some neurons (n = 5), we measured in the same cells the cGMP dynamics and the cytosolic Ca^{2+} response. One example is presented in Figure 3F and G. For technical reasons, only the 380 nm component of the fura-2 indicator is reported (Figure 3G). A decrease in the 380 nm component, as shown in Figure

3G, corresponds to an increase in $[Ca^{2+}]_i$. With no exception, when a rise in cGMP was observed a Ca^{2+} signal was also detected; and vice versa, no rise in Ca^{2+} was observed in cells not responding to odors with a cGMP increase. Nonspecific effects of odors on Ca^{2+} and cGMP levels were excluded because the odor mix had no effect on the majority of OSNs tested (~70%), although the nonresponsive neurons presented a normal rise in Ca^{2+} (Figure 1H) or cGMP when subsequently tested with KCl (Figure 3H). Moreover, upon odor stimulation, no Ca^{2+} or cGMP rise could be observed in HEK cells expressing the cGMP sensor (Figure 3I) and/or loaded with fura-2 (data not shown).

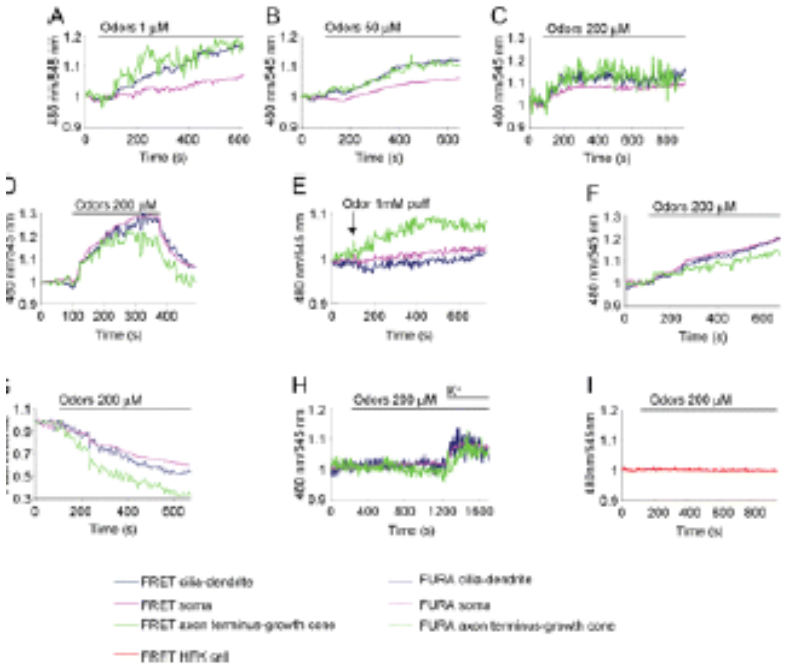

Figure 3: cGMP dynamics in OSNs upon physiological stimuli. **A – E**, examples of cGMP kinetics in OSNs treated with different concentrations of odors, bath applied: odors 1 µM (**A**); odors 50 µM (**B**); odors 200 µM (**C**); odors 200 µM bath applied for 5 – 7 min and then washed away (**D**); cGMP rise in response to odors (1 mM in the pipette) focally applied to the axon terminal (**E**). **F**, **G**, examples of cGMP dynamics (FRET, 480/545 nm)(**F**) and calcium dynamics (fura-2, 380 nm component)(**G**) in the same neuron, transfected with the sensor for cGMP and loaded with fura-2, treated with odors (200 µM, bath applied). **H**, example of cGMP dynamics in an OSN non responsive to odors (200 µM, bath applied), but responsive to KCl (50 mM) subsequently bath applied. **I**, example of cGMP dynamics in a HEK cell, not expressing OR (used as controls), treated with odors (200 µM, bath applied). Solid lines: cGMP dynamics (**A – F**, **H**); dotted lines: Ca^{2+} dynamics (**G**). Blue line, cilia - dendrite; pink line, soma; green line, axon terminus - growth cone; red line, cGMP kinetics in HEK cell (**I**).

3.4 Molecular mechanism underpinning cGMP increase

The question then arises as to the molecular mechanism underpinning the cGMP increase upon odor treatment. Since the OSNs express both soluble and particulate GCs, we first investigated which enzyme is activated upon OR

stimulation. We analyzed the ability of the inhibitor LY83583 to block sGC activity in living OSNs. cGMP increase, upon sGC stimulation by the NO donor SNAP, was abolished in presence of the sGC inhibitor LY83583 (Figure 4A; n = 10). However, when the same neuron was subsequently stimulated with SNAP alone, after washing away the inhibitor, it exhibited a prompt cGMP response (Figure 4B). To assess the role of sGC in the cGMP rise upon odor stimulation, OSNs were stimulated with odors in the presence of the inhibitor LY83583. In these conditions, no cGMP increase could be detected in the entire OSN (Figure 4C). However, a rise in cGMP, in the same neuron, was observed after washing away the inhibitor and the subsequent application of odors (Figure 4D).

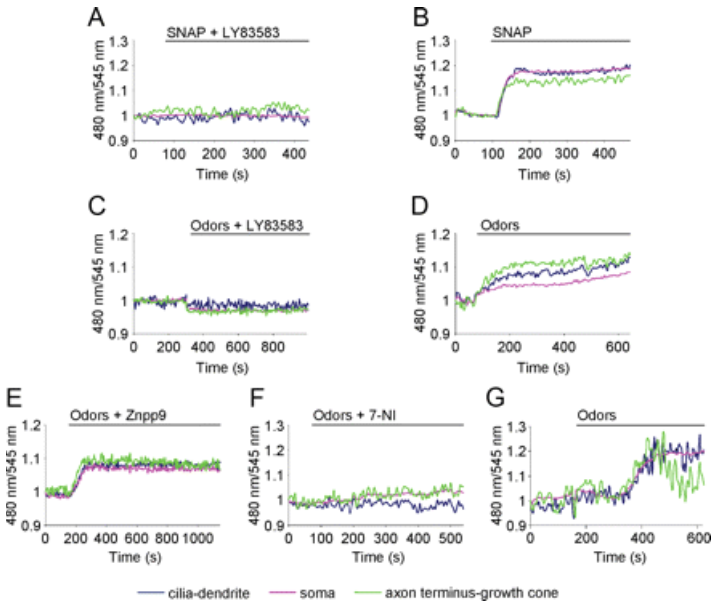

Figure 4: Molecular mechanism of GC activation. **A, B**, examples of cGMP dynamics in the same OSN treated with the NO donor SNAP (300 µM) along with the sGC inhibitor LY83583 (10 µM)(**A**), and with SNAP after washing away the inhibitor LY83583 (**B**). **C, D**, the same OSN treated with odors (200 µM) in the presence of sGC inhibitor LY83583 (10 µM)(**C**), and with odors only (200 µM) after washing away the inhibitor LY83583 **(D**). **E**, an OSN treated with odors (200 µM) in the presence of HO inhibitor ZnPP9 (10 µM). **F, G**, the same OSN treated with odors (200 µM) in the presence of NOS inhibitor 7 - NI (30 µM)(**F**), and with odors only (200 µM) after washing away the inhibitor 7 - NI (**G**). Stimuli were all bath applied. Blue line, cilia - dendrite; pink line, soma; green line, axon terminus - growth cone.

It is known that sGCs are activated by gaseous messengers, NO or CO according to the stage of development of the OSNs. NO is thought to act only during development and in regenerating axons, while CO is active in adult OSNs (Roskams et al., 1994). Odor treatment in the presence of ZnPP9 (Figure 4E), an inhibitor of HO, which synthesizes CO, caused a cGMP increase that

was indistinguishable from that of controls (odors without ZnPP9). Again, the time to reach half - maximal concentration was faster at cilia - dendrite and axon terminus - growth cone than at the soma level (n = 7, $t_{1/2}$: cilia - dendrite = 2.9 ± 0.7 min; soma = 3.4 ± 0.6 min; axon terminus - growth cone = 2.9 ± 0.5 min; *t* test $t_{1/2}$: cilia - dendrite - soma, **p* = 0.03; axon terminus – growth cone - soma, **p* = 0.04; cilia - dendrite - axon terminus – growth cone, *p* = 0.9). On the contrary, OSNs treated with odors in the presence of 7 - NI, an inhibitor of NOS, which synthesized NO, did not show any rise in cGMP levels (Figure 4F). The same neurons, after washing away the inhibitor, presented a positive response to the odor mixture applied subsequently (n = 5; Figure 4G).

The next question is to determine the mechanism coupling sGC to OR activation. The most obvious candidate is cAMP, which is synthesized upon odorant binding to their receptors. To test this hypothesis, OSNs were treated with odors in the presence of the AC blocker SQ22536 (incubated for 15 min before odor application). Under these conditions, odor stimulation did not induce any rise in cGMP. However, when these same neurons not responsive to the odor mix in the presence of SQ22536, were subsequently challenged with odors after washing away the inhibitor, they exhibited a prompt rise in cGMP (n = 5; Figure 5A, B). To confirm that cGMP increases were causally dependent on the cAMP rise, the OSNs transfected with the sensor for cGMP were treated with forskolin, a generic AC activator. After treatment with forskolin, an increase in cGMP was observed in all neurons (Figure 5C; n = 5, $t_{1/2}$: cilia - dendrite = 1.7 ± 0.2 min; soma = 2 ± 0.4 min; axon terminus – growth cone = 1.7 ± 0.4 min). Unlike the case of odors (when only a fraction of the neurons tested responded with a cGMP rise) the vast majority (90%) of the OSNs tested responded to forskolin.

The final and most important mechanistic question is to assess how cAMP can activate sGC. We first considered the possibility that the link between cAMP and sGC was PKA, the principal target of cAMP. However, when OSNs were treated with the odor mixture in the presence of a PKA inhibitor (H89 or KT5720), they presented a rise in cGMP as in controls (i.e., neurons treated with odors only)(Figure 5D; n = 10, $t_{1/2}$: cilia - dendrite = 2.9 ± 0.5 min; soma = 3.4 ± 0.5 min; axon terminus - growth cone = 2.7 ± 0.5 min; *t* test $t_{1/2}$: cilia - dendrite - soma, **p* = 0.04; axon terminus - growth cone - soma, ***p* = 0.006;

cilia - dendrite - axon terminus – growth cone, p = 0.3). The other potential target of cAMP is Epac, directly activated by cAMP (Bos 2003). Since we are studying developing neurons, we analyzed the expression of Epac1 in a primary culture of OSNs. As shown in Figure 5E, Epac1 is homogeneously expressed in the entire OSN, including the axon terminus. Given that no selective inhibitor of Epac is commercially available, we treated OSNs with 8 – CPT – 2' – O – Me - cAMP, a selective and potent activator of Epac with no effect on PKA (Enserink et al., 2002). Moreover, 8 – CPT – 2' – O – Me - cAMP is also known to be totally ineffective on cAMP - dependent ion channels (Bos 2003). OSNs treated with Epac activator presented a prompt rise in cGMP in the whole neuron (Figure 5F; n = 8, $t_{1/2}$: cilia - dendrite = 2.4 ± 0.3 min; soma = 2.8 ± 0.4 min; axon terminus - growth cone = 2.1 ± 0.4 min) and, also in this case, as for the other pharmacological agents, the vast majority (90%) of the tested neurons responded to the Epac activator. NOS is known to be activated by Ca^{2+} - calmodulin. Thus, the simplest explanation for the above results is that NO production (and thus sGC activation) would be dependent on cAMP – triggered Ca^{2+} increases (through CNG channels and other mechanisms). Indeed, a Ca^{2+} increase resulted in a clear increase in cGMP in the OSN (Figure 5G; n = 4, $t_{1/2}$: cilia - dendrite = 2.6 ± 0.4 min; soma = 2.9 ± 0.3 min; axon terminus - growth cone = 2.5 ± 0.3 min).

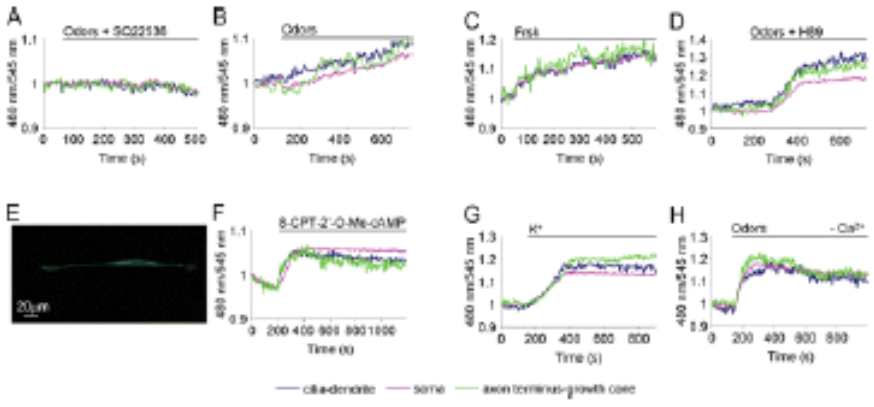

Figure 5: Molecular mechanism underpinning cGMP rise. **A**, **B**, examples of the spatio - temporal dynamics of cGMP in the same OSN treated with odors (200 µM) in presence of AC inhibitor SQ22536 (30 µM)(**A**) and with odors only (200 µM) after washing away the inhibitor SQ22356 (**B**). **C**, **D**, OSNs treated with Frsk (25 µM), AC activator (**C**), and odors (200 µM) in the presence of the PKA inhibitor H89 (10 µM)(**D**). **E**, example of an OSN immunopositive for Epac1. The immunofluorescence is present in the entire neuron. Scale bar, 20 µM. **F – H**, examples of cGMP dynamics in OSNs treated with Epac activator 8-CPT-2'-O-Me-cAMP (30 µM)(**F**), KCl (50 mM)(**G**), and odors (200 µM), in a Ca^{2+} - free Ringer's solution (**H**). Stimuli were all bath applied. Blue line, cilia - dendrite; pink line, soma; green line, axon terminus - growth cone.

We next challenged the OSNs with odors while bathed in a Ca^{2+} - free Ringer's solution (supplemented with 1mM EGTA), thus preventing any influx of Ca^{2+} from the medium. However, in these conditions, a clear rise in cGMP was still observed, indicating that odors may also cause the release of Ca^{2+} from intracellular stores. The time to reach half - maximal concentration ($t_{1/2}$) was longer, although not significantly, with respect to that observed in OSNs in normal Ringer's solution (Figure 5H; n = 12, $t_{1/2}$: cilia - dendrite = 3.2 $\pm$ 0.6 min; soma = 3.7 $\pm$ 0.7 min; axon terminus - growth cone = 3.1 $\pm$ 0.6 min; *t* test $t_{1/2}$: cilia - dendrite - soma, **p* = 0.01; axon terminus - growth cone - soma, ***p* = 0.005; cilia - dendrite - axon terminus - growth cone, *p* = 0.4). Furthermore, the number of responsive neurons in Ca^{2+} - free Ringer's solution was slightly lower (22 vs 30%) than in normal solution. These results suggested that the release of Ca^{2+} from intracellular stores is sufficient, in most cells, to activate NOS and thus to cause a rise of cGMP.

How could Epac activation induce Ca^{2+} mobilization from stores? One likely possibility is via the production of IP3. Indeed, among the targets of Epac there is PLCε, whose activation results in diacylglycerol and IP3 formation and subsequent release of Ca^{2+} from stores (Schmidt et al., 2001; Bos 2003). To test this possibility, OSNs were loaded with the Ca^{2+} indicator fura-2 and then challenged with forskolin (25 μM, n = 11; Figure 6A), with the Epac activator 8 – CPT – 2' – O – Me - cAMP (30 μM, n = 10; Figure 6B), or with odors (n = 3, data not shown) while bathed in a Ca^{2+} - free Ringer's solution. A slow and sustained rise in $[Ca^{2+}]_i$ was observed under these conditions. In a few cells, we observed a lag phase between the application of the stimulus and the onset of the response. The most important IP3 – sensitive Ca^{2+} store in non muscle cells is the endoplasmic reticulum (ER). To evaluate the ER distribution in the OSNs, the cells were immunostained with antibodies against two canonical markers of the organelle, SERCA and calreticulin (Rizzuto and Pozzan, 2006). As shown in Figure 6C and D, both antibodies decorated a delicate reticular structure in dendrite, soma, and axon. To directly evaluate the release of Ca^{2+} from the ER, primary cultures of OSNs were transiently transfected with D1ER, a genetically encoded Ca^{2+} sensor targeted to the ER lumen (Rudolf et al., 2006). OSNs transfected with D1ER (Figure 6E) presented a diffuse fluorescence in dendrite, soma and axon similar to the labeling observed in OSNs immunostained with

antibodies against SERCA and calreticulin (Figure 6C, D). Changes in $[Ca^{2+}]$ER result in modifications of FRET in D1ER and can be conveniently monitored by the changes of the YFP/CFP fluorescence emission ratio (545/480 nm). A drop in $[Ca^{2+}]$ER is associated to a reduction of the YFP/CFP fluorescence emission ratio (545/480 nm). As shown in Figure 6F, OSNs transfected with D1ER and challenged, in normal Ca^{2+} - containing medium, with the Epac activator (30 μM, n = 6) presented a slow and sustained drop in $[Ca^{2+}]$ER (corresponding to Ca^{2+} release from stores) in dendrite, soma, and axon terminus. As well, when OSNs, transfected with D1ER, were treated with odors (200 μM), a slow and prolonged reduction in $[Ca^{2+}]$ER signal was observed in the entire OSN (n = 8; Figure 6G). When the same experiments were performed in Ca^{2+} - free Ringer's solution, the $[Ca^{2+}]$ER drop was similar or larger to the one observed in Ca^{2+} - containing medium.

Most important from a mechanistic point of view, the Ca^{2+} release from the ER was abolished when responsive neurons were subsequently rechallenged with odors in the presence of the PLCε blocker, U73122 (30 μM, incubated for 15 min before odor application; n = 6; Figure 6H). To exclude the possibility that the lack of response to odors in the presence of the inhibitor of PLCε was due to desensitization of the OR after the first stimulation, the odor mix was first applied in the presence of the inhibitor and subsequently after washing away the inhibitor. No release of Ca^{2+} was detected at all in the presence of the inhibitor, whereas it was observed upon removal of the blocker (data not shown). To directly investigate the role of Ca^{2+} release from stores, via PLCε, in cGMP synthesis, OSNs transfected with the sensor for cGMP, Cygnet 2.1 (while bathed in Ca^{2+} - free Ringer's solution) were treated with odors in the presence of the inhibitor of PLCε. Under these conditions, no rise of cGMP could be detected. However, after washing away the inhibitor, the same neurons presented a clear rise in cGMP (n = 5; Figure 6I – J).

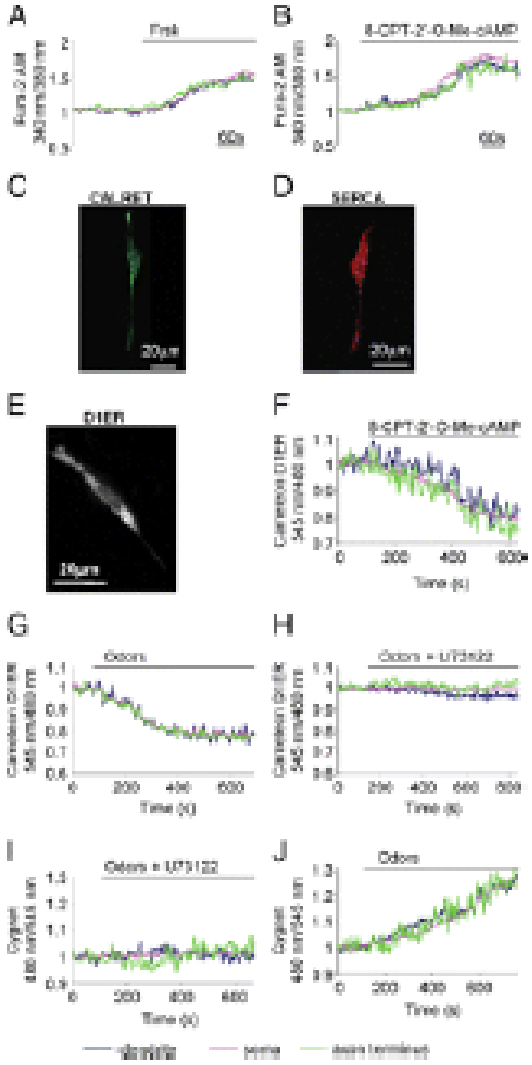

Figure 6: Mobilization of Ca^{2+} from stores and cGMP synthesis. **A**, **B**, normalized fluorescence ratio changes (340/380 nm) in OSNs loaded with fura-2 and challenged with Frsk (25 μM), an AC activator (**A**) and Epac activator 8-CPT-2′-O-Me-cAMP (30 μM)(**B**). **C**, **D**, examples of OSNs immunopositive for two canonical ER markers: calreticulin (**C**) and SERCA (**D**). **E**, example of an OSN transiently transfected with the genetically encoded Ca^{2+} sensor, targeted to the ER lumen D1ER. **F – H**, Ca^{2+} dynamics in OSNs transiently transfected with D1ER and treated with Epac activator 8-CPT-2′-O-Me-cAMP (30 μM)(**F**). **G**, **H**, the same neuron, treated with odors (200 μM)(**G**) and with odors in the presence of the PLCε inhibitor U73122 (30 μM)(**H**). **I**, **J**, cGMP dynamics in the same OSN transiently transfected with the sensor for cGMP, Cygnet, and challenged with odors (200 μM) in the presence of the PLCε inhibitor U73122 (30 μM)(**I**) and with odors only (200 μM), and after washing away the inhibitor (**J**). Stimuli were all bath applied. In **A**, **B**, **I**, and **J**, OSNs were bathed in Ca^{2+} - free Ringer's solution. Blue line, cilia - dendrite; pink line, soma; green line, axon terminus – growth cone. Scale bar, 20 μm.

3.5 cGMP action at the nuclear level

cGMP can exert its action both locally at the cilia - dendrite and at the axon terminus where it is produced. However, since it is involved in long - term response to odors, it may also act at the nuclear level, regulating gene expression (e.g., via P - CREB). To investigate this possibility, we treated OSNs with 8Br - cGMP (bath applied), a membrane - permeable analogue of cGMP, and we looked for P - CREB at the nuclear level (n = 4 cultures). Upon treatment with 8Br - cGMP, OSNs exhibited an increased immunopositive labeling for P - CREB in the nuclei (Figure 7A–C; P - CREB level, controls vs treated, *t* test, ***p = 0.001). The question then arises as to the physiological significance of these findings *in vivo*. To assess whether the cGMP produced

upon activation of the OR at the axon terminus can exert its action not only locally, but also at the nuclear level, 8Br – cGMP was applied to the olfactory bulbs *in vivo*. Within 30 – 40 min from 8Br - cGMP application it was possible to detect a large increase in P - CREB in the nuclei of OSNs, in a small dorsal portion (14%), only in few slices of the epithelium, approximately corresponding to the dorsal portion (20%) of the OB bathed with 8Br - cGMP (n = 4 mice, P - CREB level, controls vs 8Br - cGMP, *t* test, ***p = 0.001; Figure *7*D – H). Finally, and most relevant, local odor application on the bulbs was followed by the presence of P - CREB in the OSN nuclei within 30 – 40 min (n = 4 mice, P - CREB level, controls vs odors, *t* test, *p = 0.02; Figure 7I). However, when odors were applied on the bulbs in presence of the sGC inhibitor LY83583 (n = 5 mice), we could still reveal the presence of P - CREB in the nuclei, as shown in Figure *7J* and *K* (P - CREB level, controls vs odors + LY83583, *t* test, *p = 0.03; P - CREB level, odors vs odors + LY83583, p = 0.8). Together, these results indicate that a rise in cGMP is sufficient, but not necessary, to induce phosphorylation of CREB at the nuclear level.

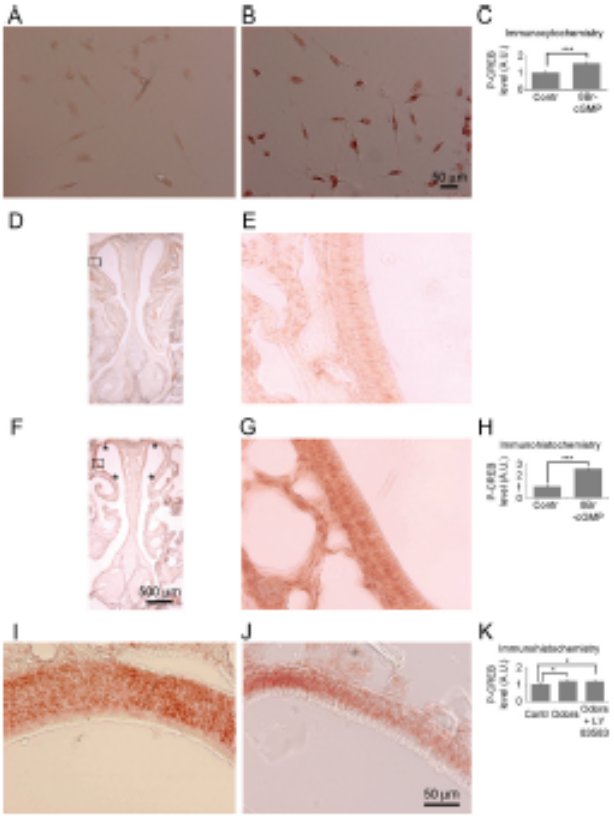

Figure 7: Phosphorylation of CREB in OSNs. **A**, **B**, primary culture of OSNs immunostained with an antibody against P - CREB in controls (i.e., OSNs treated with Ringer's solution)(**A**) and after treatment with the membrane - permeable cGMP analog 8Br-cGMP (50 µM)(**B**). **C**, summary of the experiments performed in **A** and **B**, normalized P - CREB level (***p < 0.001). **D**, **F**, coronal sections of the olfactory epithelium immunostained with an antibody against P - CREB after application of Ringer's solution (controls)(**D**) and 8-BrcGMP (250 µM)(**F**) at the axon terminus of the OSNs in the olfactory bulb *in vivo*. Asterisks signify the portion of the epithelium with increased P - CREB levels. Scale bars: **D**, **F**, 500 µm; **E**, **G**, higher magnification (20x) of the epithelium indicated in the squares in **D** and **F**, respectively. **H**, summary of experiments in **D – G** (normalized P - CREB level, ***p < 0.001). **I**, **J**, portions of coronal sections of the olfactory epithelium immunostained with an antibody against P - CREB, after odors (1 mM)(**I**) and odors (1 mM) in the presence of the sGC inhibitor LY83583 (250 µM) were applied at the axon terminus of the OSNs in the olfactory bulb *in vivo*. **K**, summary of experiments performed in **I** and **J**, normalized P - CREB level, controls versus odors, *p = 0.02; controls versus odors + LY83583, *p = 0.03; odors versus odors + LY83583, p = 0.8. A.U, Arbitrary units. Scale bar, 50 µm.

3.6 Ca^{2+} dynamics in OSN axon terminus – growth cone in response to extracts from the olfactory bulb

The question then arose on the possible natural ligands able to activate and trigger the intracellular cascade of cAMP, Ca^{2+} and cGMP coupled to the OR expressed at the axon temrinus - growth cone. Our hypothesis was that a few molecules, present in gradient in the OB, could bind and activate the OR. To ascertain this hypothesis, primary cultures of OSNs were loaded with the Ca^{2+} indicator fura-2 and challenged with both lysate and dialysate from the olfactory bulb, focally applied to the axon terminus – growth cone with a glass pipette (puff). As shown in Figure 8, an immediate and transient rise in $[Ca^{2+}]_i$ could be observed in the axon terminal of OSNs in response to both stimuli (lysate: n = 62, response ($\Delta R/R_0$ %) = 101.9 ± 13.3, responsive cells 56.4%; dyalisate: n = 73, response ($\Delta R/R_0$ %) = 42.1 ± 7.0, responsive cells 42.4%; t test lysate – dialysate, ***p = 0.0002).

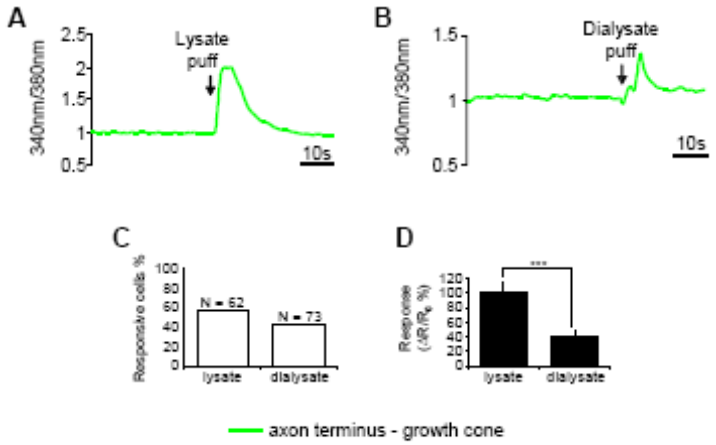

Figure 8: Ca^{2+} dynamics in OSN axon terminal in response to extracts from the OB. **A**, **B**, examples of normalized fluorescence ratio changes (340/380 nm) in OSNs loaded with fura-2 and challenged with bulb lysate (**A**), bulb dyalisate (**B**), focally applied to the axon terminus – growth cone with a glass pipette (puff). **C**, summary of responsive cells (%). **D**, summary of the response, measured as increment (%) of the ratio at the peak of the response (R_{max}) respect to the ratio at baseline (R_0), $\Delta R/R_0$ (%), where $\Delta R = R_{max} - R_0$ (P = 0.0002***, bars, SEM). Green line, axon terminus – growth cone.

In order to fractionate the OB dialysate we decided to perform a gel filtration (GF) chromatography from which three fractions were obtained. After testing all of them on OSNs, we found that only the third peak (GF fract3) was able to induce a Ca^{2+} rise in the axon terminal of OSNs loaded with the Ca^{2+} indicator fura-2 (Figure 9; GF fract1: n = 21, responsive cells 0%; GF fract2: n = 20,

responsive cells 0%; GF fract3: n = 31, responsive cells 25.8%, response ($\Delta R/R_0$ %) = 55.8 ± 13.9). To further fractionate the GF fract3, an ion exchange chromatography (IEC) was performed and we obtained four peaks. Among these fractions, the first and the second one (IEC fract1 and IEC fract2) were able to elicit higher Ca^{2+} responses in a larger number of cells (Figure 9; IEC fract1: n = 92, responsive cells 43.5%, response ($\Delta R/R_0$ %) = 188.1 ± 22.5; IEC fract2: n = 95, responsive cells 44.3%, response ($\Delta R/R_0$ %) = 119.9 ± 18.1; IEC fract3: n = 20, responsive cells 5%, response ($\Delta R/R_0$ %) = 10.6 ; IEC fract4: n = 20, responsive cells 10%, response ($\Delta R/R_0$ %) = 46.3 ± 29.3).

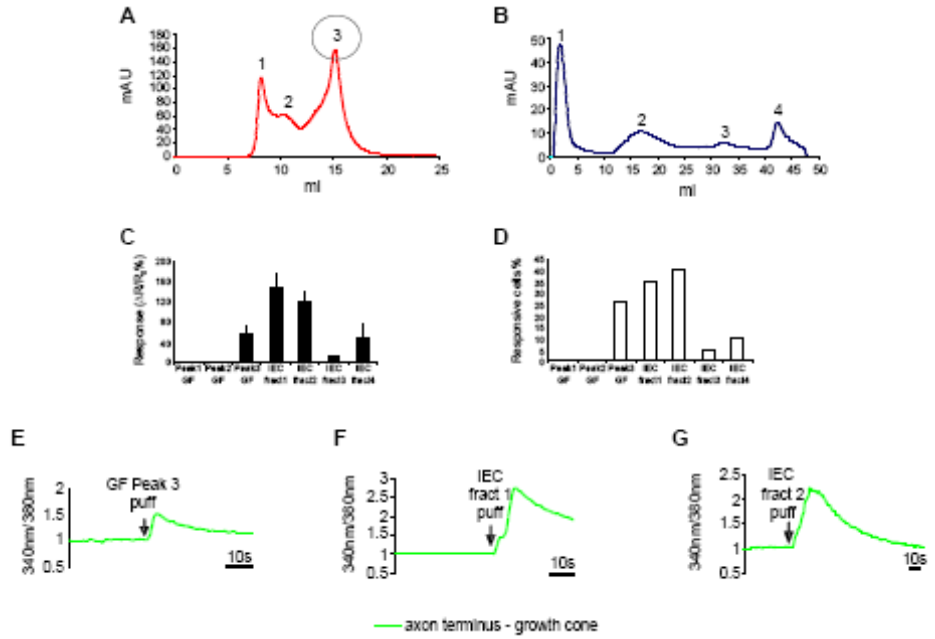

Figure 9: Ca^{2+} dynamics in OSN axon terminal in response to chromatographic products. **A**, chromatogram of the gel filtration chromatography of the dyalisate from the OB. **B**, chromatogram of the ion exchange chromatography of the third peak product of the gel filtration chromatography. **C**, summary of Ca^{2+} response $\Delta R/R_0$ %, bars, SEM. **D**, summary of responsive cells (%). **E – G**, examples of Ca^{2+} dynamics in OSNs loaded with fura-2 and challenged with different chromatographic peaks, focally applied to the axon terminus – growth cone.

To assess whether the molecules present in the active pools were proteins we denatured the active pools of molecules by heating or treating with protease K and we then applied them to the OSNs. Namely, OSNs were loaded with the Ca^{2+} indicator fura-2 and focally challenged at the axon terminus – growth cone with IEC fract1 heated at 99° C. In these condition s the majority of cells tested did not exhibit any rise in Ca^{2+} , but a few residual Ca^{2+} responses were observed in a few cells (heated IEC fract1: n = 21, response ($\Delta R/R_0$ %) = 80.5 ± 41.1, responsive cells 19%). However, when the IEC fract1 was treated with

protease K, an enzyme known to digest proteins, the Ca^{2+} responses were completely abolished (Figure 10). On the other hand, the heating at 99° C of IEC fract2 was sufficient to completely abolish its activity on the OSN axon terminal (heated fract2: n = 20, responsive cells 0%; Figure 10). These data demonstrate that this pool of molecules from the olfactory bulb is constituted by proteins.

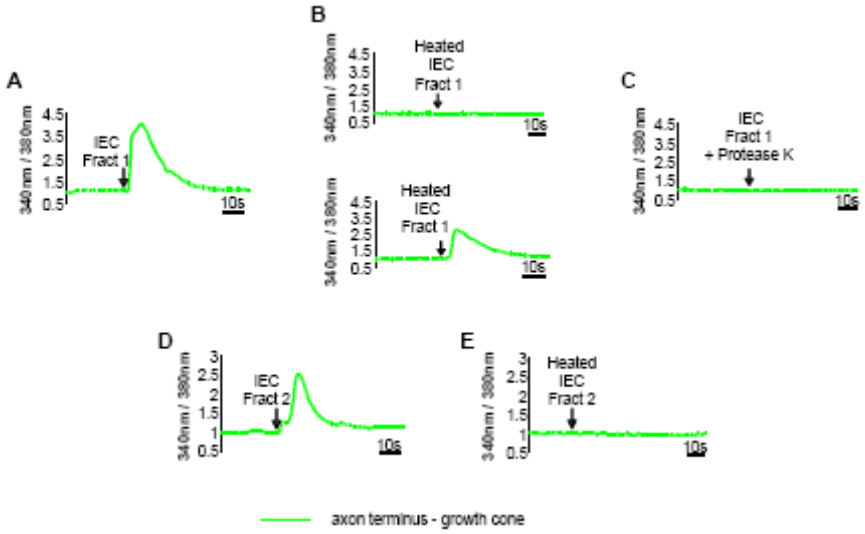

Figure 10: IEC fract1 and IEC fract2 are composed by proteins. **A – E**, examples of normalized fluorescence ratio changes (340/380 nm) in OSNs loaded with fura-2 and challenged with the IEC fract1 product (**A**), the same chromatogram product heated at 99° C (**B**) or treated with protease K (**C**), the IEC fract2 (**D**) and the same chromatogram product heated at 99° C (**E**).

3.7 Ca^{2+} dynamics in HEK cells challenged with IEC fractions and odors

To ascertain that the Ca^{2+} rises observed in the OSN axon terminal upon stimulation with the OB extracts were due to the activation of the odorant receptor at this location, we tested these same molecules from the olfactory bulb on HEK cells, transfected with different types of ORs. HEK cells transfected with the empty pCI vector (without the OR) were used as controls. As expected, no Ca^{2+} rise was observed in response to odors (100 μM, bath applied), in HEK cells loaded with the Ca^{2+} indicator fura-2 and transfected with the empty vector (not expressing the OR gene). However, the same cells challenged with a puff of IEC fraction 1 showed a clear and prompt rise in Ca^{2+} (IEC fract1: n = 16, response ($\Delta R/R_0$ %) = 55.2 ± 22.5, responsive cells 25%; Figure 11). ATP (100 μM, bath applied) or carbachol (CCH, 100 μM, bath

applied) were used as controls of vitality. These data suggest that IEC fract1 may elicit an increase in $[Ca^{2+}]_i$ through a different pathway to that involving the activation of the odorant receptor.

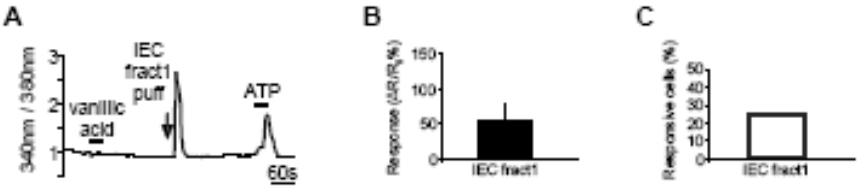

Figure 11: Ca^{2+} dynamics in HEK cells challenged with IEC fract1 and odors. **A**, example of normalized fluorescence ratio changes (340/380 nm) in a HEK cell transfected with the pCI vector (without the OR), loaded with fura-2 and challenged with an odor (vanillic acid, 100 μM), IEC fract1 puff and ATP (100 μM, used as control of vitality). **B**, summary of the response $\Delta R/R_0$ (%), bars, SEM. **C**, summary of responsive cells (%).

When HEK cells loaded with fura-2 were transfected with the empty pCI vector (without the OR) and focally stimulated with IEC fract2, they did not exhibit any rise in Ca^{2+} (IEC fract2: n = 76, responsive cells 0%; Figure 12). However, the same HEK cells showed an increase in Ca^{2+} levels when challenged with ATP or CCH (100 μM, bath applied).

IEC fract2 was then tested on HEK cells transfected with different types of ORs (OREG, ORS6, Olfr62, OR23, ORM71) and loaded with the calcium indicator fura-2. In these conditions, similar Ca^{2+} responses were elicited by the IEC fract2 (locally applied) and the specific ligand (i.e. odor, locally applied) for the OR transfected in the HEK cells (100 μM, bath applied). Only HEK cells expressing the OR23 did not present a rise in Ca^{2+} upon stimulation with IEC fract2, although they exhibited a prompt rise in Ca^{2+} upon stimulation with lyral (the specific ligand of OR23)(ORS6: n = 63, response ($\Delta R/R_0$ %) = 77.0 ± 11.9, responsive cells 28.6%; Olfr62: n = 122, response ($\Delta R/R_0$ %) = 46.2 ± 5.9, responsive cells 18%; OR23: n = 58, responsive cells 0%; OREG: n = 78, response ($\Delta R/R_0$ %) = 91.3 ± 6.5, responsive cells 71.8%; M71: n = 63, response ($\Delta R/R_0$ %) = 81.3 ± 20.5, responsive cells 6.3%; Figure 12).

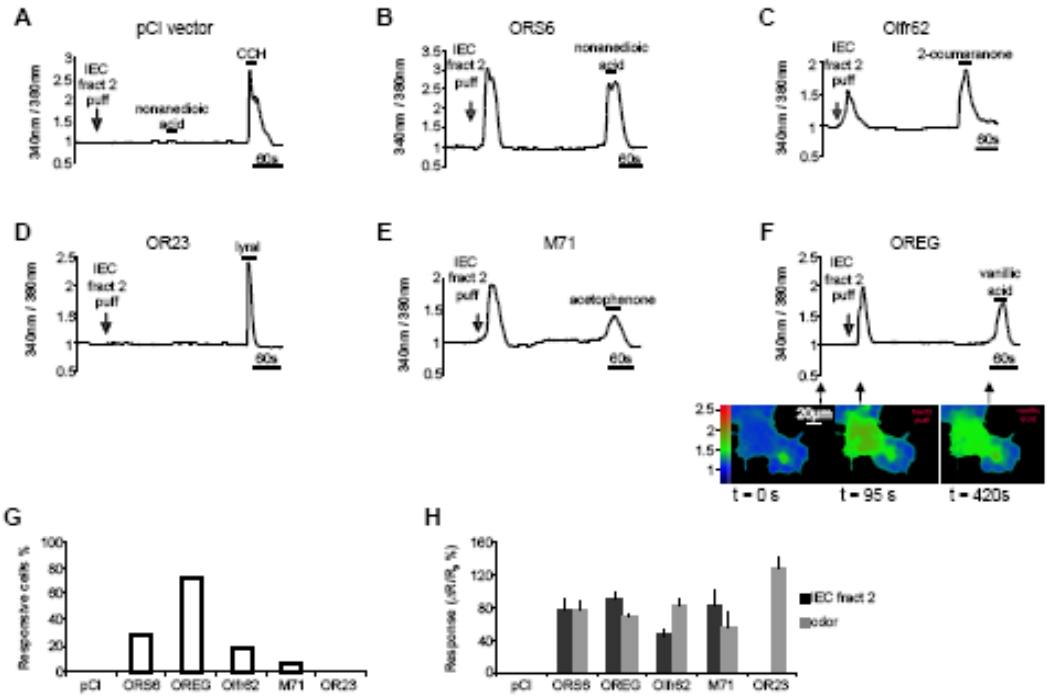

Figure 12: IEC fract2 activates odorant receptors in HEK cells. **A**, example of normalized fluorescence ratio changes (340/380 nm) in a HEK cell transfected with the pCI vector (without the OR), loaded with fura-2 and challenged with a puff of IEC fract2, an odor (nonanedioic acid, 100 µM) and carbachol (CCH, 100 µM, used as control of vitality). **B – F**, examples of Ca^{2+} dynamics in HEK cells transfected with different ORs, loaded with fura-2 and challenged with a puff of IEC fract2 and the odor specific for the transfected OR. **F**, bottom, representative pseudocolor images of the Ca^{2+} responses in a HEK cell transfected with OREG, before (time = 0 s) and after a IEC fract2 puff (time = 95 s) and vanillic acid (100 µM, time = 420 s). **G**, summary of responsive cells (%). **H**, summary of the response $\Delta R/R_0$ %, bars, SEM.

3.8 Ringer's solution or cerebellum lysate do not activate the OR in HEK cells and in OSN axon terminal

It is known that the odorant receptor responds not only to odorants, but also to mechanical stimuli, such as pressure (Grosmaitre et al., 2007). In order to assess whether the Ca^{2+} rises observed in HEK cells could be due to the mechanical activation of the OR, we performed a series of control experiments on HEK cells and OSNs challenged with Ringer's solution or cerebellum lysate, locally applied with a glass pipette (the concentration of the cerebellum lysate in the pipette was 1 µg/µL). HEK cells were transfected with the different types of ORs and loaded with the Ca^{2+} indicator fura-2. As shown in Figure 13, when the cells were challenged with the Ringer's solution, the majority of them did not exhibit any Ca^{2+} rise (ORS6: n = 30, responsive cells 0%; OREG: n = 50,

responsive cells 0%; Olfr62: n = 33, response ($\Delta R/R_0$ %) = 112.2 ± 27.3, responsive cells 6.1%). However, the same cells non responsive to Ringer's solution presented an immediate and transient rise in Ca^{2+} when stimulated with the odor specific for the transfected OR (100 μM, bath applied). Similar results were found when HEK cells transfected with the different ORs and loaded with fura-2 were challenged with the cerebellum lysate (Figure 13; ORS6: n = 62, responsive cells 0%; OREG: n = 63, response ($\Delta R/R_0$ %) = 86.1 ± 66.8, responsive cells 3.2%; Olfr62: n = 37, responsive cells 0%). Also in this case, HEK cells non responsive to the cerebellum lysate exhibited a prompt Ca^{2+} response when challenged with the odor specific for the transfected OR (100 μM, bath applied). These data exclude a possible activation of the OR by the mechanical pressure of stimuli locally applied and confirm that in HEK cells the odorant receptor is activated by the pool of molecules from the olfactory bulb.

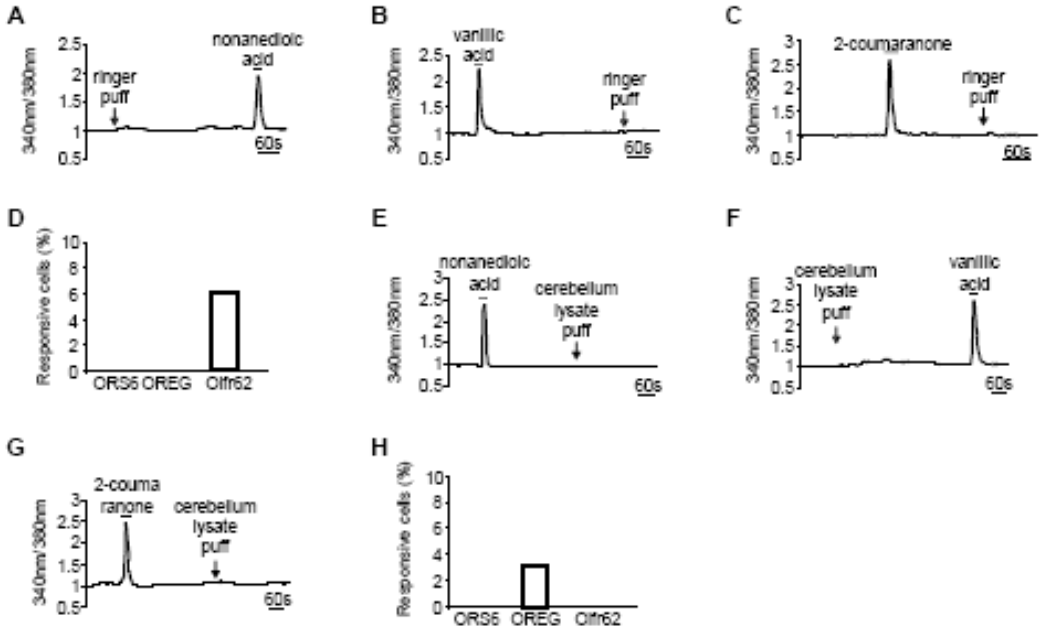

Figure 13: Ca^{2+} dynamics in HEK cells challenged with Ringer's solution or cerebellum lysate. **A – C**, examples of normalized fluorescence ratio changes (340/380 nm) in HEK cells transfected with different ORs, loaded with fura-2 and challenged with a Ringer's solution puff and the odor specific for the transfected OR (100 μM, bath applied). **D**, summary of responsive cells (%) to the Ringer's solution. **E – G**, examples of normalized fluorescence ratio changes in HEK cells transfected with different ORs, loaded with fura-2 and challenged with a cerebellum lysate puff and the odor specific for the transfected OR (100 μM, bath applied). **H**, summary of responsive cells (%) to the cerebellum lysate.

To exclude a possible activation of the OR by the pressure of the stimuli locally applied with a glass pipette at the axon terminal of OSNs, we performed a series of control experiments in which OSNs were loaded with the calcium

indicator fura-2 and challenged with Ringer's solution and cerebellum lysate, focally applied to the axon terminus – growth cone with a glass pipette. In these conditions, no rise in Ca^{2+} was detected in OSNs (Ringer's solution: n = 11, responsive cells 0%; cerebellum lysate: n = 26, responsive cells 0%). However, the same OSNs non responsive to these two unspecific stimuli, showed a clear and prompt rise in $[Ca^{2+}]$ when loaded with the Ca^{2+} indicator fura-2 and treated with forskolin (frsk, 25 μM, bath applied), a generic adenylyl cyclase (AC) activator (Figure 14). These results indicate that Ca^{2+} signal induced by chromatographic products from the OB extract is certainly due to this pool of molecules and not to any unspecific stimulus (i. e. mechanical stimulus).

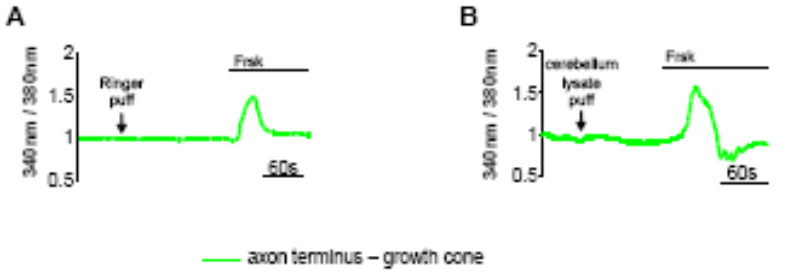

Figure 14: Ringer's solution or cerebellum lysate do not elicit Ca^{2+} rise in OSN axon termini. **A – B**, examples of normalized fluorescence ratio changes (340/380 nm) in OSNs loaded with fura-2 and challenged with a Ringer's solution puff (**A**) and a cerebellum lysate puff (**B**), focally applied to the axon terminus – growth cone, and Frsk (25 μM, bath applied).

3.9 Stimulation with IEC fract2 induces Ca^{2+} entry in OSNs via activation of CNG channels

We then investigated whether the increase in $[Ca^{2+}]$ in the axon terminus – growth cone of OSNs upon stimulation with IEC fract2, was due to the influx of Ca^{2+} through CNG channels. To assess this possibility, we performed Ca^{2+} imaging experiments on OSN axon terminal in presence of SQ22536, an adenylyl cyclase blocker (30 μM, bath applied). These experiments were performed in presence of tetrodotoxin (TTX, 4 μM) in the bath, to prevent any Ca^{2+} influx through the voltage – gated Ca^{2+} channels. OSNs were loaded with the Ca^{2+} indicator fura-2 and focally challenged to the axon terminal with a IEC fract2. As shown in Figure 15, when the OSNs were stimulated with IEC fract2 in presence of the AC inhibitor, they did not present any change in $[Ca^{2+}]$. However, the same non responsive OSNs in presence of SQ22563, exhibited a clear and prompt rise in Ca^{2+} when the inhibitor was washed away and the cells

were subsequently challenged with IEC fract2 (with SQ: n = 68, response ($\Delta R/R_0$ %) = 17.1 ± 7.5, responsive cells 8.8%; w/o SQ: n = 68, response ($\Delta R/R_0$ %) = 80.6 ± 25.2, , responsive cells 17.6%, *p = 0.02). These data demonstrate that the Ca^{2+} rises observed in OSN axon terminus – growth cone upon stimulation with IEC fraction 2 are due to the influx of Ca^{2+} through the CNG channels.

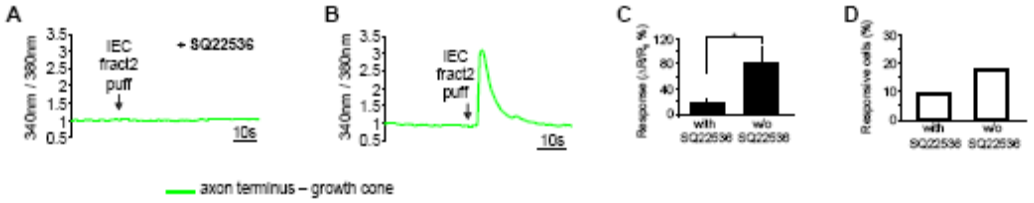

Figure 15: Ca^{2+} influx through CNG channels in OSNs challenged with IEC fract2. **A – B**, examples of normalized fluorescence ratio changes (340/380 nm) in OSNs loaded with fura-2 and focally challenged at the axon terminus – growth cone with IEC fract2 in presence of SQ22536 (**A**) and without SQ22536 (**B**). **C**, summary of Ca^{2+} response ($\Delta R/R_0$ %), bars, SEM. **D**, summary of responsive cells (%).

3.10 cAMP dynamics in OSNs in response to IEC fraction 2

In OSNs Ca^{2+} dynamics is strictly dependent on cAMP kinetics. We then studied the spatio – temporal dynamics of cAMP in OSN axon terminus – growth cone upon stimulation with IEC fraction 2. Primary cultures of OSNs transiently transfected with the genetically encoded sensor for cAMP (Epac) were challenged with IEC fraction 2, focally applied to the axon terminal, and forskolin, a generic activator of ACs (frsk 25 μM, bath applied). As shown in Figure 16, IEC fract2 was able to elicit a slow and sustained rise in cAMP in the axon terminal of OSNs (n = 84, response ($\Delta R/R_0$ %) = 4.32 ± 0.56, t ½ = 68.6 ± 6.4 s, responsive cells 16.7%). In several cases the cAMP signal partially return to baseline (data not shown). Taken together, these results indicate that IEC fract2 is able to induce not only local increases in [Ca^{2+}] but also in [cAMP] when focally applied to the OSN axon terminus – growth cone.

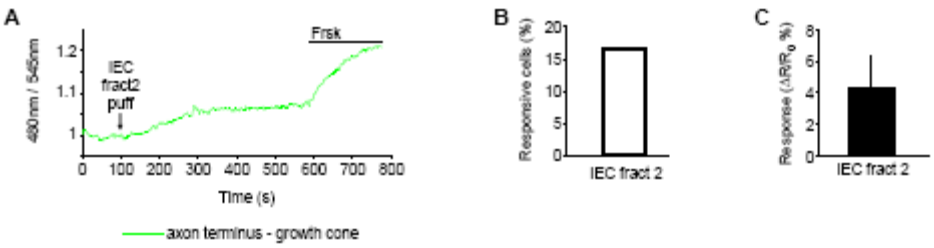

Figure 16: cAMP dynamics in OSNs in response to IEC fract2. **A**, example of cAMP dynamics indicated as normalized kinetics of fluorescence emission intensity (480/545 nm) in an OSN transfected with the sensor for cAMP and challenged with IEC fract2, focally applied to the axon terminus – growth cone, and forskolin (frsk, 25 μM), bath applied. **B**, summary of responsive cells (%). **C**, summary of the response $\Delta R/R_0$ %, bars, SEM.

3.11 Real - time imaging of axon turning behavior

To assess the physiological meaning of Ca^{2+} and cAMP rises on the behavior of the OSN growth cone, real - time imaging experiments on isolated OSNs were performed (see *Material and methods* for details). We first analyzed the turning behaviour of OSN growth cones in response to gradients of molecules known to modulate cAMP and Ca^{2+} levels at the axon terminus - growth cone, such as forskolin (5 mM in the pipette), a generic activator of adenylyl cyclase, and odors (1 mM in the pipette). As shown in Figure 17, both forskolin and odors were able to induce a turning response in the growth cone of OSNs either toward and away from the source of the stimulus. The capability of the pool of active molecules from the olfactory bulb to regulate the axon terminal behaviour was also assessed (the concentration of IEC fract2 in the pipette was 5 μg/μL). Also in this case, the growth cone showed both attractive and repulsive turning responses (Ringer's solution: n = 14, responsive cells 0%; frsk: n = 26, turning angle (°) = 17.6 ± 3.8, responsive cells 38.5%; odors: n = 60, turning angle (°) = 11.1 ± 0.7, responsive cells 35%, IEC fract2: n = 42, turning angle (°) = 17.6 ± 2.3, responsive cells 50%). These data demonstrate that gradients of the abovementioned molecules, including the pool of active molecules from the olfactory bulb, are able to modulate the turning behaviour of the OSN axons. Therefore, through the activation of the OR expressed at the axon terminus – growth cone, they could contribute in providing the axons with instruction to reach the proper target.

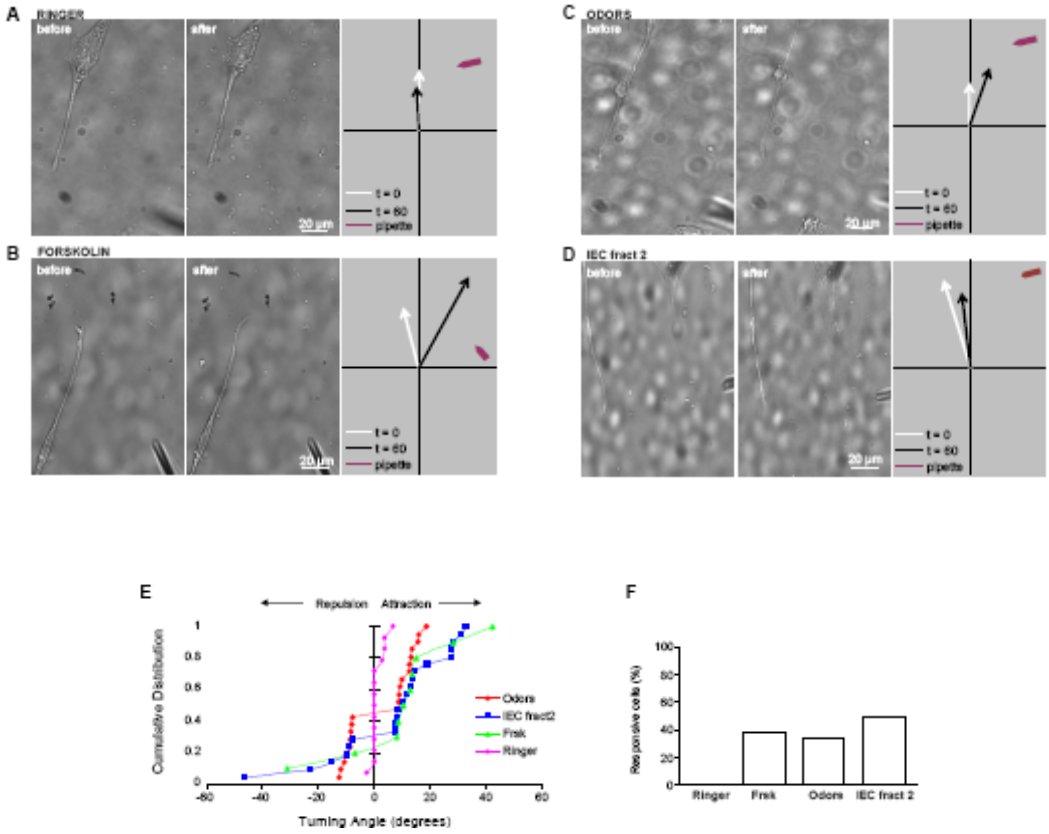

Figure 17: Real – time imaging of axon turning behavior. **A – D**, images of OSN growth cones before and after the application of a gradient of Ringer's solution (**A**), forskolin (**B**), odors (**C**) and IEC fract2 (**D**). **A' – D'**, scheme depicting the direction changes after the stimulation period. The arrows represent the growth cone orientation at the beginning (white) and at the end (black) of the entire stimulation period. Purple head arrow corresponds to the pipette direction. **E**, cumulative distribution of growth cone turning angles. **F**, summary of responsive cells (%).

3.12 Ca^{2+} dynamics in OSNs and HEK cells upon stimulation with Reverse – Phase Chromatography products of Ion Exchange Chromatography

To further fractionate the IEC fract2, a reverse – phase chromatography (RPC) was performed. From this chromatography several different peaks were obtained that were tested on the axon terminus – growth cone of OSNs. Primary cultures of OSNs were loaded with fura-2 and challenged with different RPC products. As shown in Figure 18, almost all fractions tested were able to induce a Ca^{2+} response in the axon terminal of OSNs (Peak 22.5: n = 22, response $\Delta R/R_0$ % = 47.5 ± 5.7, responsive cells 36.4%; Peak 23.8: n = 24, response $\Delta R/R_0$ % = 87.6 ± 0, responsive cells 4.2%; Peak 25.5: n = 28, response $\Delta R/R_0$ % = 13.3 ± 1.7, responsive cells 17.8%; Peak 27: n = 58,

response $\Delta R/R_0$ % = 17.6 ± 3.0, responsive cells 13.8%; Peak 28.5: n = 47, response $\Delta R/R_0$ % = 26.8 ± 8.3, responsive cells 19.1%; Peak 30.2: n = 19, response $\Delta R/R_0$ % = 11.5 ± 1.6, responsive cells 10.5%; Peak 32.6: n = 11, response $\Delta R/R_0$ % = 0, responsive cells 0%; Peak 34.1: n = 25, response $\Delta R/R_0$ % = 29.1 ± 14.4, responsive cells 24%; Peak 36.1: n = 9, response $\Delta R/R_0$ % = 0, responsive cells 0%).

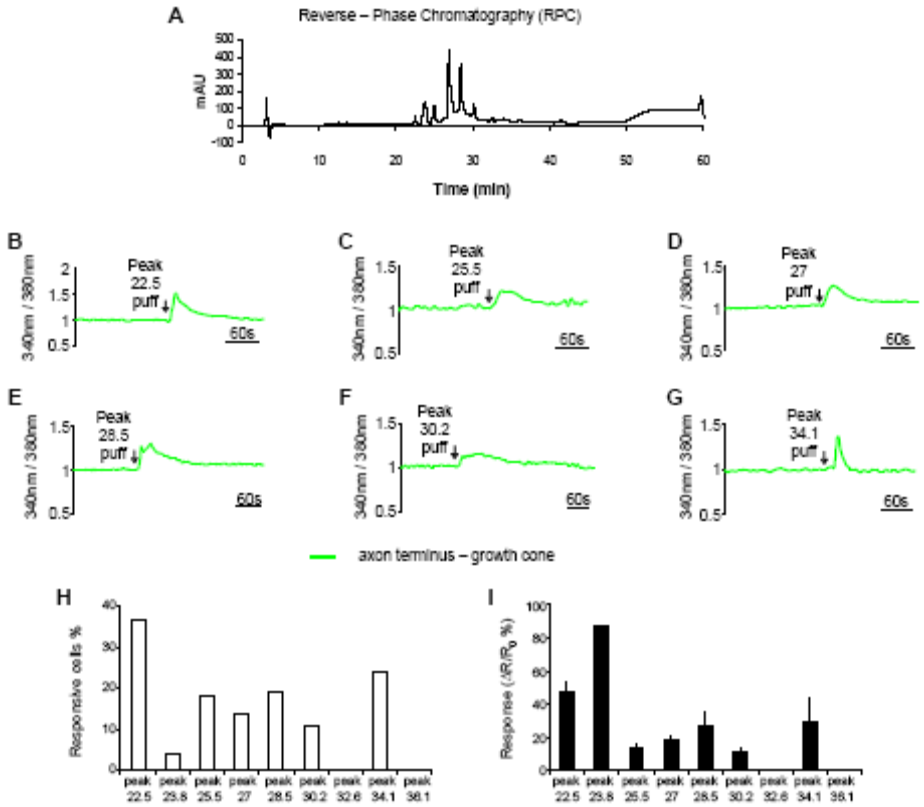

Figure 18: Ca^{2+} dynamics in OSNs challenged with RPC products. **A**, chromatogram of the reverse – phase chromatography of the IEC fract2. **B - G**, examples of Ca^{2+} dynamics in OSNs loaded with fura-2 and challenged with different RPC products, focally applied to the axon terminus – growth cone. **H**, summary of responsive cells (%). **I**, summary of Ca^{2+} response $\Delta R/R_0$ (%), bars, SEM.

However, when the same RPC products were tested on HEK cells transfected with different types of ORs, only some of these fractions were able to activate the odorant receptor (Figure 19). Indeed, only a few RPC peaks induced a clear and prompt rise in Ca^{2+} also in HEK cells transfected with the empty pCI vector (without the OR)(Peak 22.5: OREG: n = 97, response ($\Delta R/R_0$ %) = 46.5 ± 8.7, responsive cells 7.2%; Peak 27: OREG: n = 73, responsive cells 0%; ORS6: n = 14, responsive cells 0%; Olfr62: n = 6, response ($\Delta R/R_0$ %) = 27.3 ± 7.0, responsive cells 83.3%; Peak 28.5: pCI: n = 58, response ($\Delta R/R_0$ %) = 92.3 ±

17.4, responsive cells 22.4%; Peak 30.2: pCI: n = 65, response ($\Delta R/R_0$ %) = 35.7 ± 21.9, responsive cells 4.6%; Peak 34.1: OREG: n = 32, response ($\Delta R/R_0$ %) = 10.1 ± 0, responsive cells 6.2%).

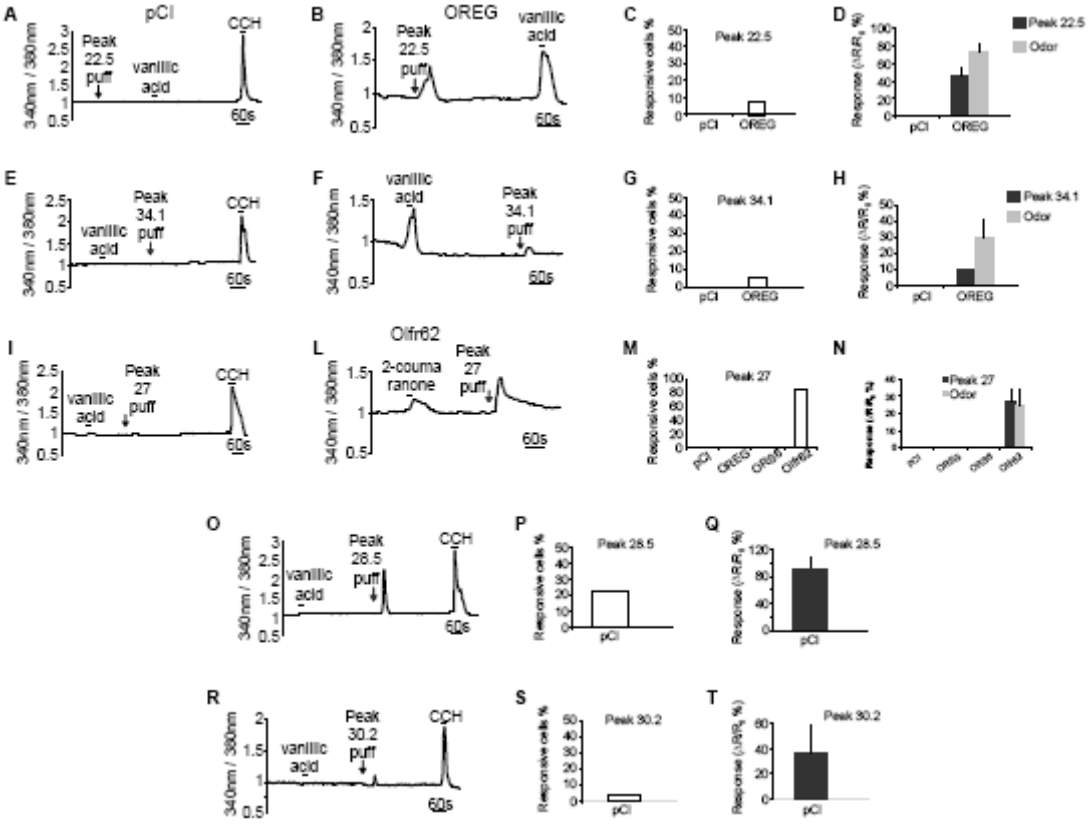

Figure 19: Only some RPC peaks are able to activate the OR expressed in HEK cells. **A, E, I, O, R**, examples of Ca^{2+} dynamics in HEK cells transfected with pCI vector, loaded with fura-2 and challenged with an odor (vanillic acid, 100 µM, bath applied) and different RPC products (puff). **B, F, L**, examples of Ca^{2+} dynamics in HEK cells transfected with different ORs, loaded with fura-2 and challenged with RPC products and the odor specific for the transfected OR. **C, G, M, P, S**, summary of responsive cells (%). **D, H, N, Q, T**, summary of Ca^{2+} response $\Delta R/R_0$ (%), bars, SEM.

4. Discussion

In this study, we analyzed the mechanisms of activation and the function of the odorant receptor expressed at the axon terminus – growth cone of the olfactory sensory neurons. In particular, in this project we studied the spatio - temporal dynamics of cGMP in living olfactory sensory neurons transfected with a genetically encoded sensor for cGMP, and we found that upon pharmacological and physiological stimuli a rise in cGMP is observed in the entire olfactory sensory neuron, from the cilia to the axon terminal. Upon stimulation with SNAP or ANP, known to activate soluble and particulate GCs respectively, a prompt and sustained increase in cGMP was observed in the entire neuron, without a lag phase between the stimulus application and the onset of the response. The time to reach the half - maximal response (t ½) was faster at the axon terminus - growth cone and at the cilia - dendrite than at the soma, only in neurons treated with ANP. These results are in agreement with the different distribution of the two forms of guanylyl cyclases. The lack of zaprinast effect on cGMP under basal conditions suggests that, although the drug is a potent inhibitor of cGMP - PDE, other PDEs (i.e., PDE1 and 2) could hydrolyze cGMP. This can also explain the lack of a larger response to ANP added subsequently to zaprinast. Moreover, it may indicate that the basal activity of the GCs is very low. As to the effect of IBMX on cGMP level, this most likely depends on the cAMP rise induced by the drug (Maritan et al., 2009), followed by a rise in Ca^{2+} and NOS activation (see below). The results with zaprinast are in contrast with those obtained in previous studies (Moon et al., 1998, 2005). This discrepancy could be due to the different preparations and/or to the different techniques used (radioimmunoassay in tissue extracts). When olfactory sensory neurons were challenged with an odormix, a slow and sustained increase in cGMP was observed in the whole neuron. The time to reach the half - maximal response ($t_{1/2}$) was faster at the cilia - dendrite and at the axon terminus - growth cone than at the soma level. This latter observation demonstrates that in the axon terminus - growth cone the cGMP rise does not derive from diffusion of cGMP produced at the cilia - dendrite level. This conclusion was confirmed by local stimulation of the odorant receptor at the axon terminus - growth cone with

odors, focally applied with a pipette. In these conditions, the cGMP increase was detected exclusively at the axon terminal.

As to the rise of cGMP at the soma upon odor stimulation, the kinetics of the cGMP signal we observed seems to be consistent with the diffusion of cGMP from the other compartments, although we cannot exclude, in olfactory sensory neurons *in vitro*, a low expression of the odorant receptor at the soma. Alternatively, the Ca^{2+} increase coupled to odor - olfactory receptor activation at the cilia - dendrite and at the axon terminus - growth cone, may diffuse and cause NOS activation and cGMP production directly at the soma. The main question addressed here is the mechanism underpinning the cGMP generation in the olfactory sensory neurons. We found that odors give rise to the cGMP increase by sGC activation via NO. Due to the temporal pattern of expression, it has been suggested that NO - cGMP (Kafitz et al., 2000; Chen et al., 2004) could play a role during development and in regeneration while CO - cGMP may be involved in the setting of long - term odor response in adult olfactory sensory neurons (Ingi and Ronnett, 1995). The local synthesis of cGMP that we found in developing axons is consistent with this hypothesis. In particular, the odor - dependent cGMP increases were completely abolished by NOS blockade and totally insensitive to HO inhibition. To be noted, olfactory sensory neurons constantly regenerate *in vivo*, thus there is always a subpopulation of developing neurons. The synthesis of cGMP at the axon terminus is of relevance since in other systems it has been shown that the cAMP/cGMP ratio plays a critical role in the axon guidance processes (Nishiyama et al., 2003). Moreover, Murphy and Isaacson (2003) suggested that cGMP and cAMP can modulate synaptic transmission between olfactory sensory neurons and postsynaptic cells. Therefore, these two cyclic nucleotides could contribute to axon pathfinding.

As to the coupling between the odorant receptor and NOS/sGC, some evidence supports the idea that cAMP and Ca^{2+} play essential roles, in particular the following: (1) a cAMP increase is necessary for the odor - dependent cGMP synthesis, since, blocking the AC, odors were unable to increase cGMP; (2) pharmacological increases in cAMP, as induced by either forskolin or IBMX, result in clear increases in cGMP. Furthermore, we demonstrate that the link between cAMP and NOS/sGC is represented by a cytoplasmic Ca^{2+} increase,

generated by plasma membrane Ca^{2+} channel activation and Ca^{2+} release from stores controlled by Epac. This mechanism is in agreement with the well known Ca^{2+} - calmodulin dependency of neuronal NOS (Breer and Shepherd, 1993), with Ca^{2+} influx through CNG channels by cAMP, and with the finding that a rise in $[Ca^{2+}]_c$, elicited solely by K^+ depolarization, results in an increase in cGMP. The link between Ca^{2+} and cGMP via the NOS - sGC activation is further supported by the fact that the sustained cGMP signal reflects the sustained Ca^{2+} signal, suggesting a prolonged Ca^{2+} - dependent activation of NOS - sGC. The contribution of the Ca^{2+} release from stores in olfactory sensory neuron signalling is still controversial, and different results have been obtained in different preparations (Zufall et al., 2000; Otsuguro et al., 2005). We found that cAMP, produced upon forskolin or odor administration in Ca^2 - free medium, can induce an increase in $[Ca^{2+}]_c$. This Ca^{2+} signal is due to Ca^{2+} release from the endoplasmic reticulum, as we directly demonstrated in olfactory sensory neurons transfected with a genetically encoded Ca^{2+} sensor specifically targeted to the endoplasmic reticulum lumen. Furthermore, we show that the link between cAMP - Epac activation and the release of Ca^{2+} from the endoplasmic reticulum is represented by PLCε, as demonstrated by the absence of Ca^{2+} release in olfactory sensory neurons treated with odors in the presence of PLCε inhibitor. cGMP has always been associated with long - term responses, such as odor adaptation (Zufall and Leinders - Zufall 1998), neuronal development and regeneration (Chen et al., 2003), and olfactory imprinting (Dittman et al., 1997). cGMP may also be involved in regulating gene expression (i.e., via CREB phosphorylation). In this work we show that 8 Br - cGMP induces phosphorylation of CREB in olfactory sensory neurons not only *in vitro* (Moon et al., 1999), but also *in vivo*, when the cGMP analogue is applied to the olfactory bulb. Phosphorylation of CREB, due to 8Br - cGMP is likely due to (1) cytosolic Ca^{2+} rise, due to cGMP opening of CNG channels at the axon terminus (Murphy and Isaacson, 2003), and (2) PKG activation and translocation into the nucleus (Gudi et al., 1997). Interestingly, we also demonstrated that odors applied on the olfactory bulb in live animals can induce P - CREB in the nuclei of olfactory sensory neurons. However, in this latter case, the phosphorylation of CREB did not depend critically on cGMP production. Indeed, P - CREB formation in the nuclei of olfactory sensory

neurons was still observed upon odor treatment in the presence of the sGC inhibitor LY83583. These results can be explained by the presence of several mechanisms potentially involved in the phosphorylation of CREB, upon the activation of the odorant receptor. The increases of cAMP and Ca^{2+}, through CNG channels and voltage - gated Ca^{2+} channels, result in a rise of nuclear Ca^{2+} that can be followed by phosphorylation of CREB by CaM kinases. Ca^{2+} may also diffuse from the synapse to the cell body through a regenerative mechanism (i.e., Ca^{2+} - induced Ca^{2+} release)(Rizzuto and Pozzan, 2006). Furthermore, in a previous work (Maritan et al., 2009), we found that a focal application of odors at the axon terminal in cultured neurons was followed by nuclear translocation of the catalytic subunit of PKA, which can in turn induce CREB phosphorylation. Thus, diffusion of the catalytic subunit of PKA could be another possibility. These different scenarios suggest that both PKA and Ca^{2+} are likely to be involved in the phosphorylation of CREB. Together, the present data suggest that cGMP, although not involved in initial stimulus detection events for its slow kinetics, could play several functions in olfactory sensory neurons long - term cellular responses coupled to odorant receptor activation. On the one hand, the local production of cGMP at the axon terminus – growth cone may be important in axon targeting/transmitter release, and, on the other hand, by activating CREB phosphorylation at the nuclear level, it could regulate gene expression independently, or in synergy, with cAMP and Ca^{2+} (Imai and Sakano, 2007). Therefore, we suggest that not only the odorant receptor derived signal, cAMP (Imai et al., 2006), but also cGMP could play a key role in axon targeting acting both locally and at the nuclear level. In this scheme, the presence of Epac in the signalling pathway leading to cGMP synthesis appears particularly relevant. Indeed, in other systems it has been shown that Epac is involved, along with cyclic nucleotides, in neurite outgrowth and turning (Murray et al., 2008).

We then investigated the possible mechanism of activation of the odorant receptor expressed at the axon terminus – growth cone, to assess which ligands can bind and activate the intracellular signalling cascade that includes cAMP, Ca^{2+} and cGMP. We hypothesized that a few molecules expressed in gradient in the olfactory bulb could bind and activate the odorant receptor at the axon terminal of olfactory sensory neurons. By studying the spatio - temporal

dynamics of Ca^{2+} and cAMP in response to lysate or dialysate of the olfactory bulb, locally applied at the axon terminal, we found that a focal increase of cAMP and/or Ca^{2+} was observed only in the axon terminus – growth cone of olfactory sensory neurons. The olfactory bulb dialysate was then fractionated by a gel filtration (GF) chromatography. We found that only the third fraction of the GF chromatography was able to elicit a Ca^{2+} rise in the olfactory sensory neurons. Therefore, this pool of molecules was sub – fractionated through an ion exchange chromatography (IEC), from which four different peaks (IEC fract1, IEC fract2, IEC fract3 and IEC fract4) were obtained. Again we found that only a few of them, namely IEC frac1 and 2, were capable of inducing Ca^{2+} responses in a large number of olfactory sensory neurons.

We found that the active pools of molecules, when heated or treated with protease K, lost their ability to induce a rise in Ca^{2+} in olfactory sensory neurons. These data suggest that the active components of these pools are proteins or peptides. Although the heating was sufficient to completely abolish IEC fract2 activity, a subsequent treatment with protease K was necessary with IEC fract1. These results could be due to the various proteins constituting these two pools and to the different action of heating and protease K. The heating denaturates proteins disrupting hydrogen bonds and non – polar hydrophobic interaction; thus, it only alters the secondary and tertiary structure of a protein without breaking peptide bonds. On the other hand, protease K is a high activity serine protease that digests proteins degrading peptide bonds. Moreover, these data are consistent with the results obtained with HEK cells (see below), in which only IEC fract2 is able to activate the odorant receptor (IEC fract1 induces a Ca^{2+} rise also in absence of the odorant receptor).

To assess whether the rise in Ca^{2+} and cAMP was due to the activation of the odorant receptor, we tested both IEC fract1 and IEC fract2 on HEK cells expressing specific odorant receptors (OREG, ORS6, Olfr62, OR23 and ORM71) and loaded with fura-2. Our data indicate that only IEC fract2 induces a rise in Ca^{2+} via activation of the odorant receptor. IEC fract1 may act through a signalling pathway that differs from that involving the odorant receptor since it elicits Ca^{2+} rises also in HEK cells lacking the odorant receptor.

We then proved that the increase in Ca^{2+} levels, upon stimulation with IEC fract2, is due to the opening of CNG channels. Ca^{2+} dynamics in the axon

terminus – growth cone were analyzed upon stimulation with IEC fract2 in presence of the AC blocker SQ22536. In these conditions no rise in Ca^{2+} was observed. However, when the inhibitor was washed away and the same cell subsequently re – challenged with IEC fract2, an immediate and transient rise in Ca^{2+} was found. Since IEC fract2 was first applied in presence of inhibitor and subsequently after washing away the inhibitor, we can exclude the possibility that the lack of response to the molecules from the bulb in presence of SQ22536 was due to desensitization of the odorant receptor.

It is known that the odorant receptor responds not only to odorants but also to mechanical stimuli, such as the pressure of the puff (Grosmaitre et al., 2007). We demonstrate that the Ca^{2+} increases observed in HEK cells and at the olfactory sensory neuron growth cone are due the IEC fract2 – induced activation of the odorant receptor and not to a mechanical stimulus. Indeed, the control experiments on HEK cells and olfactory sensory neuron axon terminal clearly showed that Ringer's solution or cerebellum lysate, focally applied, did not elicit any Ca^{2+} response in the axon terminal. These results corroborate our hypothesis on the possible role of molecules from the bulb in the activation of the odorant receptor expressed at the growth cone.

Since in olfactory sensory neurons the Ca^{2+} dynamics is strictly dependent on cAMP kinetics, we studied the spatio - temporal dynamics of cAMP in olfactory sensory neurons challenged with IEC fract2, locally applied at the axon terminal, and we found a slow and sustained rise in cAMP exclusively in this compartment. These data confirm that this pool of molecules from the olfactory bulb is able to induce a cAMP rise in the axon terminal of olfactory sensory neurons, that in turn leads to the opening of CNG channels with the subsequent increase in Ca^{2+} levels.

Ca^{2+}, cAMP and cGMP have been shown to play a pivotal role in axon elongation and turning. To assess whether the second messengers locally produced at the axon terminus – growth cone could have a similar role in olfactory sensory neurons, we performed real - time imaging experiments on isolated sensory neurons. We found that molecules able to modulate cAMP and Ca^{2+} concentration, such as forskolin, odors and also IEC fract2, were capable of modulating the turning behavior of the axon terminal of olfactory sensory neurons. We found both attractive and repulsive responses. This is not

surprising since previous studies demonstrated that different levels of cAMP at the axon terminal may result in opposite turning behaviors of the growth cone in response to the same guidance cues (Song et al., 1997, Song et al., 1998).

Finally, IEC fract2 was sub – fractionated through a reverse – phase chromatography (RPC) and we found that only a few fractions were able to activate the odorant receptor expressed in HEK cells.

All together our data demonstrate that the odorant receptor expressed at the axon terminus – growth cone is active and coupled to local increases of cAMP, Ca^{2+} and cGMP. These molecules can exert their action locally, modulating the turning behaviour of the growth cone in response to gradients of axon guidance molecules. They could also act at the nuclear level, modulating gene expression via CREB phosphorylation. Finally we found that the odorant receptor expressed at the axon terminal can be activated by a pool of molecules from the olfactory bulb. Our data suggest that this pool of active molecules could contribute in providing the axons of the olfactory sensory neurons with instructions to reach the proper target.

5. Bibliography

Arctander, S. (1969). “Perfume and flavour chemicals.” (Aroma chemicals)(Las Vegas, NV: Steffen’s Arctander’ s Publications).

Barnea, G., S. O'Donnell, et al. (2004). "Odorant receptors on axon termini in the brain." Science 304(5676): 1468.

Belluscio, L., G. H. Gold, et al. (1998). "Mice deficient in G(olf) are anosmic." Neuron 20(1): 69-81.

Bhandawat, V., J. Reisert, et al. (2005). "Elementary response of olfactory receptor neurons to odorants." Science 308(5730): 1931-4.

Bhandawat, V., J. Reisert, et al. (2010). "Signaling by olfactory receptor neurons near threshold." Proc Natl Acad Sci U S A 107(43): 18682-7.

Bos, J. L. (2003). "Epac: a new cAMP target and new avenues in cAMP research." Nat Rev Mol Cell Biol 4(9): 733-8.

Bozza, T., P. Feinstein, et al. (2002). "Odorant receptor expression defines functional units in the mouse olfactory system." J Neurosci 22(8): 3033-43.

Bozza, T. C. and J. S. Kauer (1998). "Odorant response properties of convergent olfactory receptor neurons." J Neurosci 18(12): 4560-9.

Bradley, J., J. Reisert, et al. (2005). "Regulation of cyclic nucleotide-gated channels." Curr Opin Neurobiol 15(3): 343-9.

Breer, H. and G. M. Shepherd (1993). "Implications of the NO/cGMP system for olfaction." Trends Neurosci 16(1): 5-9.

Campbell, D. S. and C. E. Holt (2001). "Chemotropic responses of retinal growth cones mediated by rapid local protein synthesis and degradation." Neuron 32(6): 1013-26.

Chen, J., Y. Tu, et al. (2004). "The localization of neuronal nitric oxide synthase may influence its role in neuronal precursor proliferation and synaptic maintenance." Dev Biol 269(1): 165-82.

Chen, J., Y. Tu, et al. (2003). "Heme oxygenase-1 and heme oxygenase-2 have distinct roles in the proliferation and survival of olfactory receptor neurons mediated by cGMP and bilirubin, respectively." J Neurochem 85(5): 1247-61.

Chesler, A. T., D. J. Zou, et al. (2007). "A G protein/cAMP signal cascade is

required for axonal convergence into olfactory glomeruli." Proc Natl Acad Sci U S A 104(3): 1039-44.

Chess, A., I. Simon, et al. (1994). "Allelic inactivation regulates olfactory receptor gene expression." Cell 78(5): 823-34.

Cho, J. H., M. Lepine, et al. (2007). "Requirement for Slit-1 and Robo-2 in zonal segregation of olfactory sensory neuron axons in the main olfactory bulb." J Neurosci 27(34): 9094-104.

Cloutier, J. F., R. J. Giger, et al. (2002). "Neuropilin-2 mediates axonal fasciculation, zonal segregation, but not axonal convergence, of primary accessory olfactory neurons." Neuron 33(6): 877-92.

Cloutier, J. F., A. Sahay, et al. (2004). "Differential requirements for semaphorin 3F and Slit-1 in axonal targeting, fasciculation, and segregation of olfactory sensory neuron projections." J Neurosci 24(41): 9087-96.

Col, J. A., T. Matsuo, et al. (2007). "Adenylyl cyclase-dependent axonal targeting in the olfactory system." Development 134(13): 2481-9.

Connelly, T., A. Savigner, et al. (2013). "Spontaneous and sensory-evoked activity in mouse olfactory sensory neurons with defined odorant receptors." J Neurophysiol 110(1): 55-62.

Cutforth, T., L. Moring, et al. (2003). "Axonal ephrin-As and odorant receptors: coordinate determination of the olfactory sensory map." Cell 114(3): 311-22.

Dittman, A. H., T. P. Quinn, et al. (1997). "Sensitization of olfactory guanylyl cyclase to a specific imprinted odorant in coho salmon." Neuron 19(2): 381-9.

Dontchev, V. D. and P. C. Letourneau (2002). "Nerve growth factor and semaphorin 3A signaling pathways interact in regulating sensory neuronal growth cone motility." J Neurosci 22(15): 6659-69.

Dubacq, C., S. Jamet, et al. (2009). "Evidence for developmentally regulated local translation of odorant receptor mRNAs in the axons of olfactory sensory neurons." J Neurosci 29(33): 10184-90.

Dunn, T. A., D. R. Storm, et al. (2009). "Calcium-dependent increases in protein kinase-A activity in mouse retinal ganglion cells are mediated by multiple adenylate cyclases." PLoS One 4(11): e7877.

Enserink, J. M., A. E. Christensen, et al. (2002). "A novel Epac-specific cAMP

analogue demonstrates independent regulation of Rap1 and ERK." Nat Cell Biol 4(11): 901-6.

Feinstein, P., T. Bozza, et al. (2004). "Axon guidance of mouse olfactory sensory neurons by odorant receptors and the beta2 adrenergic receptor." Cell 117(6): 833-46.

Feinstein, P. and P. Mombaerts (2004). "A contextual model for axonal sorting into glomeruli in the mouse olfactory system." Cell 117(6): 817-31.

Firestein, S. (2001). "How the olfactory system makes sense of scents." Nature 413(6852): 211-8.

Galli, L. and Maffei, L. (1988). “Spontaneous impulse activity of rat retinal ganglion cells in prenatal life.” Science 242: 90-91.

Glusman, G., I. Yanai, et al. (2001). "The complete human olfactory subgenome." Genome Res 11(5): 685-702.

Gomez, T. M. and J. Q. Zheng (2006). "The molecular basis for calcium-dependent axon pathfinding." Nat Rev Neurosci 7(2): 115-25.

Gordon, S. E. and W. N. Zagotta (1995). "Subunit interactions in coordination of Ni^{2+} in cyclic nucleotide-gated channels." Proc Natl Acad Sci U S A 92(22): 10222-6.

Greene, L. A., S. A. Drexler, et al. (1986). "Selective inhibition of responses to nerve growth factor and of microtubule-associated protein phosphorylation by activators of adenylate cyclase." J Cell Biol 103(5): 1967-78.

Grosmaitre, X., L. C. Santarelli, et al. (2007). "Dual functions of mammalian olfactory sensory neurons as odor detectors and mechanical sensors." Nat Neurosci 10(3): 348-54.

Gudi, T., S. M. Lohmann, et al. (1997). "Regulation of gene expression by cyclic GMP-dependent protein kinase requires nuclear translocation of the kinase: identification of a nuclear localization signal." Mol Cell Biol 17(9): 5244-54.

Hallem, E. A., M. G. Ho, et al. (2004). "The molecular basis of odor coding in the Drosophila antenna." Cell 117(7): 965-79.

Hamilton, K. A., T. Heinbockel, et al. (2005). "Properties of external plexiform layer interneurons in mouse olfactory bulb slices." Neuroscience 133(3): 819-29.

Henley, J. and M. M. Poo (2004). "Guiding neuronal growth cones using Ca^{2+} signals." Trends Cell Biol 14(6): 320-30.

Honda, A., S. R. Adams, et al. (2001). "Spatiotemporal dynamics of guanosine 3',5'-cyclic monophosphate revealed by a genetically encoded, fluorescent indicator." Proc Natl Acad Sci U S A 98(5): 2437-42.

Hong, K., M. Nishiyama, et al. (2000). "Calcium signalling in the guidance of nerve growth by netrin-1." Nature 403(6765): 93-8.

Huber, A. B., A. L. Kolodkin, et al. (2003). "Signaling at the growth cone: ligand-receptor complexes and the control of axon growth and guidance." Annu Rev Neurosci 26: 509-63.

Imai, T. and H. Sakano (2007). "Roles of odorant receptors in projecting axons in the mouse olfactory system." Curr Opin Neurobiol 17(5): 507-15.

Imai, T., M. Suzuki, et al. (2006). "Odorant receptor-derived cAMP signals direct axonal targeting." Science 314(5799): 657-61.

Ingi, T. and G. V. Ronnett (1995). "Direct demonstration of a physiological role for carbon monoxide in olfactory receptor neurons." J Neurosci 15(12): 8214-22.

Juilfs, D. M., H. J. Fulle, et al. (1997). "A subset of olfactory neurons that selectively express cGMP-stimulated phosphodiesterase (PDE2) and guanylyl cyclase-D define a unique olfactory signal transduction pathway." Proc Natl Acad Sci U S A 94(7): 3388-95.

Kafitz, K. W., T. Leinders-Zufall, et al. (2000). "Cyclic GMP evoked calcium transients in olfactory receptor cell growth cones." Neuroreport 11(4): 677-81.

Kaupp, U. B. and R. Seifert (2002). "Cyclic nucleotide-gated ion channels." Physiol Rev 82(3): 769-824.

Kuhn, M. (2003). "Structure, regulation, and function of mammalian membrane guanylyl cyclase receptors, with a focus on guanylyl cyclase-A." Circ Res 93(8): 700-9.

Lankford, K. L., F. G. DeMello, et al. (1988). "D1-type dopamine receptors inhibit growth cone motility in cultured retina neurons: evidence that neurotransmitters act as morphogenic growth regulators in the developing central nervous system." Proc Natl Acad Sci U S A 85(12): 4567-71.

Leinders-Zufall, T., M. N. Rand, et al. (1997). "Calcium entry through cyclic nucleotide-gated channels in individual cilia of olfactory receptor cells: spatiotemporal dynamics." J Neurosci 17(11): 4136-48.

Leinders-Zufall, T., G. M. Shepherd, et al. (1996). "Modulation by cyclic GMP of the odour sensitivity of vertebrate olfactory receptor cells." Proc Biol Sci 263(1371): 803-11.

Leinders-Zufall, T. and F. Zufall (1995). "Block of cyclic nucleotide-gated channels in salamander olfactory receptor neurons by the guanylyl cyclase inhibitor LY83583." J Neurophysiol 74(6): 2759-62.

Lin, D. M., F. Wang, et al. (2000). "Formation of precise connections in the olfactory bulb occurs in the absence of odorant-evoked neuronal activity." Neuron 26(1): 69-80.

Liu, N., Shields, CB., Rojsen, FJ. (1998). “Primary culture of adult mouse olfactory receptor neurons.” Exp Neurol 151: 173-183.

Lledo, P. M., G. Gheusi, et al. (2005). "Information processing in the mammalian olfactory system." Physiol Rev 85(1): 281-317.

Lodovichi, C., L. Belluscio, et al. (2003). "Functional topography of connections linking mirror-symmetric maps in the mouse olfactory bulb." Neuron 38(2): 265-76.

Lohof, A. M., M. Quillan, et al. (1992). "Asymmetric modulation of cytosolic cAMP activity induces growth cone turning." J Neurosci 12(4):1253-61.

Lugnier, C. (2006). "Cyclic nucleotide phosphodiesterase (PDE) superfamily: a new target for the development of specific therapeutic agents." Pharmacol Ther 109(3): 366-98.

Malnic, B., J. Hirono, et al. (1999). "Combinatorial receptor codes for odors." Cell 96(5): 713-23.

Maritan, M., G. Monaco, et al. (2009). "Odorant receptors at the growth cone are coupled to localized cAMP and Ca^{2+} increases." Proc Natl Acad Sci U S A 106(9): 3537-42.

Matthews, H. R. and J. Reisert (2003). "Calcium, the two-faced messenger of olfactory transduction and adaptation." Curr Opin Neurobiol 13(4): 469-75.

Meister, M., R. O. Wong, et al. (1991). "Synchronous bursts of action potentials in ganglion cells of the developing mammalian retina." Science

252(5008): 939-43.

Menini, A. (1999). "Calcium signalling and regulation in olfactory neurons." Curr Opin Neurobiol 9(4): 419-26.

Ming, G. L., H. J. Song, et al. (1997). "cAMP-dependent growth cone guidance by netrin-1." Neuron 19(6): 1225-35.

Miyamichi, K., S. Serizawa, et al. (2005). "Continuous and overlapping expression domains of odorant receptor genes in the olfactory epithelium determine the dorsal/ventral positioning of glomeruli in the olfactory bulb." J Neurosci 25(14): 3586-92.

Mombaerts, P., F. Wang, et al. (1996). "Visualizing an olfactory sensory map." Cell 87(4): 675-86.

Monti-Graziadei, G. A., F. L. Margolis, et al. (1977). "Immunocytochemistry of the olfactory marker protein." J Histochem Cytochem 25(12): 1311-6.

Monti-Graziadei, G. A., R. S. Stanley, et al. (1980). "The olfactory marker protein in the olfactory system of the mouse during development." Neuroscience 5(7): 1239-52.

Moon, C., P. Jaberi, et al. (1998). "Calcium-sensitive particulate guanylyl cyclase as a modulator of cAMP in olfactory receptor neurons." J Neurosci 18(9): 3195-205.

Moon, C., P. J. Simpson, et al. (2005). "Regulation of intracellular cyclic GMP levels in olfactory sensory neurons." J Neurochem 95(1): 200-9.

Moon, C., Y. K. Sung, et al. (1999). "Odorants induce the phosphorylation of the cAMP response element binding protein in olfactory receptor neurons." Proc Natl Acad Sci U S A 96(25): 14605-10.

Mori, K., H. Nagao, et al. (1999). "The olfactory bulb: coding and processing of odor molecule information." Science 286(5440): 711-5.

Murphy, G. J. and J. S. Isaacson (2003). "Presynaptic cyclic nucleotide-gated ion channels modulate neurotransmission in the mammalian olfactory bulb." Neuron 37(4): 639-47.

Murray, A. J. and D. A. Shewan (2008). "Epac mediates cyclic AMP-dependent axon growth, guidance and regeneration." Mol Cell Neurosci 38(4): 578-88.

Murthy, V. N (2011). "Olfactory maps in the brain." Annu Rev Neurosci 34: 233-58.

Nakamura, T. (2000). "Cellular and molecular constituents of olfactory sensation in vertebrates." Comp Biochem Physiol A Mol Integr Physiol 126(1): 17-32.

Nakamura, T. and G. H. Gold (1987). "A cyclic nucleotide-gated conductance in olfactory receptor cilia." Nature 325(6103): 442-4.

Nikolaev, V. O., S. Gambaryan, et al. (2006). "Fluorescent sensors for rapid monitoring of intracellular cGMP." Nat Methods 3(1): 23-5.

Nishiyama, M., A. Hoshino, et al. (2003). "Cyclic AMP/GMP-dependent modulation of Ca^{2+} channels sets the polarity of nerve growth-cone turning." Nature 423(6943): 990-5.

Noe, J., E. Tareilus, et al. (1997). "Sodium/calcium exchanger in rat olfactory neurons." Neurochem Int 30(6): 523-31.

Otsuguro, K., S. H. Gautam, et al. (2005). "Characterization of forskolin-induced Ca^{2+} signals in rat olfactory receptor neurons." J Pharmacol Sci 97(4): 510-8.

Pifferi, S., A. Boccaccio, et al. (2006). "Cyclic nucleotide-gated ion channels in sensory transduction." FEBS Lett 580(12): 2853-9.

Ponsioen, B., J. Zhao, et al. (2004). "Detecting cAMP-induced Epac activation by fluorescence resonance energy transfer: Epac as a novel cAMP indicator." EMBO Rep 5(12): 1176-80.

Reisert, J. (2010). "Origin of basal activity in mammalian olfactory receptor neurons." J Gen Physiol 136(5): 529-40.

Ressler, K. J., S. L. Sullivan, et al. (1994). "Information coding in the olfactory system: evidence for a stereotyped and highly organized epitope map in the olfactory bulb." Cell 79(7): 1245-55.

Rizzuto, R. and T. Pozzan (2006). "Microdomains of intracellular Ca^{2+}: molecular determinants and functional consequences." Physiol Rev 86(1): 369-408.

Ronnett, G. V., L. D. Hester, et al. (1991). "Primary culture of neonatal rat olfactory neurons." J Neurosci 11(5): 1243-55.

Roskams, A. J., D. S. Bredt, et al. (1994). "Nitric oxide mediates the formation of synaptic connections in developing and regenerating olfactory receptor neurons." Neuron 13(2): 289-99.

Royal, S. J. and B. Key (1999). "Development of P2 olfactory glomeruli in P2-

internal ribosome entry site-tau-LacZ transgenic mice." J Neurosci 19(22): 9856-64.

Rydel, RE and Greene, LA (1988). “cAMP analogs promote survival and neurite outgrowth in cultures of rat sympathetic and sensory neurons independently of nerve growth factors.” Proc Natl Acad Sci USA 85: 1257-1261.

Rudolf, R., P. J. Magalhaes, et al. (2006). "Direct in vivo monitoring of sarcoplasmic reticulum Ca^{2+} and cytosolic cAMP dynamics in mouse skeletal muscle." J Cell Biol 173(2): 187-93.

Sadana, R. and C. W. Dessauer (2009). "Physiological roles for G protein-regulated adenylyl cyclase isoforms: insights from knockout and overexpression studies." Neurosignals 17(1): 5-22.

Sakano, H. (2010). “Neural map formation in the mouse olfactory system.” Neuron 67: 530-542.

Sano, M., R. Katoh-Semba, et al. (1990). "Changes in levels of microtubule-associated proteins in relation to the outgrowth of neurites from PC12D cells, a forskolin- and nerve growth factor-responsive subline of PC12 pheochromocytoma cells." Brain Res 510(2): 269-76.

Schmidt, M., S. Evellin, et al. (2001). "A new phospholipase-C-calcium signalling pathway mediated by cyclic AMP and a Rap GTPase." Nat Cell Biol 3(11): 1020-4.

Schwarting, G. A., C. Kostek, et al. (2000). "Semaphorin 3A is required for guidance of olfactory axons in mice." J Neurosci 20(20): 7691-7.

Scolnick, J. A., K. Cui, et al. (2008). "Role of IGF signaling in olfactory sensory map formation and axon guidance." Neuron 57(6): 847-57.

Serizawa, S., K. Miyamichi, et al. (2003). "Negative feedback regulation ensures the one receptor-one olfactory neuron rule in mouse." Science 302(5653): 2088-94.

Serizawa, S., K. Miyamichi, et al. (2004). "One neuron-one receptor rule in the mouse olfactory system." Trends Genet 20(12): 648-53.

Serizawa, S., K. Miyamichi, et al. (2005). "Negative feedback regulation ensures the one neuron-one receptor rule in the mouse olfactory system." Chem Senses 30 Suppl 1: i99-100.

Serizawa, S., K. Miyamichi, et al. (2006). "A neuronal identity code for the

odorant receptor-specific and activity-dependent axon sorting." Cell 127(5): 1057-69.

Shepherd, G. “The synaptic organization of the brain.” Oxford: Oxford University Press 1998.

Shigeoka, T., B. Lu, et al. (2013). "Cell biology in neuroscience: RNA-based mechanisms underlying axon guidance." J Cell Biol 202(7): 991-9.

Shipley, M. T. and M. Ennis (1996). "Functional organization of olfactory system." J Neurobiol 30(1): 123-76.

Song, H., G. Ming, et al. (1998). "Conversion of neuronal growth cone responses from repulsion to attraction by cyclic nucleotides." Science 281(5382): 1515-8.

Song, H. J., G. L. Ming, et al. (1997). "cAMP-induced switching in turning direction of nerve growth cones." Nature 388(6639): 275-9.

Strotmann, J. and H. Breer (2006). "Formation of glomerular maps in the olfactory system." Semin Cell Dev Biol 17(4): 402-10.

Strotmann, J., O. Levai, et al. (2004). "Olfactory receptor proteins in axonal processes of chemosensory neurons." J Neurosci 24(35): 7754-61.

Takeuchi, H., K. Inokuchi, et al. (2010). "Sequential arrival and graded secretion of Sema3F by olfactory neuron axons specify map topography at the bulb." Cell 141(6): 1056-67.

Taniguchi, M., H. Nagao, et al. (2003). "Distorted odor maps in the olfactory bulb of semaphorin 3A-deficient mice." J Neurosci 23(4): 1390-7.

Touhara, K., S. Sengoku, et al. (1999). "Functional identification and reconstitution of an odorant receptor in single olfactory neurons." Proc Natl Acad Sci U S A 96(7): 4040-5.

Treloar, H. B., P. Feinstein, et al. (2002). "Specificity of glomerular targeting by olfactory sensory axons." J Neurosci 22(7): 2469-77.

Tsuda, M., K. Ono, et al. (1989). "Neurite outgrowth from mouse neuroblastoma and cerebellar cells induced by the protein kinase inhibitor H-7." Neurosci Lett 105(3): 241-5.

Van Wagenen, S. and V. Rehder (1999). "Regulation of neuronal growth cone filopodia by nitric oxide." J Neurobiol 39(2): 168-85.

Vassar, R., S. K. Chao, et al. (1994). "Topographic organization of sensory projections to the olfactory bulb." Cell 79(6): 981-91.

Verma, A., D. J. Hirsch, et al. (1993). "Carbon monoxide: a putative neural messenger." Science 259(5093): 381-4.

Wang, F., A. Nemes, et al. (1998). "Odorant receptors govern the formation of a precise topographic map." Cell 93(1): 47-60.

Wen, Z., C. Guirland, et al. (2004). "A CaMKII/calcineurin switch controls the direction of Ca^{2+}-dependent growth cone guidance." Neuron 43(6): 835-46.

West, A. E. and M. E. Greenberg (2011). "Neuronal activity-regulated gene transcription in synapse development and cognitive function." Cold Spring Harb Perspect Biol 3(6).

Wong, S. T., K. Trinh, et al. (2000). "Disruption of the type III adenylyl cyclase gene leads to peripheral and behavioral anosmia in transgenic mice." Neuron 27(3): 487-97.

Yan, Z., J. Tan, et al. (2008). "Precise circuitry links bilaterally symmetric olfactory maps." Neuron 58(4): 613-24.

Yu, C. R., J. Power, et al. (2004). "Spontaneous neural activity is required for the establishment and maintenance of the olfactory sensory map." Neuron 42(4): 553-66.

Zaccolo, M., F. De Giorgi, et al. (2000). "A genetically encoded, fluorescent indicator for cyclic AMP in living cells." Nat Cell Biol 2(1): 25-9.

Zaccolo, M. and T. Pozzan (2002). "Discrete microdomains with high concentration of cAMP in stimulated rat neonatal cardiac myocytes." Science 295(5560): 1711-5.

Zhang, LI. and Poo, MM. (2001). “Electrical activity and development of neural circuits.” Nat Neurosci 4, Suppl: 1207-1214.

Zheng, C., P. Feinstein, et al. (2000). "Peripheral olfactory projections are differentially affected in mice deficient in a cyclic nucleotide-gated channel subunit." Neuron 26(1): 81-91.

Zheng, J. Q., M. Felder, et al. (1994). "Turning of nerve growth cones induced by neurotransmitters." Nature 368(6467): 140-4.

Zou, D. J., A. T. Chesler, et al. (2007). "Absence of adenylyl cyclase 3 perturbs peripheral olfactory projections in mice." J Neurosci 27(25): 6675-83.

Zozulya, S., F. Echeverri, et al. (2001). "The human olfactory receptor repertoire." Genome Biol 2(6): RESEARCH0018.

Zufall, F. and T. Leinders-Zufall (1998). "Role of cyclic GMP in olfactory transduction and adaptation." Ann N Y Acad Sci 855: 199-204.

Zufall, F., T. Leinders-Zufall, et al. (2000). "Amplification of odor-induced Ca^{2+} transients by store-operated Ca^{2+} release and its role in olfactory signal transduction." J Neurophysiol 83(1): 501-12.

6. Acknowledgements

I would like to thank my supervisor Claudia Lodovichi for giving me the opportunity to take up my PhD in her laboratory, during which I could follow an interesting project and achieve a professional growth.

Thanks to all my colleagues.

A special thank to my family, to have always believed in me, even when I was not able to do it. Thanks to my mum, to have listen to me also in difficult moments and for being always, even when the others turned them back. Thanks to my dad, for the practical advices and for his jokes that make me smile also when I don't want to smile. Thanks to Cora, the best sister of the world, for her continuous support and for helping me in difficult choices. Thanks to Livio and to Argo, my wonderful and very sweet nephew, that every day makes me proud of his smiles and conquests.

A special thank also to my grand mothers and to my aunt Rosy, for her support and for all sweets that get me up during my nights in Padova.

Thanks to Giuly, for her wonderful friendship.

6. Ringraziamenti

Vorrei ringraziare la Dott.ssa Claudia Lodovichi per avermi dato l'opportunità di svolgere il mio dottorato nel suo laboratorio, dove ho potuto partecipare ad un interessante progetto e crescere professionalmente.

Grazie anche a tutti i miei colleghi.

Un grazie tutto speciale va alla mia famiglia, per aver sempre creduto in me, anche quando io non ci riuscivo. Grazie alla mia mamma, per avermi ascoltato nei momenti difficili e per esserci sempre, anche quando tutti gli altri mi voltano le spalle. Grazie al mio papà, per i consigli pratici e le battute di spirito che mi hanno fatto sorridere anche quando non ne avevo voglia. Grazie a Cora, la sorella migliore del mondo, che mi ha sempre incoraggiata e aiutata nelle scelte difficili. Grazie a Livio e al mio bellissimo e dolcissimo Argo, che ogni giorno mi riempie di orgoglio con i suoi sorrisi sdentati e le sue conquiste!

Un grazie speciale anche alle mie nonne e alla zia Rosy, per esserci sempre e per tutte le cose buone che mi hanno tirato su il morale nelle mie serate a Padova.

Grazie a Giuly, un'amica come lei è cosa rara!